รายงานการวิจัย

การกำจัดแอมโมเนียจากอากาศเสียของโรงงานอุตสาหกรรมน้ำยางข้นด้วยถ่านกัมมันต์ที่อิ่มตัวด้วยสารเคมี

งบประมาณแผ่นดิน 2552

คณะผู้วิจัย

นางจรรยา อินทมณี หัวหน้าโครงการวิจัย

ผู้ช่วยศาสตราจารย์ ดร.จันทิมา ชั่งสิริพร ผู้ร่วมวิจัย

รองศาสตราจารย์ ดร.จรัญ บุญกาญจน์ ผู้ร่วมวิจัย

บทคัดย่อ

แอมโมเนียเป็นสารเคมีซึ่งใช้ในโรงงานอุตสาหกรรมหลายประเภท การแพร่กระจายของแอมโมเนียในอากาศโดยไม่ได้ทำการบำบัดก่อนนั้นจะส่งผลเสียให้กับมนุษย์และสิ่งแวดล้อมอย่างมาก ดังนั้นงานวิจัยนี้จึงทำการศึกษาถึงการกำจัดก๊าซแอมโมเนียในอากาศเสียโดยใช้วิธีการดูดซับด้วยตัวดูดซับชนิดถ่านกัมมันต์จากไม้ยางพาราและถ่านไม้ยางพารา ซึ่งทำการปรับปรุงสภาพพื้นผิวโดยใช้กรดซัลฟิวริก เพื่อให้ได้ประสิทธิภาพในการกำจัดแอมโมเนียในอากาศเสียที่สูงขึ้นและสามารถนำตัวดูดซับกลับมาใช้ซ้ำได้ สำหรับในงานวิจัยนี้ได้แบ่งการศึกษาออกเป็น 4 ส่วน คือ การผลิตถ่านกัมมันต์ (activated carbon) จากไม้ยางพาราโดยกรดซัลฟิวริกและกรดฟอสฟอริก การผลิตถ่าน (biochar) จากไม้ยางพารา การกำจัดแอมโมเนียในอากาศเสียโดยตัวดูดซับที่ผ่านการทำให้อิ่มตัวโดยกรดซัลฟิวริก และการฟื้นฟูสภาพตัวดูดซับ โดยทำการศึกษาเปรียบเทียบประสิทธิการกำจัดแอมโมเนียในอากาศเสียระหว่างถ่านกัมมันต์กับถ่านจากไม้ยางพารา การสร้างแบบจำลองทางคณิตศาสตร์ของระบบและหาสภาวะที่เหมาะสมในการบำบัดแอมโมเนียในอากาศเสียด้วยวิธีพื้นผิวตอบสนอง (RSM)

การผลิตถ่านกัมมันต์จากไม้ยางพาราโดยการกระตุ้นทางเคมีด้วยกรดเพื่อใช้ในการบำบัดแอมโมเนียในอากาศเสีย ทำได้โดยการเตรียมปีกไม้ขนาด 1×1×1 cm. ทำการกระตุ้นด้วยกรดซัลฟิวริกและกรดฟอสฟอริกที่ความเข้มข้น 20-80% โดยวิธีแช่และเผาในสภาวะไร้อากาศ พบว่า การกระตุ้นด้วยกรดฟอสฟอริกทำให้ได้ร้อยละผลได้ (% yield) ที่ดีถึง 52% ส่วนการกระตุ้นด้วยกรดซัลฟิวริกทำให้พื้นที่ผิวของถ่านกัมมันต์ที่มากกว่า การกระตุ้นด้วยกรดซัลฟิวริกความเข้มข้น 50% ทำให้ได้พื้นที่ผิว BET สูงถึง 558 m^2/g และมีพื้นที่ผิว Micropore สูงถึง 466 m^2/g การผลิตถ่านกัมมันต์จากไม้ยางพาราด้วยการใช้กรด 2 ชนิดมาผสมกัน พบว่า อัตราส่วนที่เหมาะสม คือ กรดฟอสฟอริก 50% และ กรดซัลฟิวริก 40% โดยทำการเผาที่อุณหภูมิ 400°C เป็นเวลา 2 ชั่วโมง ทำให้ได้ผลได้ของถ่านกัมมันต์จากไม้ยางพาราเป็น 40% มีพื้นที่ผิว BET 1200 m^2/g และพื้นที่ผิว Micropore 700 m^2/g และสภาวะที่เหมาะสมในการผลิตถ่านไม้ยางพารา คือ ใช้อุณหภูมิในการเผา 500°C เป็นเวลา 2 ชั่วโมง ทำให้ได้ผลได้ของถ่านไม้ยางพาราเป็น 25% พื้นที่ผิว BET 3 m^2/g

ทำการปรับสภาพพื้นผิวถ่านกัมมันต์จากไม้ยางพาราและถ่านไม้ยางพาราที่ผลิตได้ด้วยกรดซัลฟิวริกที่ความเข้มข้น 40 ถึง 80% สำหรับการดูดซับแอมโมเนียในอากาศเสียด้วยระบบหอแบบเบดนิ่ง (fixed bed) โดยตัวแปรที่ศึกษาได้แก่ อัตราการไหลของอากาศเสีย ความเข้มข้นของแอมโมเนีย และความเข้มข้นของกรดที่ใช้ในการปรับสภาพผิว พบว่าเมื่อใช้ความเข้มข้นของกรด

สำหรับการปรับสภาพพื้นผิวตัวดูดซับเพิ่มสูงขึ้น อัตราการไหลของอากาศเสียและความเข้มข้นของแอมโมเนียลดลง ส่งผลให้ประสิทธิภาพในการกำจัดแอมโมเนียเพิ่มสูงขึ้น และจากการศึกษาประสิทธิภาพการดูดซับก๊าซแอมโมเนียในอากาศเสียระหว่างถ่านกัมมันต์จากไม้ยางพาราและถ่านไม้ยางพารามีค่าใกล้เคียงกัน ซึ่งความเข้มข้นของกรดซัลฟิวริกที่เหมาะสมในการปรับสภาพผิวคือ 80% โดยให้ประสิทธิภาพในการดูดซับแอมโมเนียที่ความเข้มข้น 800 ppmv ที่อัตราการไหล 2 ลิตร/นาที สูงถึง 90% นอกจากนี้จากการเกิดปฏิกิริยาระหว่างแอมโมเนียในอากาศเสียกับกรดซัลฟิวริกที่ผิวของถ่านไม้ จะทำให้ได้ผลผลิตพลอยได้เป็นแอมโมเนียมซัลเฟท ($(NH_4)_2SO_4$) ซึ่งสามารถใช้เป็นปุ๋ยไนโตรเจนในการปลูกพืช

การออกแบบการทดลองสำหรับการทดสอบการใช้ถ่านไม้ยางพาราในกระบวนการดูดซับแอมโมเนียในอากาศเสียใช้วิธีการพื้นผิวตอบสนอง ด้วยการออกแบบส่วนประสมกลาง (CCD) และสมการควอดราติก (quadratic) เพื่อหาความสัมพันธ์ระหว่างตัวแปรดำเนินการและผลตอบสนอง ทำการวิเคราะห์ความแปรปรวนด้วย ANOVA โดยผลตอบสนอง (response) ของสมการพื้นผิว คือ ระยะเวลาการดูดซับที่ประสิทธิภาพการดูดซับแอมโมเนียลดลง 50% พบว่า แบบจำลองที่ได้มีความสอดคล้องกับค่าที่ได้จากการทดลองจริง (R^2= 0.9137) และสภาวะที่เหมาะสมที่ได้จากแบบจำลองในการดูดซับแอมโมเนียที่ความเข้มข้น 300 ppmv อัตราการไหล 2.1 ลิตรต่อนาที คือ ใช้กรดซัลฟิวริก 72% ในการปรับสภาพพื้นผิวถ่านไม้ยางพารา ซึ่งจะทำให้ได้ระยะเวลาการดูดซับถึง 219 นาทีซึ่งให้ค่าใกล้เคียงกับผลการทดลองจริง

การปรับฟื้นผิวสภาพถ่านไม้ยางพาราหลังจากใช้งานในการดูดซับแอมโมเนียในอากาศเสียทำได้โดยใช้วิธีการล้างด้วยน้ำร้อน เนื่องจากแอมโมเนียมซัลเฟตสามารถละลายน้ำได้ดี โดยช่วงอุณหภูมิที่ศึกษาอยู่ระหว่าง 30-100°C ทำการปรับสภาพถ่านไม้ที่ผ่านการปรับฟื้นผิวสภาพด้วยกรดซัลฟิวริก และทำการทดสอบประสิทธิภาพการนำกลับไปใช้ใหม่ซ้ำ 2 ครั้งในการดูดซับก๊าซแอมโมเนียจากอากาศเสียในหอดูดซับ ด้วยกราฟเบรกทรูของการดูดซับแอมโมเนีย พบว่ากราฟเบรกทรูของการดูดซับแอมโมเนีย ในครั้งที่ 2 จะให้ระยะเวลาในการดูดซับมากกว่าครั้งที่ 1 และให้ระยะเวลาการดูดซับสูงถึง 9 ชั่วโมง ที่อุณหภูมิของน้ำร้อน 100°C นอกจากนี้ยังพบว่าเมื่ออุณหภูมิสูงขึ้นจะทำให้ระยะเวลาการดูดซับเพิ่มขึ้นด้วย

ผลจากงานวิจัยชิ้นนี้สามารถนำไปประยุกต์ใช้ในการกำจัดก๊าซแอมโมเนีย ภายในโรงงานอุตสาหกรรมเช่น โรงงานน้ำยางข้น โรงงานผลิตปุ๋ยเคมี เป็นต้น เพื่อลดผลกระทบต่อมนุษย์และสิ่งแวดล้อม จากการปลดปล่อยก๊าซแอมโมเนียสู่บรรยากาศ

ABSTRACT

NH_3 is a common chemical used in various industries. Emission of NH_3 contaminated waste air to atmosphere without treatment has affected to human and environment. This research studied the removal of NH_3 in waste air by using adsorption methods. The adsorbent selected to apply for this work was rubber wood activated carbon and rubber wood biochar which were modified surface properties by H_2SO_4 for higher of NH_3 removal efficiency and reusable. This study was divided into four parts: preparation of rubber wood activated carbon with H_2SO_4 and H_3PO_4 and preparation rubber wood biochar, NH_3 treatment in waste air using adsorbents impregnated with H_2SO_4 and regeneration, Comparison study of NH_3 adsorption from waste air using acid modification rubber wood activated carbon and biochar, and modeling and optimization of ammonia treatment by acidic biochar using response surface methodology (RSM).

The production of rubber wood activated carbon by chemical activation from off-cut rubber wood (dimension of 1×1×1 cm) was studied for applying in waste air treatment system. Sulfuric acid (H_2SO_4) and phosphoric acid (H_3PO_4) at concentration rang of 20-80 % were chosen for using as chemical activation. H_3PO_4 activation got higher carbon yield than activated carbon deriving from H_2SO_4 activation but the properties of BET and micropore surface area were less. H_2SO_4 concentrations of 50% provided the highest BET and micropore surface area at 558 m^2/g and 466 m^2/g, respectively. From the advantage of H_3PO_4 and H_2SO_4 on rubber wood activated carbon production, the mixed acid between H_3PO_4 and H_2SO_4 was applied. The mixing composition of H_3PO_4 50 % w/w and H_2SO_4 40 % w/w was found more effectively in terms of yield, BET, and micropores surface. The optimum condition for activated carbon preparation was obtained from 400°C and 2 hour activation which provided 40% yield, 1200 m^2/g BET surface area and 700 m^2/g micropores surface areas and The optimum condition for biochar preparation was obtained from 500°C and 2 hour activation which provided 25% yield, 3 m^2/g BET surface area.

Rubber wood activated carbon (RWAC) and rubber wood biochar (RWB) were impregnated by 40-80% H_2SO_4 acid to get acidic adsorbents (RWACs and RWBs). Adsorption parameters of the fixed bed column with continuous mode were studied including waste air flow

rate, initial NH_3 concentration, and acid concentration using the adsorbents. The results demonstrated that increasing in NH_3 inlet concentration and waste air flow rate were decreased NH_3 adsorption efficiency. On the other hand, when increasing H_2SO_4 concentration, the NH_3 removal efficiency from waste air was increased. From the removal efficiency and breakthrough curve of the NH_3 adsorption, RWBs was slightly less removal efficiency and adsorption time than RWACs. The optimum condition for NH_3 removal from waste air using RWBs are 80% w/w H_2SO_4 which was provided the NH_3 removal efficiency reach to 90% for NH_3 inlet concentration 800 ppmv of waste air flow rate 2 l/min. By-product of the treatment is ammonium sulfate ($(NH_4)_2SO_4$) which is a good nitrogen fertilizer for plants.

Response surface methodology (RSM) is employed to optimize the process parameters of NH_3 adsorption. Based on the central composite design (CCD), quadratic model was developed to correlate the process variables to the response. The most influential factor on each experimental response was identified from analysis of variance (ANOVA). The values of adsorption time at 50% NH_3 removal efficiency obtained through the developed model are found to agree well with their corresponding experimental data (R^2= 0.9137). The optimum condition for the NH_3 adsorption by acidic rubber wood biochar is impregnation with 72% H_2SO_4 for removing NH_3 at 300 ppmv of inlet concentration on 2.1 l/min waste air flow rate to give the adsorption time to 219 min which was validated with experimental result.

Regeneration of the spent RWBs by desorption performing with leaching water was investigated at temperature of 30-100°C. The regenerated RWBs was re-soaked with 70% H_2SO_4 solution to refresh the activity of the acidic adsorbent and reused for NH_3 removal from waste air in the adsorption column for 3 times. The efficiency of this procedure was evaluated by breakthrough curve of the 1st and 2nd adsorption test. The breakthrough time of NH_3 adsorption by the 2nd regeneration was higher than 1st regeneration and provided the adsorption time to 9 h at 100°C temp of water. Furthermore, increasing the leaching temperature was also increasing adsorption time

The results from this research can be applied to NH_3 adsorption in industries were concern with NH_3 such as concentrated latex industry and fertilizer industry etc. for reducing the effect of NH_3 emission to human and environment in the atmosphere.

กิตติกรรมประกาศ

งานวิจัยนี้ได้รับทุนอุดหนุนการวิจัยจากเงินงบประมาณแผ่นดิน ประจำปี 2552 ขอขอบคุณบริษัท วู้ดเวอร์คแอดวานส์ จำกัด ที่ให้ความอนุเคราะห์ไม้ยางพาราในการผลิตถ่านกัมมันต์ ขอขอบคุณภาควิชาวิศวกรรมเคมี ที่ให้ความอนุเคราะห์สถานที่และครุภัณฑ์ในการทำวิจัย สุดท้ายขอขอบคุณบุคลากรในภาควิชาฯ ทุกท่านที่ให้ความช่วยเหลือในทุกๆ ด้าน จนกระทั่งงานวิจัยสำเร็จลุล่วงด้วยดี

คณะผู้วิจัย

CONTENTS

CONTENTS (Continued)

CONTENTS (Continued)

CONTENTS (Continued)

LIST OF TABLES

LIST OF TABLES (Continued)

LIST OF TABLES (Continued)

LIST OF TABLES (Continued)

LIST OF TABLES (Continued)

LIST OF FIGURES

LIST OF FIGURES (Continued)

LIST OF FIGURES (Continued)

LIST OF FIGURES (Continued)

CHAPTER 1

INTRODUCTION

1.1 Rational / Problem statement

The increase in atmospheric pollution caused by gases such as ammonia (NH_3) has been shown to be a global problem. Ammonia, a colorless, pungent, and corrosive gas, is one of the most abundant nitrogen-containing compounds in the atmosphere, after nitrogen (N_2) and nitrous oxide (N_2O) (Guo et al. 2004). Ammonia can be smelt at as low level as 50 ppmv in the air. Breathing levels of NH_3 at 50–100 ppmv can give rise to eye, throat, and nose irritation. The US Occupational Safety and Health Administration (OSHA) has set a limit of 50 ppmv over an 8-h work day or 40-h work week for ammonia vapor in ambient air. Ammonia gas is mainly used in the fertilizer industry as a raw material for the production of ammonium solution, nitrate and phosphate, calcium and sodium nitrate, ammonium sulphate, ammonium superphosphates, and urea (Rodrigues et al., 2007). This gas is also an important raw material in the manufacturing of concentrated rubber latex, nitric acid, synthetic urea, plastics, varnishes, fungicides, germicides, and disinfectants. It is employed as a coolant gas in refrigeration systems, in the pharmaceutical, tanning, and mirror silvering industries, as well as in the production of military explosives.

In concentrated rubber latex industry, ammonia gas is added in raw latex with concentration of 0.05-0.20% to preserve and protect from bacterial attack during the production steps. The latex will later be centrifuged (by a centrifuging machine) to get rid of water and other particles and produce concentrated latex as main product and skim latex as by product. Ammonia gas is more added to the concentrated latex product to preserve and prevent from rubber coagulating during storage and transportation. In the skim latex by product (0.3% ammonia) (De and White, 2001), the ammonia has to be repelled to atmosphere before adding sulfuric acid to produce skim rubber. Therefore, the releasing of ammonia gas from all production areas of concentrated rubber latex industry generates very bad smell in the work place. Ammonia is a noxious gas that can cause serious damage to human health and to the environment. Therefore, it is important to find ways to efficiently control the emission of this gas.

Many techniques, including catalytic decomposition, reaction of NH_3 with another gas, adsorption by solids, absorption with chemical solutions, and combustion have been used to eliminate NH_3 emissions or remove them from flue gases before emission into the atmosphere. Among these techniques, the removal of NH_3 using dry adsorbents such as activated carbons is a promising approach that has attracted much attention due to its simplicity and economy in configuration and operation (Guo et al. 2004). Fixed-bed downflow adsorption column is simply applied for waste gas adsorption system (Rodrigues et al., 2007 and Liang-hsing et al. 2006). Downflow is preferred because upflow at high rates might fluidize the particles, causing attrition and loss of fines (McCabe et al., 2005). Recently, the adsorption properties of the carbon adsorbent can be improved by impregnating it with acid or base solution depending on a kind of the adsorbate. In case of NH_3 adsorption, after using the H_2SO_4 impregnated activated carbon, $(NH_4)_2SO_4$ by product is generated at surface and pore of the carbon (Liang-hsing et al. 2006).

The symmetric adsorption time ($t_{1/2}$) of adsorbent is defined as the ideal time at a proportion of 50% NH_3 adsorption efficiency for an operating curve or breakthrough curve at $C_i/C_o = 0.5$ (McCabe et al., 2005). The operating curves can be plotted between NH_3 adsorption efficiency versus operating time of waste air flowed through the bed and the breakthrough curve can be also plotted between concentration and time for waste air leaving the bed. The $t_{1/2}$ can represent the adsorption capacity of the adsorbent and can be used for design of the adsorption column. At the higher $t_{1/2}$, the adsorption time was longer thus the absorbate was more adsorbed on the adsorbent and affected to higher adsorption capacity. Moreover, $t_{1/2}$ can be determined the length of pack bed by material balance (McCabe et al., 2005).

Activated carbon is the trade name for highly porous products, made of carbonaceous raw materials, with a large internal surface of 400-1600 m^2/g and a large pore volume of more than 30 $cm^3/100$ g. Activated carbon can be designed for adsorption of specific adsorbate by using appropriate precursor and optimizing the activation process conditions. Either physical or chemical activation method has been used for manufacturing from a wide variety of precursor materials (Srinivasakannan and Bakar, 2004). The main forms of activated carbon consist of 3 types such as: granular, powder, and extruded activated carbon. Granular activated carbon has a relatively larger particle size compared to powder activated carbon and

consequently, presents a smaller external surface. These carbons are therefore preferred for all absorption of gases and vapors as their rate of diffusion are faster. Granulated activated carbons (GAC) are used for water treatment, deodorization and separation of components of flow system.GAC is designated by mesh sizes such as 8×20, 20×40, or 8×30 for liquid phase applications and 4×6, 4×8 or 4×10 mesh. (http://en.wikipedia.org/wiki/Activated_carbon).

Biochar is a form of charcoal produced by thermal decomposition of biomass under limited or absence of oxygen supply at relative low temperatures know as pyrolysis (<700 ^{o}C) (Yu et al., 2011 and Duku et al., 2011). Biochar persists in the environment due to the reduction of microbial decomposition in biomass. Intuitively, generating the highest-value target products and adding value to residue products are both essential for sustainable biomass conversion to energy. The residual biochar would improve the overall economic efficiency of pyrolysis. Biochar has potential to apply in many works such as filter pyrolysis gas, base product for production of nitrogen fertilizer, activated carbon production. The biochar has been suggested as a farm fertilizer, a way to improve forest productivity, and a soil amendment (Dumroese et al., 2011). biochar has been an alternative adsorbent for adsorption in fixed-bed reactor. Impregnation with H_2SO_4 can be performed for modified the surface property to increasing the NH_3 adsorption efficiency.

Rubber wood (Hevea brasiliensis) is one of the main plantation crops in South East Asia with an estimated plantation area of 2.72 million hectares in Thailand. The rubber trees are cut after their latex yielding period of around 25 years and the wood would be utilized for many downstream processing. It is estimated that a gross yield of rubber wood per ha would be around 6.4 m^3. In the process of converting the raw logs rubber wood into the sawn timber, large amounts of residual biomass are generated. The rubber wood becomes raw material for sawmills and wood product factories, e.g., furniture, kitchenware, and wooden toys. The rubber wood residues comprise of small branches left in the plantation (54% of total biomass) and sawmill wastes (32%). On an annual basis, rubber wood residues in the forms of sawdust and wood off-cuts in the saw mills, small branches left in the farm, and wood residue in the factories are estimated at 4125 $\times 10^3$, 6917$\times 10^3$ and 833$\times 10^3$ t (Krukanot and Prasertsan, 2004). Rubber wood sawdust has been used to produce activated carbon with high surface area of 1496-m^2/g (Srinivasakannan and bakar, 2001) but the particle size is too small to apply as adsorbent in

adsorption column. So, production of adsorbent using off-cut rubber wood biomass from rubber wood industry is very interesting to make high value added of them.

Regeneration of spent adsorbent follow-up step after breakthrough in the air treatment system is necessary using desorption techniques to save cost of buying the new adsorbent. A variety of regeneration techniques, e.g. thermal regeneration, wet air oxidation, and chemical regeneration, are applied for exhausted adsorbent. And the one technique that interesting for regeneration the spent adsorbent is leaching with hot water at temperature up to 100^{o}C, which can provide the adsorption capacity more than 95% of the initial adsorbent (Berčič et al., 1996). Liang-hsing et al. (2006) found aqueous solution after steaming the activated carbon which was spent to adsorb NH_3 by acidic activated carbon that is ammonium sulfate solution ($(NH_4)_2SO_4$). This is the perfect fertilizer use for right at the farm.

Response surface methodology (RSM) is a collection of mathematical and statistical technique that can be used for studying the effect of several factors at different level and their influence on each other. Furthermore, it helps to obtain the surface plot that provides a good way for visualizing the parameter interaction. The objective of RSM is to optimize the response based on the factors investigated (Xiarchos et al., 2008). The central composite design (CCD), a design of experiments technique, was chosen to carry out the experiments at five levels respecting optimality criteria. The responses and the corresponding parameters were modeled and optimized using analysis of variance (ANOVA) to estimate the statistical parameters by means of RSM. The experimental design and optimization was generated using the Design-Expert program 8.0.6 trial version. The predicted optimum condition by RSM technique from the software was verified the result with the experimentation.

The aim of this research was an attempt to utilize off-cut rubber wood generated from sawing process for high surface area adsorbent development and evaluated the adsorption potential for NH_3 contaminated air treatment. Surface property of the activated carbon and biochar was modified using sulfuric acid to increase NH_3 adsorbing efficiency and evaluated the suitable adsorbent for NH_3 adsorption. The adsorbents were packed in the continuous down flow fixed-bed column system for NH_3 treatment. The NH_3 removal efficiency was determined according to several factors influencing the fixed bed performance and adsorption capacity. The feasibility and effectiveness of regenerating the spent activated carbon using hot water was

studied. RSM was applied to design for the experiments and find for optimum condition of the NH_3 adsorption from waste air in the fixed bed system. Three operating factors were chosen as independent variables, namely, the effects of H_2SO_4 concentration for impregnation on adsorbent, NH_3 initial concentration in waste air, and waste air flow rate. The symmetric adsorption time ($t_{1/2}$) was applied for the response of the adsorption data in the RSM solution to develop an empirical model. The advantage from this work are the reduction of NH_3 emission from industries, model formation and optimization of the NH_3 adsorption process, and the by product after regeneration of the spent adsorbent can be apply to produce fertilizer for planting.

1.2. Research Objective

1) To produce activated carbon and biochar from rubber wood off-cut and modified the adsorbent surfaces by chemical impregnation for NH_3 removal from waste air.
2) To compare the NH_3 treatment efficiency by using rubber wood activated carbon and biochar impregnated with H_2SO_4.
3) To study the NH_3 removal efficiency in packed bed system, find the optimum condition and regression model by RSM, and regenerate the used adsorbent by leaching with hot water and study for the reusing acidic adsorbents .

1.3 Scopes of Research Work

1) Activated carbon and biochar were produced and modified surface properties from rubber wood off-cut.
2) A chemical impregnation reagent for modified surface rubber wood activated carbon and biochar is H_2SO_4.
3) NH_3 simulated waste gas stream was generated by using NH_3 vapor from 25% NH_3 solution mixed with air stream and was be used for NH_3 adsorption in packed bed system.

4) Design of experiment set up and optimization condition of NH_3 adsorption determined by Design-expert software 8.0.6 trial version. RSM was applied to determine the model for predicted adsorption time in the NH_3 adsorption process by acidic rubber wood adsorbents.
5) Hot water was alternated for adsorbents defective regeneration and reusing for adsorption to twice again.

1.4 Expected Benefits

1) Improvement the adsorbents efficiency for NH_3 adsorption from waste air.
2) Value added of rubber wood biomass for solving the environmental problem.
3) The result from this work can be applied to NH_3 removal in waste air from concentrated rubber latex and other industries.
4) Modeling and optimization condition from RSM can be applied to predict the suitable condition for NH_3 adsorption by acidic adsorbents.

CHAPTER 2

CARBON ADSORBENTS

2.1 Activated carbon

Evaluation of waste biomass is getting increased attention in all over the world as it is renewable, widely available, cheap, and environmental friendly. One of the effective uses of waste biomass is the production of activated carbon by thermo-chemical conversion. The activated carbon has been produced from variety of biomass i.e., wood, rice husk, cellulose, lignin, coconut shells and palm shells, and has surface areas of 300 to 1200 m^2/g with average pore diameters of 10 to 60 Å. There are many reports on the production of activated carbon to use as adsorbent for removing hazardous compounds from industrial waste gases or wastewater, and in catalysis as support for catalyst. There are two basic processes to activate the carbon materials; physical and chemical. The effect of different chemical reagents on the production and quality of activated carbon has been studied extensively by different researchers. There are two important advantages of chemical activation in comparison to physical activation. One is the lower temperature in which the process is accomplished. The other is that the global yield of the chemical activation tends to be greater since burn off char is not required. (Singh et al., 2007)

Chemical activation processes have been carried out with acidic reagents i.e. $ZnCl_2$, H_3PO_4, HCl, and H_2SO_4 or with basic reagents KOH, K_2CO_3, NaOH, and Na_2CO_3 (Karagöz et al., 2008). Among the numerous dehydrating agents, sulfuric acid (H_2SO_4) and phosphoric acid (H_3PO_4) in particular have been widely used as chemical agent in the preparation of activated carbon. Knowledge of different variables during the activation process is very important in developing the porosity of carbon sought for a given application.

Chemical activation by H_2SO_4 improves the pore development in the carbon structure, and because of the effect of chemicals, the yields of carbon are usually high (Singh et al., 2007). Sulfuric acid activation has been applied on a wide variety of cellulosic precursors such as apricot stone (Demirbas et al., 2008), oil-palm stone (Guo and Lua, 1999), sunflower oil

cake (Karagöz et al., 2008), palm shells (Guo et al., 2004), Tamarind wood (Singh et al., 2007), olive cake (Cimino et al., 2005), sewage sludge and discarded tyres (Rozada et al., 2005), and Euphorbia rigida (Gerçel et al., 2006).

Traditional method of chemical activation by H_3PO_4 consists of the raw material with H_3PO_4 solution followed by pyrolysis in inert atmosphere at temperatures between 350 and 600°C (Girgis et al., 2007 and Budunova et al., 2006).This reagent induces important changes in the pyrolytic decomposition of the lignocellulosic materials since it promotes depolymerization, dehydration and redistribution of constituent biopolymers. It can increase the yield by favoring the conversion of aliphatic to aromatic compounds at temperatures lower than when heating in the absence of additive (Gómez-Serrano et al., 2005). H_3PO_4 has been applied on a wide variety of cellulosic precursors such as coconut shell, peach stones, cotton stalks, shells of nuts like almond, pecan, English walnut, black walnut and macadamia nut (Srinivasakannan and Bakar, 2004).

In general, it can be classified either as single-stage or two-stage activation process carried out either in an inert medium or a self-generated atmosphere. The efforts made towards developing a high surface area carbon with desired pore size by optimizing the process parameters such as the activation time, activation temperature and impregnation ratio (Srinivasakannan and Bakar, 2004). Table 2.1 and 2.2 summarizes various works with reference to the experimental conditions, quality of the product, and their critical findings of activated carbon which was activated by H_2SO_4 and H_3PO_4, respectively.

Table 2.1 Summary of earlier research works on activated carbon production from various material using sulfuric acid

References	Material	Experimental condition	Quality of the product
Guo and Lua, 1999	Oil-palm stone	- Oil palm stone was crushed and sieved to the particle sizes 1-2 mm. - 10 g of stone was impregnated at room temperature with H_2SO_4 of various concentrations (5, 10, 20, and 30%) for 12-72 h. - The impregnated samples were carbonized under N_2 (150 cm^3/ min) at 600°C for 2 h. - The resulting chars were activated with CO_2 (100 cm^3/min) at 800 °C for 1 h to produce final activated carbon products.	- BET surface area of the sample increased when the H_2SO_4 impregnation time increased from 12-24h. - Increasing in H_2SO_4 concentration can increase BET, micropore surface area, and pore volume of the activated carbon.
Guo et al., 2005	Palm shells	- Palm shells were dried, crushed, and sieved to particle size of 1.0-2.0 mm. - Palm shell 10 g was impregnated with 200 ml H_2SO_4 at concentration of 5-40% and room temperature (298 K) for 24 h. - The carbon was dried overnight at 383 K And activated under nitrogen stream (150 cm^3/min) at 573-973 K for 2h.	- BET surface area is increased by increasing in temperature (573 – 973 K) and concentration of H_2SO_4 (5-30%). - At high H_2SO_4 concentration of 40%, BET and micropore surface area is decreased.

Table 2.1 Summary of earlier research work on activated carbon production from various material using sulfuric acid (conc.)

References	Material	Experimental condition	Quality of the product
Gerçel et al., 2007	Euphorbia rigida	- Euphorbia rigida was impregnated with 50 % H_2SO_4 for 24 h and activated at 850 ^{o}C for 30 min by heating rate of 10 ^{o}C/min. - After the cooling, the activated carbon was washed with de-ionized water and dried at 105 ^{o}C.	- The Specific surface area was 741.2 m^2/g and most of the material (90%) consists of microspores structure. - Methylene blue adsorption of the activated was 114.45 mg/g
Singh et al., 2008	Tamarind wood	- The washed Tamarind wood was cut into 50.8 mm × 76.2 mm, dried 20 days in sunlight, and soaked in concentrated sulfuric acid at room temperature and pressure. - The mixture of H_2SO_4 and wood was heated at 200^{o}C and washed until acid free. - Finally, the carbon was dried at 60 ^{o}C and crushed in a small mill for 1 h.	- The BET surface area of this activated carbon is 612 m^2/g and total pore volume of 0.508 cm^3/g - Adsorption capacities of lead (II) in the activated carbon is 134.22 mg/g

Table 2.1 Summary of earlier research work on activated carbon production from various material using sulfuric acid (conc.)

References	Material	Experimental condition	Quality of the product
Karagöz et al., 2008	Sunflower oil cake	- Sun flower oil cake was immersed with H_2SO_4 at impregnation ratio of 0, 0.85, and 1.90 by continuous agitation for 24 h. - The mixture was dried at 110 ^{o}C for 24 h and carbonized at 600 ^{o}C under nitrogen flow of 30 mL/min at heating rate of 5 ^{o}C/min. - The sample was several washed with hot water and cold water to remove residual chemical and make neutral pH was dried at 110 ^{o}C for 24 h	- The specific surface area at impregnation ratio 0, 0.85 and 1.90 is 8.8, 240.02 and 114.77 m^2/g, respectively. - Adsorption of methylene blue on the activated carbon at impregnation ratio 0.85 is 16.43 mg/g.
Demirbas et al., 2008	Apricot stone	- Apricot stone was air dried, crushed, and screened to sizes of 0.5-2.0 mm. - Apricot stone of 100 g was impregnated with concentrated H_2SO_4 and activated in hot air oven at 250 ^{o}C for 24 h. - The carbonized material was washed with distilled water to remove free acid and increase to pH 6. - The carbon was dried at 105 ^{o}C and sieved to particle size of 0.8-1.6 mm.	- Bulk density, ash content, moisture, solubility in water, solubility in acid, surface area, and iodine number of activated carbon were determined as 0.46 g/cm^3, 2.28%, 7.26%, 0.65%, 1.22%, 560 m^2/g and 486 mg/g, respectively. - The maximum dye adsorption capacity on the activated carbon at 50 ^{o}C was 221.23 mg/g.

Table 2.2 Summary of earlier work on activated carbon using phosphoric acid activation (Srinivasakannan and Bakar, 2004)

Reference	Material	Experimental conditions	Quality of the product
Toles et al. 1988	Almond, pecan, walnut, macadamia shell	Nitrogen as well as self-generated atmosphere; Single as well as two-stage; S.C. Temp. - 170^{o}C; S.C.Time - 0:5 h; A.Temp.- 450^{o}C; A.Time -1 h.	S.A. ranging from 1100 to 1600 m^2/g covering var ious methods of activation.Activation in self generated atmosphere was found to give higher surface area when compared to inert activation.
Girgis and Ishak 1999	Cotton stalk	Self-generated atmosphere; Predrying followed by activation, Predrying - 110^{o}C; A.Temp. - 500^{o}C; A.Time - 2 h; I.R. - 0.5–2.1; H.R. - 5^{o}C.	S.A. of 1032 m^2/g.Predrying step is found to be important.High S.A.obtained at I.R.of 1.6 with 65% concentration.
Girgis et al. 2002	Peanut hull	Self-generated atmosphere; Single stage; A.Temp. - 500^{o}C; A. Time - 3 h or 6 h; I.R: 0.5 - 1.6.	S.A. of 1177 m^2/g with I.R. - 1, A. Time - 3 h. Porosity developed as function of increased I.R. reached maximum at I.R. - 1, where the product is essentially micro-porous with high S.A.
Ahmedna 2000	Sugarcane bagasse	Nitrogen atmosphere; two-stage activation; 2 h pre-soaked samples; S.C. Temp. - 170^{o}C; S.C. Time - 0:5 h; A.Temp. - 450^{o}C; A.Time - 1 h.	S.A. of 1200 m^2/g.A micro-pore S.A.of 78% obtained.

Table 2.2 Summary of earlier work on activated carbon using phosphoric acid activation (Srinivasakannan and Bakar, 2004) (conc.).

References	Material	Experimental conditions	Quality of the product
Garcia et al. 2001	Apple pulp	Argon atmosphere; predrying at 110°C for 4 h; A.Temp. - 450°C; A. Time - 1 h; I.R. - 0.2 - 1.5; H.R. - 10°C/min.	S.A. of 1022 m^2/g at I.R. of 0.85. At low I.R. (<43) phosphoric acid promotes the micropores whereas at intermediate and high I.R. increase in pore diameter with increase in I.R.
Dastgheib Rockstraw 2001	Pecan shell	Self-generated atmosphere; three-stage activation; liquid-stage activation at 160°C followed by primary activation at 160–210°C followed by secondary activation 300–500°Cfor 30 min I.R. of 3.	S.A. of 1071 m^2/g.Increase in S.A.until secondary activation temperature of 450°C and reduction in S.A. above 450°C.
Vernersson et al. 2002	Arundo donax cane	Self-generated atmosphere; single stage; A.Temp. - 400 - 550°C; A. Time - 1 h; I.R. - 1.5 - 2.5; H.R. - 3°C/min.	S.A. of 1333 m^2/g at I.R. of 2 at zero activation time. Reduction in surface area with increase in activation time.Pore volume increase with temperature but at the expense of micro-pore volume.
Diao et al. 2002	Grain sorghum	Nitrogen atmosphere; two-stage and three-stage; in two-stage predrying at 100°C followed by activation at 450 - 700°C. In three-stage process carbonization at 300°C for 15 min followed by impregnation and activation between 400°C and 600°C.	Two-stage S.A. of 528 m^2/g and three-stage 1522 m^2/g at 500°C with I.R. of 0.76.

Table 2.2 Summary of earlier work on activated carbon using phosphoric acid activation (Srinivasakannan and Bakar, 2004) (conc.).

References	Material	Experimental conditions	Quality of the product
Garcia et al. 2002	Apple pulp	Argon atmosphere; two stage; predried for 4 h at 110°C; A.Temp. - 450°C; A. Time - 1 h; I.R. - 0.21–1.5; H.R. - 10K/min.	S.A. of 1022 m^2/g at I.R. of 0.85. Higher temperature and longer times lead to reduction in S.A. and pore volume.As I.R.is increased the micro-pores progressively widen towards wider pores.
Kirubakaran et al.1991	Coconut shell	Nitrogen atmosphere; two stage; predried at 100°C; A.Temp. - 400–600°C; A. Time - 2 h; I.R. - 1–2.	S.A. in excess of 1000 m2/at I.R. of 1.5 at 500°C.
La 2001	Acorns, olive seeds	Self-generated atmosphere; single stage, A.Temp. - 400°C, 650°C, 800°C, A.Time - 1 h.	Highest methylene blue no.of 130 mg/g obtained at A.Temp.of 800°C.
Ruiz Bevia et al.1984	Almond shell	Nitrogen atmosphere; two-stage; predrying at 110°C for 24 h; A.Time - 2 h; A.Temp. - 600°C, 700°C; I.R. - 0.2.	Iodine number of 176 at 600°C.

(S.A.—surface area; S.C. Temp.—semi-carbonization temperature, S.C. Time—semi-carbonization time; A. Temp.—activation temperature; A. Time—activation time;I.R.—impregnation ratio; H.R.—heating rate.

2.2 Biochar (http://www.csiro.au/files/files/poei.pdf)

It is important to note that there is a wide variety of char products produced industrially. For applications such as activated carbon, char may be produced at high temperature, under long heating times and with controlled supply of oxygen. In contrast, basic techniques for manufacture of charcoal (such as clay kilns) tend to function at a lower temperature, and reaction does not proceed under tightly controlled conditions. Traditional charcoal production should be more accurately described as 'carbonisation', which involves smothering of biomass with soil prior to ignition or combustion of biomass whilst wet. Drying and roasting biomass at even lower temperatures is known as 'torrefaction'.

A charred material is also formed during 'gasification' of biomass, which involves thermal conversion at very high temperature (800°C) and in the partial presence of oxygen. This process is designed to maximize the production of synthesis gas ('syngas'). Materials produced by torrefaction and gasification differ from biochar in physico-chemical properties, such as particle pore size and heating value and have industrial applications, such as production of chemicals (methanol, ammonia, urea) rather than agricultural applications. In order to differentiate biochar from charcoal formed in natural fire, activated carbon, and other black carbon materials, the following list of terms aims to better define the different products. The differences, however, are relatively subtle since all products are obtained from the heating of carbon-rich material.

Char: the solid product arising from thermal decomposition of any natural or synthetic organic material. Examples are char from forest fire and soot resulting from the incomplete combustion of fossil hydrocarbon.

Charcoal: the carbon produced from the thermal decomposition of wood and related organic materials, mainly for use as an urban fuel for heating and cooking, but also traditional uses as soil amendment or control of odor. Temperatures in traditional kilns approach 450-500°C, which is similar to that of industrial pyrolysis but with lower yields: conversion of feedstock dry mass may be as low as 10 % compared to 35% using more formal production technology. Also, all heat as well as gaseous and liquid co-products are lost during the combustion process.

Activated carbon: manufactured by heating carbonaceous material at a high temperature (above 500°C) and over long (>10 hours) periods of time. The resulting material is characterised by a very high adsorptive capacity. It is not used as a soil amendment but has been applied for cleansing processes, such as water filtration and adsorption of gas, liquid or solid contaminants.

Black carbon: a general term that encompasses diverse and ubiquitous forms of refractory organic matter that originate from incomplete combustion. The diversity of burning conditions results in black carbon occupying a continuum of material.

Biochar is a name for charcoal when it is used for particular purposes, especially as a soil amendment. Biochar is a fine-grained and porous substance, similar in its appearance to charcoal produced by natural burning. Biochar is produced by the combustion of biomass under oxygen-limited conditions. The definition adopted by the International Biochar Initiative (IBI) furthermore specifies the need for purposeful application of the material to soil for agricultural and environmental gain. The term biochar was originally associated with a specific type of production, known as 'slow pyrolysis'. In this type of pyrolysis, oxygen is absent, heating rates are relatively slow, and peak temperatures relatively low. However, the term biochar has since been extended to products of short duration pyrolysis at higher temperatures known as 'fast pyrolysis' and novel techniques such as microwave conversion.

This is important since there is currently a much greater amount of research for char than for biochar. Biochar produced in association with bioenergy generation may be more applicable in some countries than others, depending on economic circumstance, political priorities, technology and infrastructure. The quality of biochar and char that makes it attractive as a soil amendment is its highly porous structure, potentially responsible for improved water retention and increased soil surface area. Addition of biochar to soil has also been associated with increased nutrient use efficiency, either through nutrients contained in biochar or through physico-chemical processes that allow better utilisation of soil-inherent or fertiliser-derived nutrients. Importantly, it is the apparent biological and chemical stability that allows biochar to both act as a carbon sink, as well as provide benefits to soil that are long-lived.

Using pyrolysis to turn sustainably produced biomass into a recalcitrant substance that is decomposed at a much slower rate, constitutes both a tool for carbon

sequestration and avoided emission. It is argued that sequestration of carbon in biochar allows for a much longer storage time compared with other terrestrial sequestration strategies, such as a forestation

2.3 Rubber wood (Hevea brasiliensis)

Thailand produces about one-third of the world's natural rubber. Out of 2.72 million hectares of Southern, 1.67 million hectares are rubber plantations, which make southern Thailand is the single largest rubber plantation region in the world. As the economic life of the rubber trees is 25–30 years, about 3–4% of the rubber growing area is cut down for replanting annually. Over its life time, the rubber trees store solar energy in the form of biomass, which weighs more than 180 t/ha. The rubber wood becomes raw material for sawmills and wood product factories, e.g., furniture, kitchenware and wooden toys. The rubber wood residues comprise of small branches left in the plantation (54% of total biomass) and sawmill wastes (32%). On an annual basis, rubber wood residues in the forms of sawdust and wood off-cuts in the sawmills, small branches left in the farm and wood residue in the factories are estimated at 4125 $\times 10^3$, 6917$\times 10^3$ and 833$\times 10^3$ t, respectively (Krukanont and Prasertsan., 2003). A proximate and ultimate analysis of the rubber wood is reported in Table 3.

Srinivasakannan and Bakar (2004) studied the activated carbon production from carbonaceous rubber wood sawdust using phosphoric acid. Efforts are made towards developing a high surface area activated carbon from by a two-stage activation process. The operating parameters were optimized based on product yield and iodine number. Semi-carbonization at 200°C for 15 min followed by activation at 500°C for 45 min with impregnation ratio of 1:5. The iodine number is 1096 mg/g. The corresponding BET surface area of the production condition were 1496 m^2/g with the product yield of 35% and acid from activation recovery is 90%

Kumar et al. (2005) studied the production of activated carbon from rubber wood sawdust for adsorption of Bismark Brown dye. They used 3 processes to produce the activated carbon. Process No.1 was carbon impregnation with phosphoric acid of 0.45 IR (g phosphorous: g precursor) and activated in fixed bed at 400 °C for 1 h. Process No.2 was activation in a fluidized bed reactor at 750 °C for 1 h with steam flow rate of 4 mL/min. Process No.3 was the

combination of the impregnation with phosphoric and fluidized bed process. The results were iodine number of 1052, 765 and 835 mg/g, methylene blue number of 375, 255 and 255 mg/g, and BET surface area of 954, 1092 and 822 m^2/g, respectively.

Table 2.3 Proximate and ultimate analysis of the rubber wood

Proximate analysis	
Moisture, %	45.00
Ash, %	1.59
Volatile Matter, %	45.70
Fixed Carbon, %	7.71
Ultimate analysis	
Carbon, %	25.58
Hydrogen, %	3.91
Oxygen, %	24.28
Nitrogen, %	0.14
Sulfur, %	0.02
Chlorine, %	0.01
Ash, %	1.60
Moisture, %	45.00

Source: Biomass, Biomass Clearing House (Energy for Environment Foundation, 2007)

Kalavathy et al. (2005) produced activated carbon from rubber wood sawdust for kinetic and isotherm investigation of Cu(II) adsorption. Procedure for the production was sawdust drying and mixed with phosphoric acid at a weight ratio of 1:2 and soaking for 24 h. The mixture was dried at 110 °C for 1.5 h and carbonized at 400 °C for a period of 1 h. Characteristics of the activated carbon product was BET surface area 1673.86 m^2/g, iodine number 794.53 mg/g and methylene blue number 255 mg/g. Adsorption capacity of Cu(II) with the rubber wood sawdust activated carbon is 5.729 mg/g.

CHAPTER 3

AMMONIA ADSORPTION

3.1 Ammonia adsorption technique

Ammonia (NH_3), a colorless, pungent, and corrosive gas, is one of the most abundant nitrogen-containing compounds in the atmosphere, after nitrogen (N_2) and nitrous oxide (N_2O). The global production of NH_3 by human activities (e.g., combustion of nitrogen-containing biomass and fossil fuels and use of NH_3-based fertilizers) is estimated to be 45.0 million tons per year. NH_3 can be smelt at as low level as 50 ppmv in the air. Breathing levels of 50–100 ppmv NH_3 can give rise to eye, throat, and nose irritation. The US Occupational Safety and Health Administration (OSHA) has set a limit of 50 ppmv over an 8-h work day or 40-h work week for ammonia vapor in ambient air.

Many techniques, including catalytic decomposition, reaction of NH_3 with another gas, adsorption by solids, and staged combustion processes have been used to eliminate NH_3 emissions or remove them from flue gases before emission into the atmosphere. Among these techniques, the removal of NH_3 using dry adsorbents such as activated carbons is a promising approach that has attracted much attention due to its simplicity and economy in configuration and operation. Activated carbon is one of the adsorbents most widely used for various gas separation and purification processes, owing to its distinguished properties such as extensive pore surface area, developed internal pore structure, and unique surface chemistry. The inherent nature of the precursor and conditions employed during adsorbent preparation determine the textural, chemical, and adsorptive properties of the final product of activated carbon. Commercial activated carbons can be manufactured from a variety of carbonaceous precursors including lignite and coal, peat, wood, and coconut shell. Since the price of commercial activated carbons has dropped continually over the past decade, interesting is growing in the use of other low-cost and abundantly available lingo-cellulose materials as precursors for activated carbon preparation (Gue et al., 2005).

In adsorption processes, one or more components in gas or liquid stream are adsorbed on surface of solid adsorbent and separated to accomplish the processes. In commercial processes, the adsorbent is usually in the form of small particles in a continuous fixed bed column. The flow of fluid is passed through the bed of adsorbents solid particle to separate impurity components from the fluid stream. When the bed is almost saturated, the system is stopped and regenerated by thermally or other desorption processes. The adsorbed material (adsorbate) is recovered and used for another cycle of adsorption. Applications of adsorbent particles in gas-phase adsorption include removal of water from hydrocarbon gases, sulfur compounds from natural gas, solvents from gases, and odors from air.

Rodrigues et al. (2007) studied the adsorption of NH_3 in the fixed bed of coconut shell activated carbon. They considered the initial concentrations of ammonia (C_0) and the bed temperature (T_L) on the adsorption by activated carbon. The results showed that within the NH_3 concentration range of 600–2400 ppm, adsorption capacity varied from 0.6 to 1.8 mg NH_3/g carbon at 40°C, from 0.2 to 0.7 mg NH_3/g carbon at 80°C and from 0.15 to 0.35 mg NH_3/g carbon at 120°C. These numbers highlight the tendency toward a lower adsorption capacity with increasing in temperature. Mass of the bed had no significantly influence over the adsorption capacity.

Asada et al. (2006) examined the effect of NH_3 adsorption in aqueous solution for bamboo charcoal carbonized at 400, 700 and 1000°C, and commercial activated carbon. Beside, they were also examining the change of NH_3 adsorption in aqueous solution by treatment of each adsorbent sample with diluted sulfuric acid. Bamboo charcoal carbonized at 400°C and treated with diluted sulfuric acid was the most effective for removing ammonia from the aqueous solution.

Even though activated carbons are considered as good and efficient adsorbents during initial uptake of ammonia, their applications for ammonia removal are limited. This is caused by weak adsorption forces which are employed in the removal process. NH_3 is a small molecule with a width of about 3 Å and at ambient conditions it can be strongly adsorbed only in pores similar in size to its diameter. Since the majority of an average activated carbon pore is in the range of 10-20 Å, only the small fraction of adsorbent surface is utilized. NH_3 easily desorbs from the surface when, for instance, the adsorbent is purged by air. All of the above indicate that

in order to remove ammonia, specific forces must be employed such as hydrogen bonding, acid/base interactions, complexation, precipitation, etc. Thus, many studies focus on texture and surface modifications of the solids to improve their adsorption capacity for ammonia retention (petit et al., 2007).

Canals-Batlle et al. (2007) improved the performance of activated carbon using carbonaceous adsorbents prepared from sewage sludge-based precursors and impregnated with Fe for NH_3 adsorption at ambient temperature. The preparation of highly porous adsorbents from these precursors has been described. The sludge was treated at 700°C under nitrogen flow. The paralyzed precursors were physically mixed (1/1 ratio) with alkali (either KOH or NaOH) and then activated at 700°C in a nitrogen flow (500 ml/min), using a 5°C/min heating rate and 30 min dwelling time. The process was completed by thoroughly washing off the activation by-products with HCl and H_2O, successively. The result, the high Fe content (>5 wt %) and low pH value of sewage sludge seem to balance its relatively modest porosity development (i.e., compared to the activated materials). The acid-base interaction mechanism also gives water (humidity) a critical role in the case of AC supporting metals. The effect of pre-humidification on the behavior of the sludge-derived adsorbents is not so crucial. Nevertheless, a mechanism of NH_3 removal on the surface of the activated sludge precursors based on coordination chemistry may not be eliminated.

Guo et al. (2005) investigated about adsorption of NH_3 onto activated carbons prepared from palm shells impregnated with sulfuric acid (H_2SO_4). The effects of activation temperature and acid concentration on pore surface area development were studied. Activation temperature and acid concentration were two important factors in surface area development. Increasing the activation temperature from 573 to 973 K or increasing the H_2SO_4 concentration from 5 to 30% increased the BET surface area progressively. The relatively large surface areas of the activated carbons prepared point to their potential applications in effective gas-phase adsorption. However, use of excessive H_2SO_4 (e.g., 40%) would cause over gasification of the palm-shell precursor, resulting in decreases in both BET and micropore surface areas. Adsorption tests at 323 K showed that the amounts of NH_3 adsorbed onto the chemically activated carbons, unlike those prepared by CO_2 thermal activation, were not solely a function of the specific surface

areas. Further adsorption and desorption tests also suggested combined physisorption and chemisorption of NH_3 for the chemically activated carbons.

Liang-hsing et al. (2006) employed activated carbon impregnated with H_2SO_4 (H_2SO_4/C) for removing ammonia from waste gas. The activated carbon was packed in an adsorption reactor to form a fixed bed. In order to obtain H_2SO_4/C with various levels of loadings, the concentration of H_2SO_4 solution was varied from 0 to 16 moles. The result shown that, an adsorbent with the highest absorption capacity was obtained using 11.3 mole H_2SO_4.

The mechanism by which the NH_3 was removed from the gas was speculated to consist of four steps in series: (1) NH_3 transport from waste gas stream to the external surface of the activated carbon support; (2) the adsorbed NH_3 diffuse to the pore mouth of the activated carbon; (3) NH_3 molecule diffuses through a gas-liquid interface and dissolves in the aqueous H_2SO_4 layer (Equation (3.1)); (4) aqueous NH_3 reacts with H_2SO_4 to form $(NH_4)_2SO_4$ (Equation (3.2)) which remains on the adsorbent. The reactive adsorption of NH_3 with H_2SO_4 can be shown as following equations:

$$NH_{3(g)} + H_2O_{(l)} \rightarrow NH_4OH_{(aq)} \qquad (3.1)$$

$$2NH_4OH_{(aq)} + H_2SO_{4(aq)} \rightarrow (NH_4)_2SO_{4(aq)} + 2H_2O_{(l)} \qquad (3.2)$$

Fortier et al. (2008) investigated the adsorption capacity of $ZnCl_2$-impregnated activated carbon (AC) for NH_3 removal. The result was reported in terms of stoichiometric ratio of reaction (NH_3 per $ZnCl_2$). Compared to the ratio obtained under dry conditions, the ratio is higher under humid conditions or increased NH_3 concentrations. The linear increase of the NH_3 capacity with increasing loading of $ZnCl_2$ breaks down at about 3.5 mmol $ZnCl_2$/g AC. This behavior was explained in terms of preferential adsorption of a monolayer of salt followed by aggregation of the impregnate once a monolayer is completed.

Huang et al. (2008) studied the influence of surface acidity of activated carbon on adsorption of ammonia. They modified coconut shell-based activated carbon by various acids at different concentrations. There were five different acids employed to modify the activated carbon, which included nitric acid, sulfuric acid, hydrochloric acid, phosphoric acid, and acetic acid. Experimental results showed that adsorption amounts of NH_3 on the modified activated

carbons were all enhanced. The NH_3 adsorption amounts on various activated carbons modified by different acids are in the following order: nitric acid > sulfuric acid > acetic acid ≈ phosphoric acid > hydrochloric acid.

3.2 Regeneration of NH_3 saturated adsorbents

3.2.1 Regeneration by steaming method

Liang-hsing et al. (2006) used steam for regeneration the spent adsorbent after adsorb NH_3 by acidic activated carbon which was impregnated with H_2SO_4. They employed low pressure steam at 103-105°C for washing $(NH_4)_2SO_4$ crystal that is the by-product from reaction between NH_3 and H_2SO_4 on adsorbent surface. The adsorption and regeneration cycle was repeated for 3 times to assess the re-usability of acidic activated carbon. The result show that, after the first regeneration, NH_3 removal capacity was decreased by 7% but remained rater constant in the subsequent regeneration cycles. After 3 times of regeneration, the adsorbents were unloaded and BET surface area measurement indicated that the surface area of activated carbon support was about 90% that of the fresh activated carbon. It was speculated that the surface area losses would be minimal in the subsequent regeneration cycle.

3.2.2 Regeneration by electrochemical method

Lei et al. (2009) was investigated with the objective of removing ammonia from water harmlessly by zeolites and reusing the regeneration solution in an undivided electrochemical cell assembled with a Ti/IrO_2–Pt anode and a Cu/Zn cathode. With NaCl as a supporting electrolyte, the conversion rate of ammonia adsorbed by the zeolites into nitrogen gas was more that 96%, while the conversion rate to nitrate was less than 4%; no ammonia or nitrite was detected in the solution after electrolysis. More nitrate was produced when the amount of NaCl was raised. The regeneration solution can be repeatedly reused over a long period of time with the proper amount of NaCl added to the solution. Even after the solution was reused for five

times, it could still completely regenerate the zeolites, saving both water resources and the chemical reagent.

3.2.3 Regeneration by leaching with hot water method

Berčič et al. (1996) was studied the adsorption/desorption of phenol from aqueous solutions at high temperatures on activated carbon. The adsorption capacities were determined by the semicontinuous desorption experiments carried out in a fixed bed adsorber, which was operated in liquid-full mode at a pressure of 25 bar and at temperatures up to 190 °C. It was found that in the range of phenol concentrations from 0.005 to 30 g/L. By hot water regeneration (180 °C for 150 min at a flow rate of 4.75 mL/h), 95% recovery of initial adsorption capacity of activated carbon was obtained. It is also demonstrated that the regeneration by leaching with hot water method can be used as an alternative way to regenerate spent activated carbon.

CHAPTER 4

RESPONSE SURFACE METHOLOLOGY AND OPTIMIZATION

4.1 Design of experiment (DOE)

DOE is a preplanned approach for finding cause and effect relationships. The purpose of statistically designing an experiment is to collect common relationship between various factors affecting the process towards finding the most suitable conditions. It is essential that an experimental design methodology be economical for extracting the maximum amount of complex information, a significant reduction in experimental time, saving both material and personnel cost. Central composite design (CCD), Box-Behnken and Doehlert designs (BBD) are among the principal response surface methodologies used in experimental design which the CCD has been widely used as the experimental design. This method is suitable for fitting a quadratic surface and it helps to optimize the effective parameters with a minimum number of experiments, and also to analyze the interaction between the parameters. The CCD consists of a 2^k factorial runs with 2^k axial runs and n_0 center runs. In CCD each variable is investigated at two levels and as the number of factors, k, increases the number of runs for a complete replicate of the design increases rapidly. This kind of design provides equally good predictions at points equally distant from the center, a very desirable property for Response surface methodology (RSM) (Anupam et al., 2011).

4.2 Response surface methodology (RSM)

RSM is a collection of statistical and mathematical methods that are useful for modeling and analyzing the engineering problems. In this technique, the main objective is to optimize the response surface that is influenced by various process parameters. RSM also quantifies the relationship between the controllable input parameters and the obtained response surfaces.

The design procedure for RSM is as follows:

(i) Performing a series of experiments for adequate and reliable measurement of the response of interest.

(ii) Developing a mathematical model of the second-order response surface with the best fit.

(iii) Determining the optimal set of experimental parameters that produce a maximum or minimum value of response.

(iv) Representing the direct and interactive effects of process parameters through two and three-dimensional (3-D) plots.

If all variables are assumed to be measurable, the response surface can be expressed as follows:

$$y = f(x_1, x_2, x_3, ..., x_k) \tag{4.1}$$

where y is the answer of the system, and x_i was the variables of action called factors.

The goal is to optimize the response variable (y). An important assumption is that the independent variables are continuous and controllable by experiments with negligible errors. The task then is to find a suitable approximation for the true functional relationship between independent variables and the response surface (Aslan, 2008).

4.3 Building empirical model

In the first step of RSM, a suitable approximation is introduced to find true relationship between the dependent variable and the set of independent variables, that is, the single-response modeled using the RSM correspond to independent variables. Then a mathematical model in the form of a second-order polynomial is formed to predict the response as a function of independent variables involving their interactions. Generally the behavior of the system is explained by the following quadratic equation.

$$Y = b_0 + \sum_{i=1}^{n} b_i x_i + \sum_{i=1}^{n} b_{ii} x_{ii}^2 + \sum b_{ij} x_i x_j \tag{4.2}$$

where Y is the predicted response, b_0 the offset term, bi the linear effect, b_{ii} the squared effect, b_{ij} the interaction effect and x_i and x_j represent the coded independent variables. In this work a second order polynomial equation was obtained using the natural independent variables as below:

$$Y = b_0 + b_1X_1 + b_2X_2 + b_3X_3 + b_{11}X_{11}^2 + b_{22}X_{22}^2 + b_{33}X_{33}^2 + b_{12}X_1X_2 + b_{13}X_1X_3 + b_{23}X_2X_3 \quad (4.3)$$

Multiple regression analysis technique was used to evaluate the coefficient of the model. In much RSM work it is convenient to transform the natural variables to code variables (x_i) which are usually defined to be dimensionless with mean zero and the same spread or standard divioation For statistical analysis, the experimental variables X_i have been coded as x_i according to the following Equation (4.4).

$$x_i = \frac{(X_i - X_0)}{\Delta X_i} \quad (4.4)$$

where x_i is the coded value (dimensionless) of the i^{th} independent variable, X_i is the natural value of the i^{th} independent variable, X_0 is the X_i at the center point, and ΔX_i is the step change value of the real variable i.

4.4 Statistical analysis of the experimental data (Steppan *et al.*, 1998)

Statistical methods should be used to analyze the data so that results and conclusions are objective rather than judgmental in nature. If the experiment has been designed correctly and if it has been performed according to the design, the statistical methods required are not elaborate. There are many excellent software package designed to assist in data analysis, and many of these programs used in step 4 to select the design provide a seamless, direct interface to the statistical analysis and interpretation. Because many of the questions that the experimenter wants to answer can be cast into the hypothesis-testing framework, hypothesis testing, and confidence interval estimation procedures are very useful in analyzing data from a designed experiment.

It is also usually very helpful to present the results of many experiments in term of an empirical model, that is, an equation derived from the data that expresses the relationship between the response and the important design factors. Residual analysis and model adequacy checking are also important analysis techniques. Remember that statistical methods cannot prove that a factor has a particular effect. They only provide guidelines as to reliability and validity of results. Properly applied, statistical methods do not allow anything to be proved experimentally, but they do allow us to measure the likely error in a conclusion or to attach a level of confidence to a statement. The primary advantage of statistical methods is that they add objectivity to the decision making process. Statistical technique coupled with good engineering or process knowledge and common sense will usually lead to sound conclusions.

The general approach to fitting empirical models is called regression analysis. When regression is performed, one approximates an observed, empirical variable (output, response) by an estimated one, based on a functional relationship between the estimated variable (y_{est}) and one or more regressor or input variables x_1, x_2, ...x_i. The regression analysis is often used to describe data sets, when parameters in known scientific equations have to be estimated, to develop new models describing and even predicting a specific response, or to control and optimize processes.

Developing this functional relationship to obtain expected empirical data to be explained without any residual doubt is impossible. Possible sources for error are random or measurement error, and the "lack-of-fit" error caused by the inaccuracies of our estimation function. Our ultimate goal in regression is to minimize this lack-of-fit error. The method used to find the coefficients (b_j) of general model equation is called least squares estimation. This means that the error term used in the model equations is defined as the difference between observed response variable y and estimated y_{est} for a given setting of the x_j at each data point. The desired optimum regression model then has to give us a minimum for this sum of squared errors, hence "least squares estimation method".

The test for significant of the regression model and the individual regression coefficient will be used for test the statistical significance of the model and model coefficient. In order to test the significance of the model, the assumption "The null hypothesis is true if there is

no linear relationship between any of the independent variables" is performed. This is equivalent to the equations:

$$H_0: b_1 = b_2 = \ldots b_i = 0 \quad (4.5)$$

$$H_1: b_j \neq 0 \text{ for at least one } j \quad (4.6)$$

with H_0 denoting the null hypothesis, H_1 being the rejection of the null hypothesis, and b_1-b_i representing the intercept and the regression coefficients of the i independent.

If H_0 is rejected, there is at least one independent variable significantly contributing to the linear model, and it can be concluded that there exists a functional relationship between the response and at least one of the variables. Similarly, the hypotheses for the individual coefficients b_j can be defined:

$$H_0: b_j = 0 \quad (4.7)$$

$$H_1: b_j \neq 0 \quad (4.8)$$

If H_0 is rejected, the respective coefficient significantly contributes to the model. If H_0 cannot be rejected, the corresponding variable can be eliminated from the model equation.

An analysis of variance or ANOVA-table such as Table 4.1 is commonly used to summarize the test for significance of the model. There are variations in the layout of this table.

Table 4.1 ANOVA table for a model with i regressor variables and n observations.

Source of Vriation	Sum of Squares	Degree of Freedom	Mean Square	F_0	Significance or Error Probability P
Regression Model	SSR	i	MSR=SSR/i	MSR/ MSE	$= P(H_0 : F_0 \leq F_{crit})$
Residual (Error)	SSE	n-1-i	MSE= SSE/(n-1-i)		
Total	S_{yy}	n-1			

The null hypothesis for the regression model (equation (4.6)) is simply tested by comparing the effect or variability caused by the regression model to the overall error. This comparison is based on the so-called Total Sum of Squares (S_{yy}), the Regression Sum of Squares (SSR), and the Sum of Squared Errors or Error Sum of Squares (SSE).

The test for the significance of the regression model is performed as an analysis-of variance procedure by calculating the ratio between the Regression Sum of Squares (SSR) and the Error Sum of Squares (SSE) and comparing the result to the F-statistic with the appropriate degrees of freedom at a given significance level.

$$F_0 = \frac{SSR/i}{SSE/(n-1-i)} = \frac{MSR}{MSE} \tag{4.9}$$

The null hypothesis H_0 is rejected if F_0 is greater than the corresponding critical value F_{crit} of the F-distribution for a given significance level with i and (n-1-i) degrees of freedom. In other words, for a significance level α, the hypothesis that the regression model is not significant can be rejected at the α-level if $F_0 > F_{crit} = F_{\alpha,i,n-1-i}$. Note that the significance level α stands for the probability that the null hypothesis is true, i.e., the model is not significant. Usually, significance levels α of 0.10, 0.05, and 0.01 are used to determine critical values F_{crit}, where decreasing significance levels indicate a higher confidence for the model. The values F_{crit} for the F distribution increase with decreasing significance level α and increasing degrees of freedom f_{SSR}

for the regression model, and they decrease with increasing degrees of freedom f_{SSE} for the error contribution. For a given model, the larger the value of MSR/MSE, the lower the significance level α leading to critical values for F_{crit} which are smaller than F_0, and the higher the confidence level for the significance of the model, i.e. a rejection of H_0. On the other hand, increasing the number of model terms for a given data set, i.e., increasing f_{SSR} and decreasing f_{SSE}, can lead to a decrease of MSR and an increase of MSE up to a point where the F_0 becomes smaller than F_{crit} and the model is no longer significant. If this occurs at significance levels α of higher than 0.1, the model is considered to be no longer significant. In computer programs, usually the significance level α is calculated and given in addition to the corresponding value of F_0=MSR/MSE, so we do not have to look up the values for F_{crit} in a table anymore.

If replicate measurements are present, i.e., responses based on the same settings for the independent variables, a test can be performed which gives the significance of the replicate error in comparison to the model dependent error. In other words, the test splits the Residual or Error Sum of Squares, SSE, into a contribution from the *pure error*, which is based on the replicate measurements, and a fraction which is due to the *lack of fit* based on the model performance. Similar to the F-test for significance of the model, it is also used for the test statistic of lack of fit. If F_0 is larger than the critical value F_{crit} for a given significance level α with *m-2* and *n-m* degrees of freedom, the lack of fit error is significant, i.e., there might be contributions in the regressor-response relationship not accounted for by the model. When performed on a linear (first order) model, this test indicates curvature if F_0 is significant.

The significance test on the regression model tells us if at least one of the regression coefficients is different from zero. It is necessary to test the significance of the individual coefficients. This test forms the basis for model optimization by adding or deleting coefficients (*Backward Elimination, Forward Selection, and Auto fitting*). A model with many coefficients is not necessarily the best, and a model with only a few coefficients might improve dramatically by adding another, but we have to know which coefficient actually plays a significant role in the model. The underlying null hypothesis was described above. A t-test statistic is used to test this hypothesis. Similar to the F-test used for checking the model significance, we compare the calculated t0 to the critical t-value t_{crit} for a given significance level α and the error degrees of freedom, *n-1-i*. If the calculated value for t_0 is larger than t_{crit}, we reject

the null hypothesis at the given significance level. For instance, with α=0.05, we would say that there is only a 5% error probability that the corresponding coefficient is not significant. Note that this significance is based on the presence of all the other regressor variables in the model. It might change dramatically with a different set of regressor variables.

There are parameters called R (correlation coefficient) or R^2 which somehow describe the quality of the fit. Most people consider these parameters as most important in assessing the quality of a regression model. In addition to the basic analysis of variance, the program displays some additional useful information. R^2, the coefficient of determination in Simple Linear Regression is called the coefficient of multiple determinations in Multiple Linear Regression. It is defined by the ratio of the Regression Sum of Squares (SSR) over the Total Sum of Squares (S_{yy}). Clearly, we must have $0 \leq R^2 \leq 1$ with larger values being more desirable. There are also some other R^2 like statistics displayed in the output. The adjusted R^2 is a variation of the ordinary R^2 statistic that reflects the number of factors in the model. It can be a useful statistic for more complex experiments with several design factors when we wish to evaluate the impact of increasing or decreasing the number of model term. Standard deviation is the square root of the error mean square and the coefficient of variance (CV). The CV measures the unexplained or residual variability in the data as a percentage of the mean of the response variable. PRESS stand for Prediction Error Sum of Square and it is a measure of how well the model for the experiment is likely to predict the response in a new experiment. Small values of PRESS are desirable. Alternatively one can calculate an R^2 for Prediction based on PRESS.

So, R^2, adjusted R^2, and R^2 for Prediction together are very convenient to get a quick impression of the overall fit of the model and the predictive power based on one data point removed. In a good model, these three parameters should not be too different from each other. However, for small data sets, it is very likely that every data point is influential. In these cases, a high value for R^2 for prediction cannot be expected.

After calculating a model, a thorough analysis of the residuals is very important to evaluate the adequacy of the regression. The most commonly used methods in residual analysis are:

1. Normal Probability Plots of the Residuals.
2. Plots of the Residuals vs. the Predicted Responses.
3. Outlier Analysis using threshold or cut off values.

Outlier analysis uses threshold or cut off values. In a computer program such as ER, the ranked residuals are plotted against the expected normal value or *rankit*, which is equal to the inverse of the normal cumulative distribution for a given cumulative probability. In such a plot, the points should form a straight line if the residuals are perfectly normally distributed. In reality, the plot is usually slightly s-shaped, which can be tolerated if the deviation from linearity is not too bad. A pronounced s-shape, however, indicates a distribution with heavy "tails", i.e. the residuals should be inspected for outliers.

In addition to inspecting the normal probability plots of residuals, it is helpful to plot the residuals versus the predicted responses. If the residuals are not correlated with the value of the predicted response, than this plot should look like a horizontal band on both sides of the expected average for the residuals, zero. If the pattern looks dramatically different, it indicates that the error variance is not constant and depends on the response. Usually, transformations in the regressors or the response are employed to correct this model inadequacy. The shape of the residual vs. predicted response plot can indicate which transformation of the response y could improve the model.

A regression model was used in this work to represent the result of experiments which were set by using central composite design. Typical quadratic model was employed to express the relationship between dependent and independent variables. Selection of significant variables for inclusion in this empirical model was carried out by Microsoft Excel essential regression, statistical package. The multiple regression starts with all possible quadratic terms. The value of the coefficients were then determined. Elimination of the non significant term was performed having the level of significance (P value $\leq$ 0.05) as criteria. A low P value of the particular independent variable indicates its significant role in improving the curve fitting of the model. The regression models were validated statistically by the analysis of variance (ANOVA).

4.5 Optimization (http://www.statease.com/dx8descr.html)

4.5.1 Numerical Optimization Criteria

Numerical optimization will optimize any combination of one or more goals. The goals may apply to either factors or responses. The possible goals are: maximize, minimize, target, within range, none (for responses only) and set to an exact value (factors only). A minimum and a maximum level must be provided for each parameter included in the optimization. If a response is transformed, the optimization will use either the original or transformed scale, as chosen by the current setting of the Display Options menu. A weight can be assigned to a goal to adjust the shape of its particular desirability function. The default value of one creates a linear ramp function between the low value and the goal or the high value and the goal. Increased weight (up to 10) moves the result towards the goal. Reduced weight (down to 0.1) creates the opposite effect. The "importance" of a goal can be changed in relation to the other goals. The default is for all goals to be equally important at a setting of 3 pluses (+++). If you want one goal to be most important, you could change it to 5 pluses (+++++).

4.5.2 Desirability Function

Desirability is an objective function that ranges from zero outside of the limits to one at the goal. The numerical optimization finds a point that maximizes the desirability function. The characteristics of a goal may be altered by adjusting the weight or importance. For several responses and factors, all goals get combined into one desirability function. Don't become distracted by trying to always get a very high desirability value. The value is completely dependent on how closely the lower and upper limits are set relative to the actual optimum. The goal of optimization is to find a good set of conditions that will meet all the goals, not to get to a desirability value of 1.0. Desirability is simply a mathematical method to find the optimum.

The method makes use of an objective function, D(X), called the desirability function. It reflects the desirable ranges for each response (d_i). The desirable ranges are from zero

to one (least to most desirable, respectively). The simultaneous objective function is a geometric mean of all transformed responses:

$$D = (d_1 \times d_2 \times .... \times d_n)^{\frac{1}{n}} = \left(\prod_{i=1}^{n} d_i \right)^{\frac{1}{n}} \qquad (4.10)$$

where n is the number of responses in the measure. If any of the responses or factors falls outside their desirability range, the overall function becomes zero.

For simultaneous optimization each response must have a low and high value assigned to each goal. On the worksheet, the "Goal" field for responses must be one of five choices: "none", "maximum", "minimum", "target", or "in range". Factors will always be included in the optimization, at their design range by default, or as a maximum, minimum of target goal. The meanings of the goal parameters are:

Maximum:

$d_i = 0$ if response < low value

$0 \leq d_i \leq 1$ as response varies from low to high

$d_i = 1$ if response > high value

Minimum:

$d_i = 1$ if response < low value

$1 \geq d_i \geq 0$ as response varies from low to high

$d_i = 0$ if response > high value

Target:

$d_i = 0$ if response < low value

$0 \leq d_i \leq 1$ as response varies from low to target

$1 \geq d_i \geq 0$ as response varies from target to high

$d_i = 0$ if response > high value

Range:

$d_i = 0$ if response < low value

$d_i = 1$ as response varies from low to high

$d_i = 0$ if response > high value

The d_i for "in range" are included in the product of the desirability function "D", but are not counted in determining "n": $D = (\prod d_i)^{1/n}$.

If the goal is none, the response will not be used for the optimization. Goals can be set for any number responses, factors and/or components provided at least one response is included in the goal set.

4.6 Design-Expert® V8 Software for Design of Experiments (DOE)

(http://www.statease.com/dx8descr.html)

Design-Expert software version 8 (trial version) is the product of Stat-Ease Incorporation in USA. Use this Windows®-based program to optimize the product or process. It provides many powerful statistical tools, such as:

- Two-level factorial screening designs: Identify the vital factors that affect the process or product so it can make breakthrough improvements,
- General factorial studies: Discover the best combination of categorical factors, such as source versus type of raw material supply,
- Response surface methods (RSM): Find the optimal process settings to achieve peak performance,
- Mixture design techniques: Discover the ideal recipe for the product formulation,
- Combinations of process factors, mixture components, and categorical factors.

The Design-Expert program offers rotatable 3D plots to easily view response surfaces from all angles, set flags and explores the contours on interactive 2D graphs. The numerical optimization function finds maximum desirability for dozens of responses simultaneously.

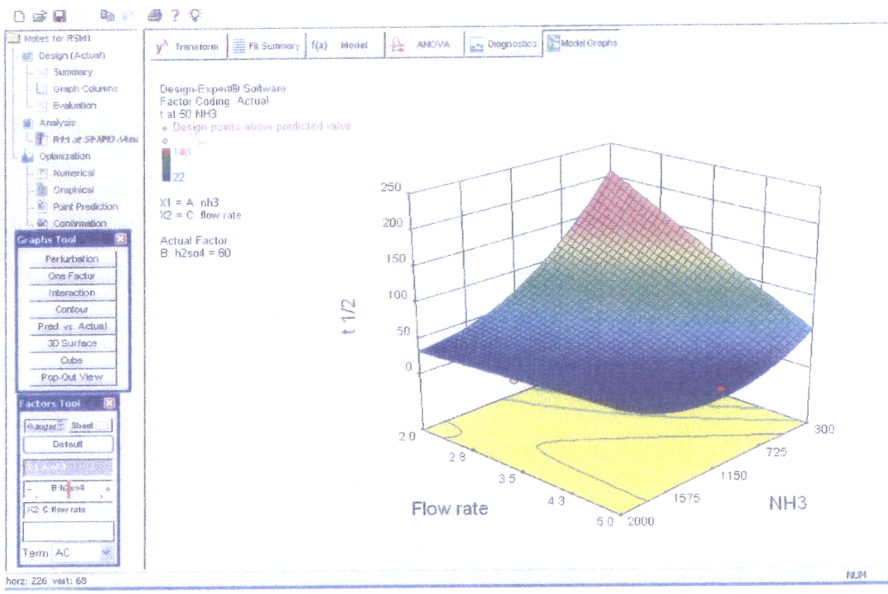

Figure 4.1 Design Expert v. 8 software window for RSM solution.

CHAPTER 5

ACTIVATED CARBON AND BIOCHAR PRODUCTION FROM RUBBER WOOD OFF-CUT

5.1 Introduction

Activated carbon has been produced from variety of biomass i.e., wood, rice husk, cellulose, lignin, coconut shells, and palm shells. The surface areas have found at 300 to 1200 m^2/g with average pore diameters of 10 to 60 Å. There have been many reports on the production of activated carbon to use as adsorbent for removing hazardous compounds from industrial waste gases or wastewater, and in catalysis as support for catalyst. There are two basic processes to activate the carbon materials; physical and chemical. The effect of different chemical reagents on the production and quality of activated carbon was studied extensively by different researchers. There are two important advantages of chemical activation in comparison to physical activation. One is the lower temperature in which the process is accomplished. The other is that the global yield of the chemical activation tends to be greater since burn off char is not required (Gue *et al.*, 2005).

There are two basic processes to activate the carbon materials; physical and chemical. The effect of different chemical reagents on the production and quality of activated carbon was studied extensively by different researchers. There are two important advantages of chemical activation in comparison to physical activation. One is the lower temperature in which the process is accomplished. The other is that the global yield of the chemical activation tends to be greater since burn off char is not required (Singh et al., 2008). Chemical activation processes have been carried out with acidic reagents i.e. $ZnCl_2$, H_3PO_4, HCl, and H_2SO_4 or with basic reagents i.e. KOH, K_2CO_3, NaOH, and Na_2CO_3 (Girgis *et al.*, 2007). Among the numerous dehydrating agents, sulfuric acid (H_2SO_4) and phosphoric acid (H_3PO_4), in particular are widely used chemical agent in the preparation of activated carbon.

H_2SO_4 improves the pore development in the activated carbon structure, and because of the effect of chemicals, the yields of carbon are usually high (Gue *et al.*, 2005). H_2SO_4 activation has been applied on a wide variety of cellulosic precursors such as apricot stone, oil-palm stone, sunflower oil cake, palm shells, Tamarind wood, olive cake, sewage sludge and discarded tyres, and Euphorbia rigida. On the other hand, activation with H_3PO_4 offers many recommending advantages over the traditional " thermal activation scheme'' as it is performed in one pyrolysis step at a much lower temperature (400-600°C), leads to a much higher carbon yield (35-50%), Moreover treatment with H_3PO_4 allows to develop both microporess and mesopores in resulting carbon materials (Girgis *et al.*, 2007). Knowledge of different variables during the activation process is very important in developing the porosity of carbon sought for a given application.

Biochar is a name for charcoal when it is used for particular purposes, especially as a soil amendment. Biochar is a fine-grained and porous substance, similar in its appearance to charcoal produced by natural burning. Biochar is produced by the combustion of biomass under oxygen-limited conditions. The definition adopted by the International Biochar Initiative (IBI) furthermore specifies the need for purposeful application of the material to soil for agricultural and environmental gain (http://www.csiro.au/files/files/poei.pdf).

Rubber wood (Hevea brasiliensis) is one of the main plantation crops in South East Asia. Rubber wood sawdust has been used to produce activated carbon with high surface area of 1496 m^2/g (Srinivasakannan and Bakar, 2004) but the particle size is too small to use as adsorbent in adsorption column. So, production of adsorbent from off-cut rubber wood biomass from rubber wood industry is very interesting to make high value added of them.

The aim of this chapter was an attempt to utilize the off-cut rubber wood generated from sawing process for adsorbent productions namely activated carbon and biochar. H_2SO_4, H_3PO_4 and mixing of H_2SO_4 - H_3PO_4 acid were used as reagents to produce rubber wood activated carbon. Concentrations of acid were varied for activated carbon production. % yield, surface area, and morphology of rubber wood activated carbon were investigated. The parameters of proportion of mixing acid between H_2SO_4-H_3PO_4, the effect of temperature and the time of carbonization on activated carbon were also study. This chapter was providing the good adsorbent for activated carbon production to using in NH_3 adsorption.

5.2 Materials and methods

5.2.1 Materials and Equipment

Rubber wood off-cut that was used as precursor material procured from Woodwork Advance Co., Ltd. (Songkhla, Thailand), and cut to $1\times1\times1$ cm^3 cubs as shown in Figure 5.1. Chemical activation for activated carbon production were H_2SO_4 95-97% (Merck, Germany) and H_3PO_4 86.1% (J.T. Backer, USA). The tube furnace (CARBOLITE CTF12/65/550) with sizing of 50 cm length and 4 cm ID was performed for carbonizing of rubber wood activated carbon. Experimental set up for carbonization the rubber wood chips was show in Figure 5.2.

(a) Raw rubber wood off-cut

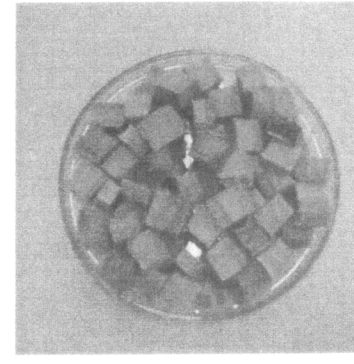

(b) Rubber wood chips

Figure 5.1 Raw rubber wood off-cut and rubber wood chips for activated carbon production.

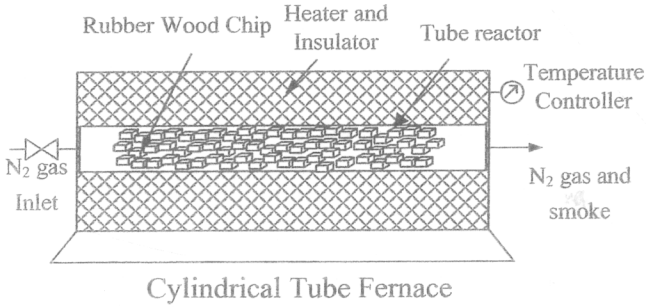

Cylindrical Tube Fernace

(a) Schematic diagram

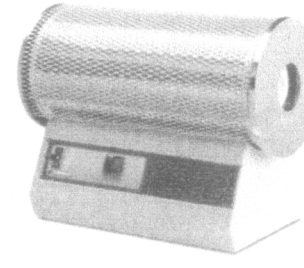

(b) Tube furnace

Figure 5.2 Cylindrical tube furnaces for activated carbon production.

5.2.2 Rubber wood activated carbon activation

1. Chemical activation conditions

A portion of 100 g of rubber wood chips was chemically activated by H_2SO_4, H_3PO_4, and mixing of H_2SO_4 - H_3PO_4 at concentration of 20–80%. The acid mixture of 250 ml was separately prepared, mixed, and immersed by the wood precursor at room temperature (30°C) for 24 hours. Figure 5.3 shows the rubber wood chips before and after chemical activation. Figure 5.3(b) was demonstrated the surface color of rubber wood chips turned to be black because there were direct contact with strong acid thus the outside texture of rubber was digested and tender.

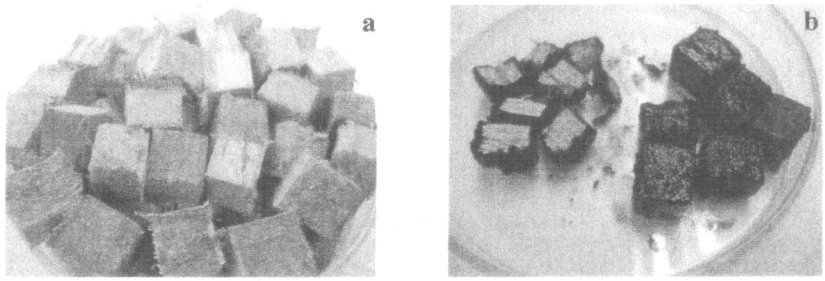

Figure 5.3 Rubber wood chips before (a) and after (b) H_2SO_4- H_3PO_4 acid activation for activated carbon production.

2. Physical activation conditions

After chemical activation, the rubber wood chips were physically activated by heating in a stainless steel tube reactor under 4 l/min nitrogen. The tube reactor was heated in a cylindrical tube furnace from room temperature to 200°C for semi-carbonization for 30 min. and heated up to 400°C – 700°C by heating rate of 10°C /min for 1-3 hours. After cooling the furnace down to room temperature, the carbon products was taken out, leached with de-ionized water, and dried in hot air oven at 110°C for 24 hours. Finally, the rubber wood chips activated carbon were obtained and the size distribution was 6.7-1.7 mm.

5.2.3 Biochar production

Rubber wood off-cut was carbonization in a stainless steel tube reactor (length 50 cm and i.d. 4 cm) under 4 l/min nitrogen at 300-500°C for 2 h (Yu et al., 2011 and Duku et al.,

2011). After cooling the furnace down to room temperature, the biochar was taken out, cut and sieved to particle size fraction of 6.7-1.70 mm.

5.2.4 Physical properties Measurements

The activated carbon and bichar were sieved to a granular size of 2.36-3.35 mm before characterization by BET and micropores surface area measurement. Weight of the raw material and activated carbon were measured and recorded. The yield (% Y_{AC}) was defined by the weight ratio of final activated carbons to the initial dried rubber wood chips. The equation applied is as follows:

$$\%Y_{AC} = \left(\frac{W_{RWAC}}{W_{RW}}\right) \times 100 \qquad (5.1)$$

where % Y_{AC} is the yield of rubber wood activated carbon, W_{RWAC} is weight of activated carbon, and W_{RW} is weight of rubber wood chips precursor.

Textural properties of adsorbents samples were determined by nitrogen adsorption at -196°C with sorptiometer (Surface Area and Pore Size Analyzers, COULTERTM SA3100™). The BET surface area was calculated from the adsorption isotherms using the Brunauer-Emmett-Teller (BET) equation (Brunauer *et al.*, 1938). Microscopic images of the rubber wood activated carbon were obtained by scanning electron microscope (JSM-5200).

5.3 Results and Discussions

5.3.1 Activated carbon

1. Morphology

Activated carbon produced from chemical activation and carbonization of rubber wood cube chips has a similar shape to raw material but smaller than initial size. The products can be shown in figure 5.4

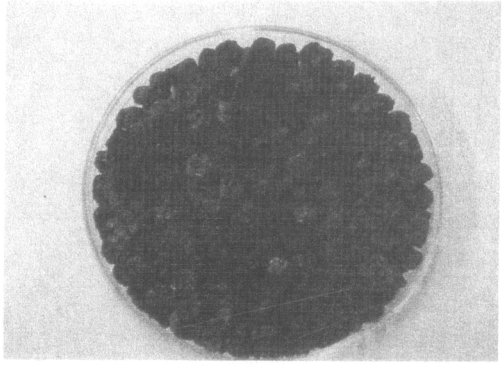

Figure 5.4 Rubber wood chips activated carbon.

From chemical activation and carbonization, the carbon product was naturally cracked to 2 parts of inner and outer wood chip part. Characteristic measured by SEM of raw wood chip and activated carbons that were activated by H_2SO_4 and H_3PO_4 can be shown in Figure 5.5 – 5.7 The results demonstrated that physical structure of the raw wood chip don't have any pore structure but has only cell bundle of wood. The structure of wood chips was modified after activation by acid H_2SO_4 and H_3PO_4 and carbonization in the tube furnace. The results shown tremendously internal surface and pore structure formed in activated carbon with H_2SO_4 and H_3PO_4 activation.

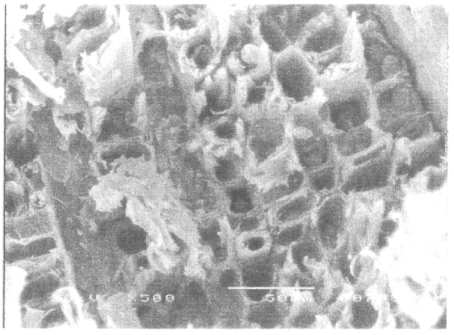

Figure 5.5 SEM photograph (500 x) of wood chips.

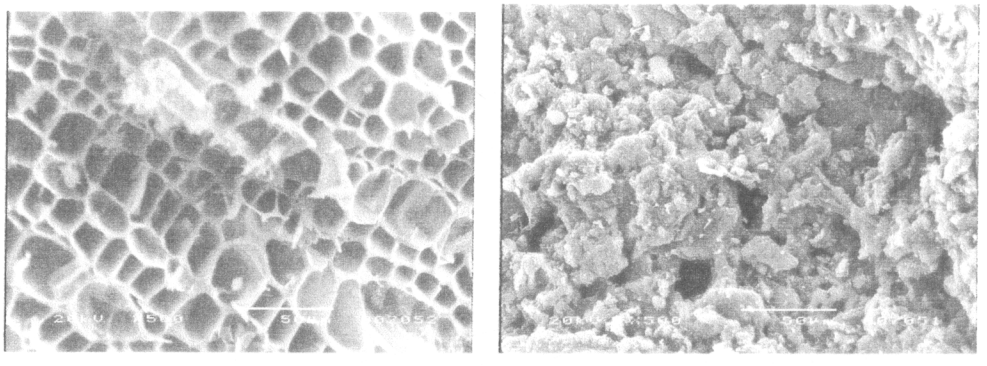

(a) The inner of activated carbon (b) The outer surface of activated carbon

Figure 5.6 SEM photographs (500 x) of activated carbon from inner (a) and outer (b) part of wood chips that was activated by H_2SO_4 (50%) acid.

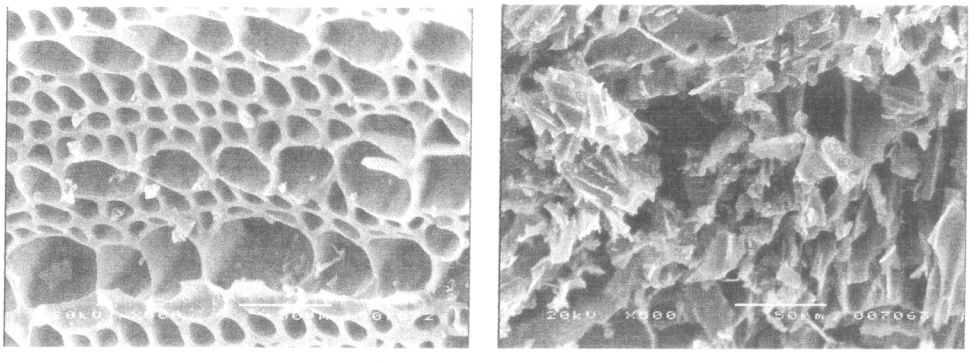

(a) The inner of activated carbon (b) The outer surface of activated carbon

Figure 5.7 SEM photographs (500 x) of activated carbon from inner (a) and outer surface (b) part of wood chips that was activated by H_3PO_4 (50%) acid.

2. Yield of activated carbon

Percentage of activated carbon yield (% yield) producing from rubber wood chips using H_2SO_4 and H_3PO_4 activation and carbonization in tube furnace at 700°C was measured. The ratio of activated carbon weight derived from the wood chip weight for activation was defined as % yield, both based on dry weight (Srinivasakannan and Bakar, 2004). The results providing the relationship between % yield and acid concentration are shown in Figure 5.8.

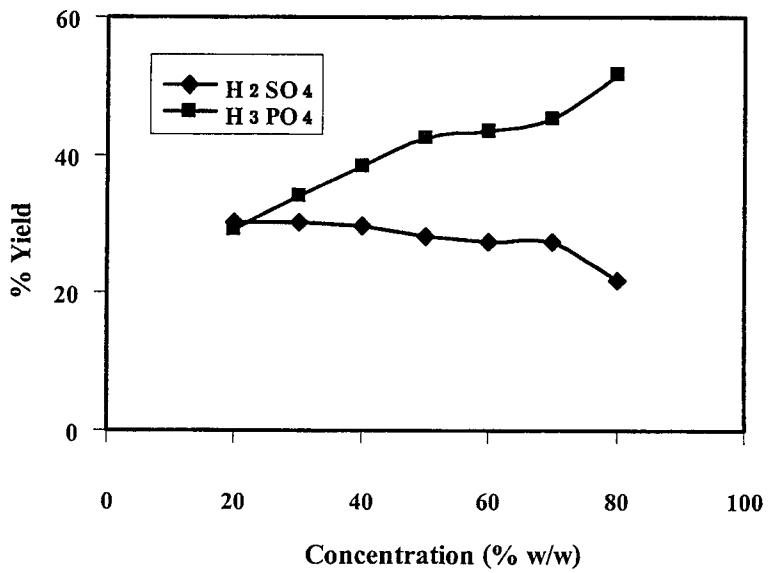

Figure 5.8 Yield (%) vs. concentration of activated carbon by H_2SO_4 and H_3PO_4 activation.

Figure 5.8 shows the effect of acid type and concentration on % yield of activated carbon. The optimum H_3PO_4 concentration for activated carbon production was 80% that provided the highest yield of 52%. From the literature, at the first stage of semi-carbonization was carried out at 200°C for activated carbon production by H_3PO_4 activation, the impregnated precursor material was found to be blackened and formed a plastic mass, which ultimately transforms to dry charcoal. Thus, increasing concentration of H_3PO_4 affected to wood texture strengthen (Srinivasakannan and Bakar, 2004).

On the other hand, at higher H_2SO_4 acid activation from 20-80 % w/w, % yield was decreased. The optimum H_2SO_4 concentration for activated carbon production was 20% that provided the highest yield of 30%. The dominant property of H_2SO_4 activation is dehydration of

material in the texture of wood, so, at the higher of H_2SO_4 concentration, the weight of activated carbon was decreased.

3. Surface Area

Effect of H_2SO_4 and H_3PO_4 concentration in the rubber wood chips activation process on BET and micropore surface area of activated carbon products are exhibited in Figure 5.8 and 5.9, respectively. Precursor was soaked in H_2SO_4 acid solution at concentration range of 20-80%. The increasing in H_2SO_4 concentration from 20-50% w/w can improve BET and micropore surface area. At 50% H_2SO_4, the highest BET and micropore surface area were 557 m^2/g and 466 m^2/g, respectively. However, at H_2SO_4 concentration was over than 60-80% w/w, the pore structure was fractured and fragmented by corrosiveness so the BET and micropore surface was decreased.

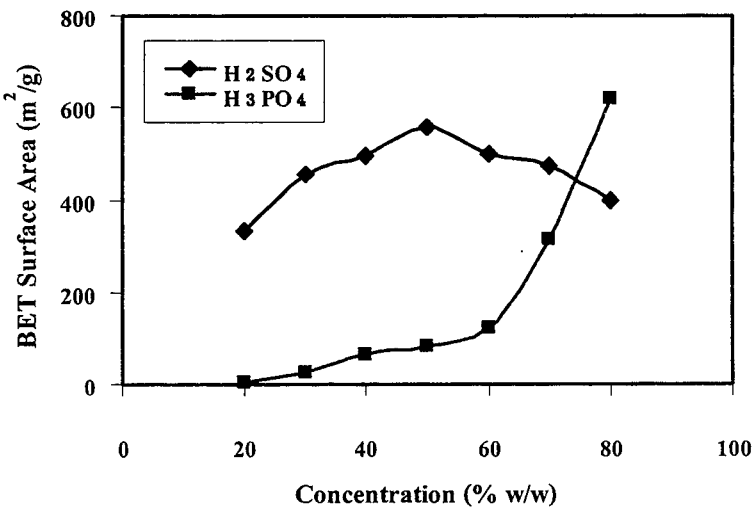

Figure 5.9 BET surface area vs. acid concentration of activated carbon production by chemically activation using H_2SO_4 and H_3PO_4

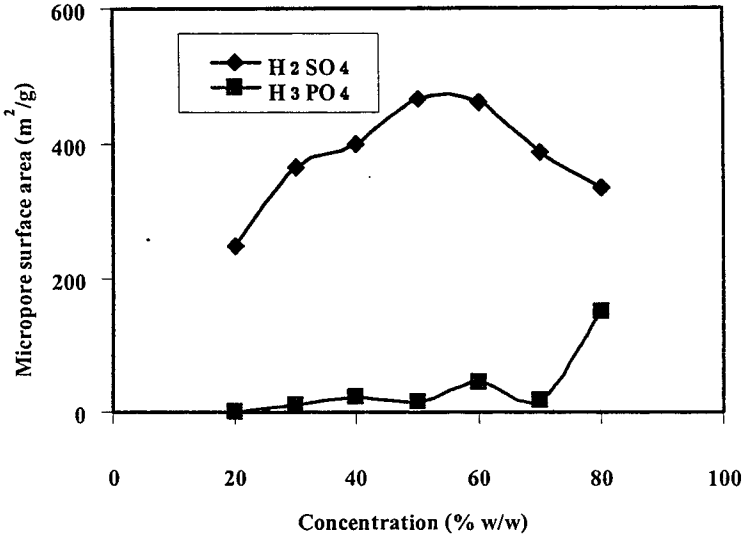

Figure 5.10 Micropore surface area vs. acid concentration of activated carbon production by chemically activation using H_2SO_4 and H_3PO_4

Activated carbon production by H_3PO_4 activation has the result of BET and micropore surface area less than using H_2SO_4 activation. Because of the acid strength of H_3PO_4 was weak in the lower concentration, still, the concentration near 85%, the acidity of H_3PO_4 was enough higher to activation (http://en.wikipedia.org/wiki/Phosphoric_acid). Thus, at 80% H_3PO_4, the BET and microspores was dominant.

4. Effect of acid mixing concentration

In case of using H_2SO_4 and H_3PO_4 mixed acid for rubber wood chips activation, activated carbon morphology is shown in figure 5.11 SEM images show for inner and outer of activated carbon surface. For the inner part, the pore structure look like honeycomb void and twisted holes. Wall of holes is thicker than activated carbon was activation with mixed H_2SO_4 and H_3PO_4. On the other hand, the surface of activated carbon was less pores and quite smooth.

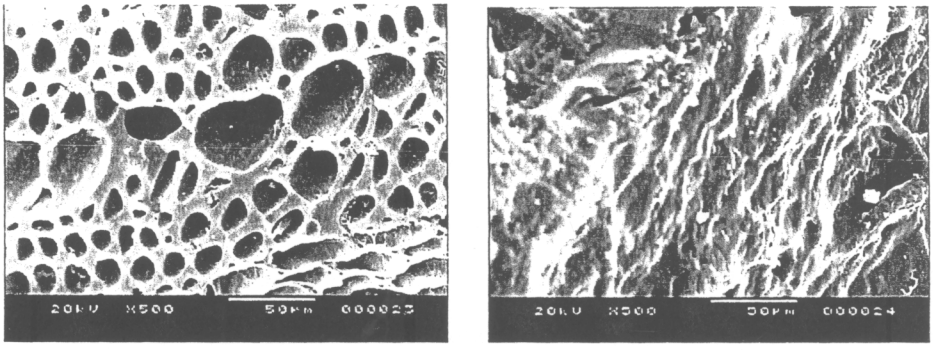

(a) The inside of activated carbon (b) The outer surface of activated carbon

Figure 5.11 SEM photographs (500 x) of internal (a) and outer surface (b) of activated carbon product that was activated by mixing acid (H_2SO_4 : H_3PO_4 ; 40 % : 40%)

The mixtures of acids between H_3PO_4 (40%-50%) and H_2SO_4 (20-50%) were prepared and used for the carbon activation to study for the effect of acid concentration on the carbon yield and surface area of rubber wood activated carbon. The physical activations were performed at 700°C carbonization temperature and 2 h activation time. Figure 5.12 shows the yield of the activated carbon according to the different acid concentration. The result showed that acid mixture in the range of H_3PO_4 40% to 50% and H_2SO_4 20% to 30% yield of activated carbon was descent. This due to rapid evolution of volatile material by H_2SO_4 to form stable compounds (tar) (Srinivasakannan and Bakar, 2004). Thus, the increasing in H_2SO_4 (30-50%) concentration in the acid mixture was not much significantly effect to the yield.

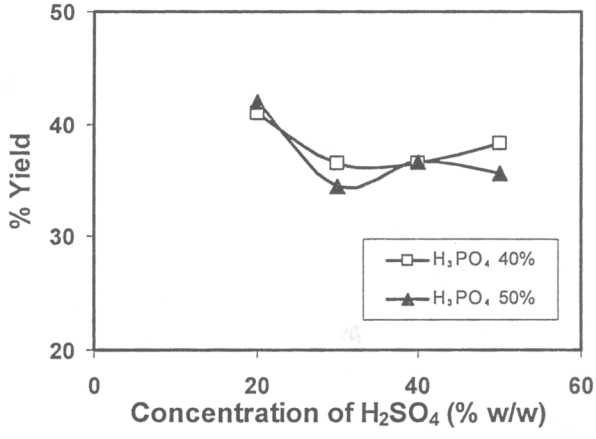

Figure 5.12 Effect of acid mixing concentration on % yield of activated carbon at carbonization temperature 700°C and time 2 h.

Figure 5.13 demonstrates BET and micropores surface area on various mixing acid concentration. Both BET and micropores surface area increased as the increasing in concentration of H_2SO_4 from 20 to 40% because H_2SO_4 was to minimize the formation of tar and any other liquids that could possibly clog up the pores and inhibit the development of the porous structures in the activated carbon (Girgis *et al.*, 2007). However, the surface areas were decreased when 50% H_2SO_4 was used. This is probably due to the surplus water vapor release via H_2SO_4 dehydration by high concentration of acid , which results in an over-gasification of the rubber wood chips precursors by converting micropores to meso- and macropores. Therefore it causes a detrimental effect on the BET and microporess surface area (Haimour and Emeish, 2006).

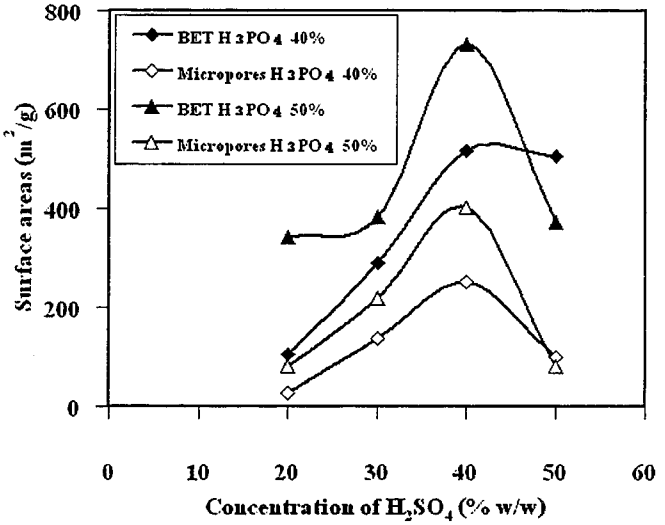

Figure 5.13 Effect of acid mixing concentration on BET and micropores surface area of activated carbon at carbonization temperature 700°C and time 2 h.

Taking into account that cellulose is one of the main components of wood, the successive reactions able to be catalyzed by protons of acid function are: the depolymerization of cellulose, the dehydration of the lignocellulosic material, the formation of aromatic rings of phosphate group. Increasing H_3PO_4 to mixed acid concentration, it takes a high rate of depolymerisation is higher. Consequently, cellulose and glycogen present the same monomers; therefore the depolymerisation reaction of cellulose can be compared to the reaction of glycogen with phosphoric acid (Haimour and Emeish, 2006). At H_3PO_4 50% w/w and H_2SO_4 40% w/w

provided the maximum BET and micropores surface area at 731.38 m^2/g and 402.54 m^2/g, respectively.

5. Effect of carbonization temperature

The effect of carbonization temperature (400-700°C) on yield of the activated carbon using acid mixing activation between H_3PO_4 50% w/w and H_2SO_4 40 % w/w at activation time 2 hours were studied and shown in Figure 5.14 The results show that when activation temperature increased the yield of activated carbon decreased. At 400°C provide the maximum yield of 40%.

For semi- carbonization at low temperature 100-200°C, dehydration can occur along the same mechanism as for acid catalyzed dehydration of alcohols. This explains the good yield in case of activation by phosphoric acid, because whatever the nature of atmosphere, dehydration can occur before wood pyrolysis and, as result, the carbon residue is strongly aromatic. In this temperature range, water coming from the wood structure is responsible for the presence of protons (Krukanot and Prasertsan, 2004). On the other hand, the H_2SO_4 compound incorporated into the interior of the rubber wood restricts the formation of tar and other liquids (e.g., acetic acid and methanol) and inhibits particle shrinkage and volume contraction (Haimour and Emeish, 2006).

In activation or carbonization at high temperature, the polymeric structure decompose and liberate most of non-carbon element, mainly hydrogen, oxygen and nitrogen in the form of tar and gases, leaving behind a rigid carbon skeleton in form of aromatic sheets and strips (Srinivasakannan and Bakar, 2004). Thus, when temperature for activation increased, yield of product decreased.

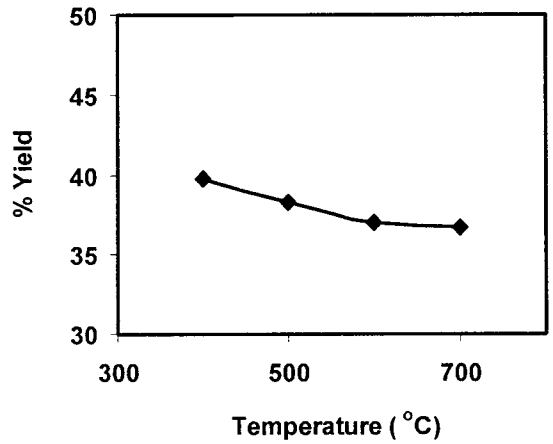

Figure 5.14 Effect of carbonization temperature on yield of activated carbon by the acid mixing of H_3PO_4 50% and H_2SO_4 40% at 2 h activation time.

In the same way, the effect of carbonization temperature on BET and microporess surface area is shown in Figure 5.15 BET and micropores surface areas of activated carbon using acid mixture decrease with the increasing in the temperature because at high temperature, micorpores structures was collapsed from meso- to macropores, so the total surface areas was decreased. The highest BET and micropores surface area at 400°C carbonization were obtained at 1200 m^2/g and 701 m^2/g, respectively.

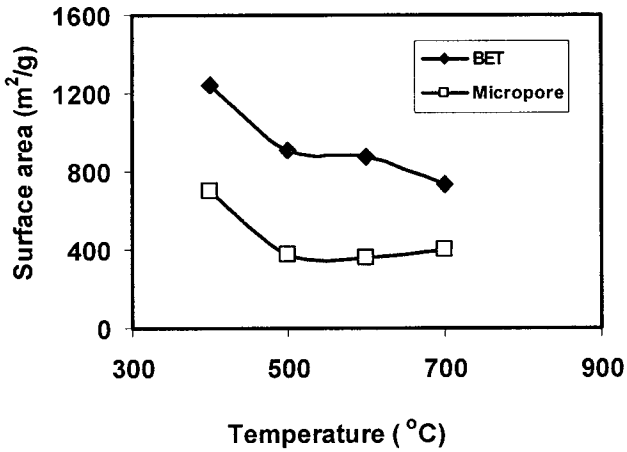

Figure 5.15 Effect of carbonizationtion temperature on BET and microporess surface areas of the activated carbon using acid mixing of H_3PO_4 50% and H_2SO_4 40% at 2 h activation time.

6. Effect of activation time

Figure 5.16 shows the results of physical activation time 1-3 hours on yield of the activated carbon using the acid mixture at activation temperature 400°C. For longer contacting time (2-3 hours) the volatile compounds evaluated to stable compounds and leaves the carboneous surface and degradation of the activated carbon becomes severe (Haimour and Emeish, 2006). Therefore, weight of activated carbon at long carbonization time was decreased.

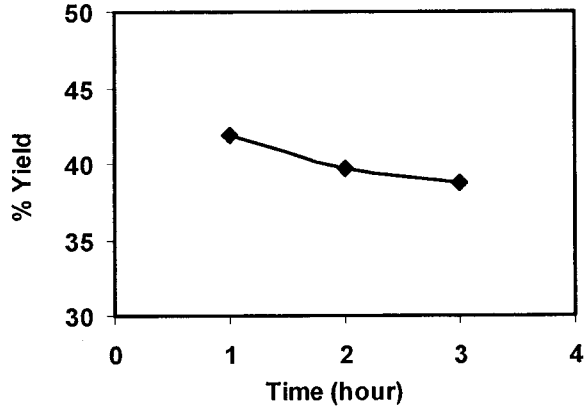

Figure 5.16 Effect of activation time on % yield of activated carbon using acid mixing of H_3PO_4 50% and H_2SO_4 40% at activation temperature of 400°C.

The effect of carbonization time on BET and microporess surface areas to the activated carbon is shown in Figure 5.17 the result demonstrated that at the carbonization time of 2 hours provided maximum BET and microporess surface areas. At 1 hour activation, the time too short to complete form the micropores in activated carbon, and at the activation time of 3 hours, micropores structure was shrunk, so the micorpores were transformed to meso- and macro consequently.

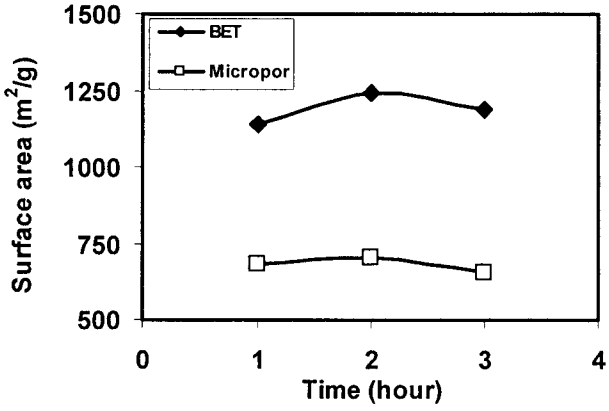

Figure 5.17 Effect of activation time on BET and micropores surface areas of the activated carbon using acid mixture of H_3PO_4 50% and H_2SO_4 40% at activation temperature 400°C.

7. Size characterization

RWAC was sieved to particle size fraction of 6.7-4.75 mm, 3.35-2.36 mm, and 2.00-1.70 mm. percentage of sieved weight was calculated and recorded for the particle size distribution. All RWAC fractions were measured for BET and micropores surface area and mixed according to the weight percent as shown in table 5.1.

Table 5.1 Characterization result of the RWAC.

Size (mm)	Weight (%)	S_{BET} (m^2/g)	$S_{micropores}$ (m^2/g)
6.70-4.75	50	8	5
3.35-2.36	40	1243	702
2.00-1.70	10	1176	484

The surface area of RWAC has associated with the particle size. The smaller size (3.35-1.70 mm) has higher surface area as it was cracked from the exterior surface of RW that was directly contacted to activating agent and exposed to the heat from furnace. On the contrary, the surface area of the larger size (6.70-4.75 mm) showed a little; because of, mixed acid unable

to permeate to inner of rubber wood textures and indirect to exposed to highly temperature from the furnace.

5.3.2 Rubber wood biochar

The % yield and BET of biochar from rubber wood off-cut were performed in Table 5.1. The result shows that the carbonization temperature at 300°C, the rubber wood off-cut was incompletely burn-off to form biochar, the colors of char was still brown as the raw wood. Thus the BET surface area approached zero. At the higher pyrolysis temperature, the yield of biochars were insignificant difference and at 500 °C was provide the maximum BET surface area to 3 m^2/g. Figure 5.18 SEM images show the pore structure of rubber wood biochar.

Table 5.2 Characterization result of rubber wood charcoal.

Carbonization temperature (°C)	**Yield (%)**	**$S_{BET}(m^2/g)$**
300	-	0
400	25	2.3
500	25	3

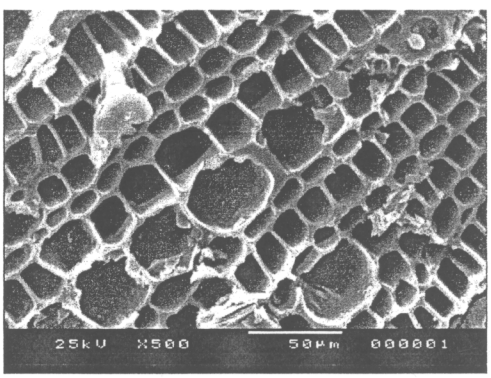

Figure 5.18 SEM photographs (500 x) of rubber wood biochar.

5.4 Conclusion

Activated carbons with relatively high yield and well developed porosity were prepared from rubber wood off-cut pre-treated with mixing acid between H_3PO_4 and H_2SO_4. Reasonably high BET surface areas and predominant microporosity of these activated carbon. The parameters were affecting to produce rubber wood chips activated carbon by mixing acid activation such as; ratio of mixed concentration between H_3PO_4 and H_2SO_4, activation temperature and time. The optimum condition for activated carbon preparation from rubber wood off-cut is the acid mixing of H_3PO_4 50% w/w and H_2SO_4 40% w/w. The temperature and time for activation performing were 400^{o}C and 2 hour that provided 40% yield of the product, 1200 m^2/g BET surface area, and 700 m^2/g micropores surface area. Rubber wood biochar was produced at 500 ^{o}C was provide the maximum yield and BET surface area were 25% and 3 m^2/g, respectively.

CHAPTER 6

NH_3 ADSORPTION FROM WASTE AIR USING ACID MODIFICATION RUBBER WOOD ACTIVATED CARBON AND BIOCHAR

6.1 Introduction

The removal of NH_3 from waste air can be performed by many technologies, for example, catalytic decomposition, reaction of NH_3 with another gas, adsorption by solid adsorbents, and incineration processes. However, it is difficulty and costly to remove the NH_3 to the levels below the specification of 50 ppmv (Gue *et al.*, 2005). Clearly, there is a need to develop an inexpensive and simple method to remove NH_3 from the waste air. Reaction between NH_3 and H_2SO_4 in wet scrubber has been selected to remove NH_3 in waste air (Liangh-hsing *et al.*, 2006). Outcome or by-product from the reaction is Ammonium sulfate $(NH_4)_2SO_4$ that can be used as nitrogen fertilizer. However, the wet scrubbing is suffers from the problems of scaling inside the tower, equipment plugging, and corrosion. Furthermore, it is costly to dispose the resulting of dilute scrubbed solution. Alternately, a fixed bed of activated carbon has been employed to adsorb and remove NH_3 from the gas stream by impregnating H_2SO_4 on activated carbon and provide high NH_3 removal efficiency (Liangh-hsing *et al.*, 2006).

Chemical reaction between NH_3 and H_2SO_4 in adsorption column is shown in equation (6.1) (Liang-hsing *et al.*, 2006). The reaction forms $(NH_4)_2SO_4$ crystal as by product which remains on the adsorbent that can be used as nitrogen fertilizer. The mechanism by which the NH_3 was removed from waste air by the chemical adsorption can be noticed in three steps: (1) NH_3 transport from waste gas stream to the external surface of the adsorbent; (2) the adsorbed NH_3 diffuse to the pore mouth and gas-liquid interface; (3) NH_3 molecule dissolves in the aqueous H_2SO_4 layer and reacts with H_2SO_4.

$$2NH_{3(g)} + H_2SO_{4(aq)} \rightarrow (NH_4)_2SO_{4(s)} \qquad (6.1)$$

Rubber wood activated carbon (RWAC) and rubber wood biochar (RWB) were produced and modified by impregnating with H_2SO_4 solution to form an acidic adsorbent (RWACs and RWBs, respectively) for NH_3 adsorption from waste air. From the previous works, the result shown that the NH_3 removal efficiency by using RWACs and RWBs can reach to 80 %.

This chapter aims to study for NH_3 removal efficiency from waste air using RWACs and RWBs. The adsorbents were packed in the continuous down flow fixed-bed column system for NH_3 treatment. The influence of initial NH_3 concentration in waste air, waste air flow rate, and concentration of H_2SO_4 impregnating on RWB were evaluated on NH_3 removal efficiency in adsorption column.

6.2 Materials and Methods

6.2.1 Materials

Rubber wood activated carbon (RWAC) and rubber wood biochar (RWB) as shown in Figure 6.1 (a) and (b) were obtained by chapter 5. H_2SO_4 95-97% and NH_3 solution 25% obtained from Merck with analytical grade were used as an impregnating reagent and precursor for generating NH_3 gas contamination, respectively.

RWAC and RWB was sieved to particle size fraction of 6.7-1.70 mm BET and Micropores surface area of each size were measured as shown in table 6.1.

Table 6.1 Characterization result of the RWAC and RWB.

Sample	Size (mm)	S_{BET} (m^2/g)	$S_{micropores}$ (m^2/g)
RWAC	6.7-1.70	1051	618
RWB	6.7-1.70	3	0

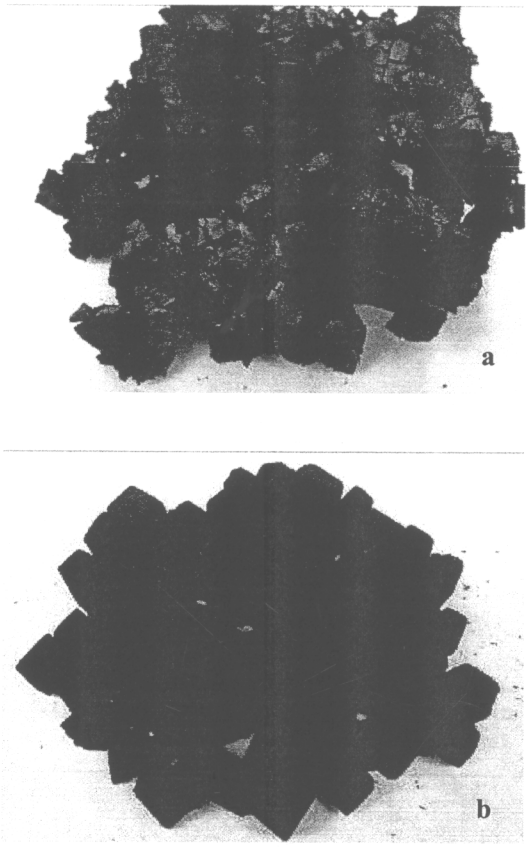

Figure 6.1 Picture of rubber wood activated carbon (RWAC) (a) and biochar (RWB) (b).

6.2.2 Acidic adsorbent preparation

The RWACs and RWBs acidic adsorbents were prepared by contacting 2 g of dried adsorbents into 10 ml of known H_2SO_4 concentration (40-80% w/w) as shown in Figure 6.2 Upon soaking time of 1 h at room temperature (28-29^{o}C), the samples was filtrated by vacuum filter then dry in hot air oven at 110^{o}C for 1 h and cooled down in glass desiccators.

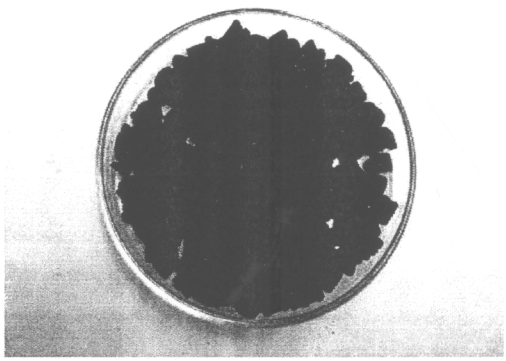

Figure 6.2 Impregnated rubber wood activated carbon (RWACs) and biochar (RWBs) with H_2SO_4.

6.2.3 Adsorption experiments

The adsorption capacities of RWACs and RWBs were tested in laboratory scale of continuous down flow fixed-bed column. The schematic diagram and experimental set up of NH_3 contaminated waste air generation and adsorption unit are demonstrated in Figure 6.3-6.4 The adsorption column was a glass with an inside diameter of 2 cm and column height of 15 cm. Fiber glass was installed in the bottom part to support adsorbents in the column as shown in Figure 6.5.

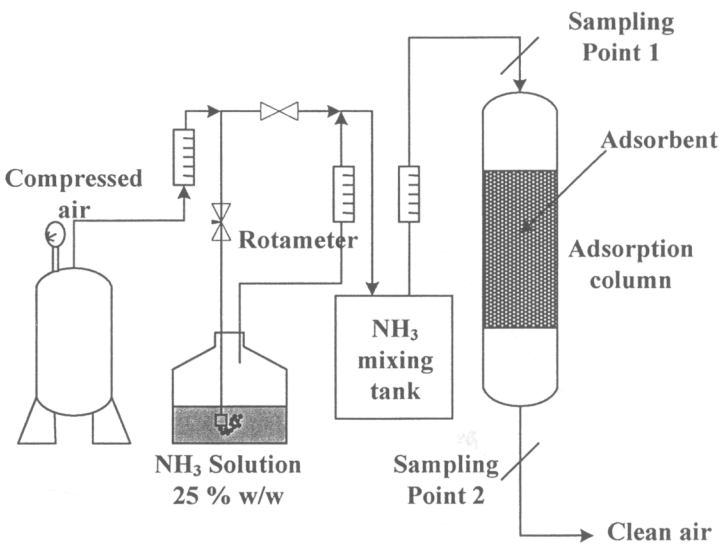

Figure 6.3 Schematic diagram of NH_3 contaminated waste air treatment system by adsorption.

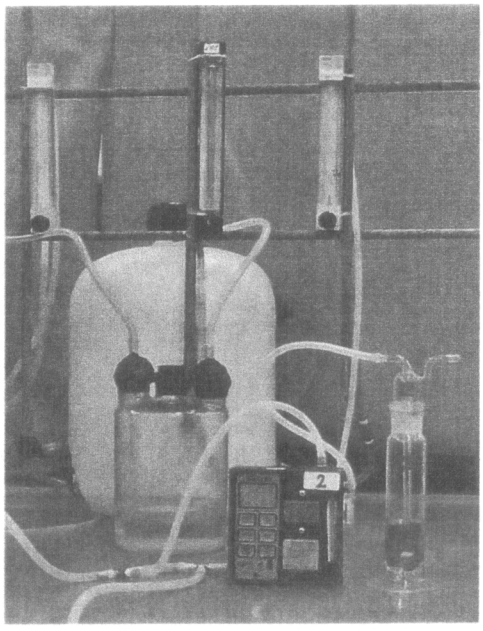

Figure 6.4 Experimental set up of NH_3 contaminated waste air preparing section and analyzer.

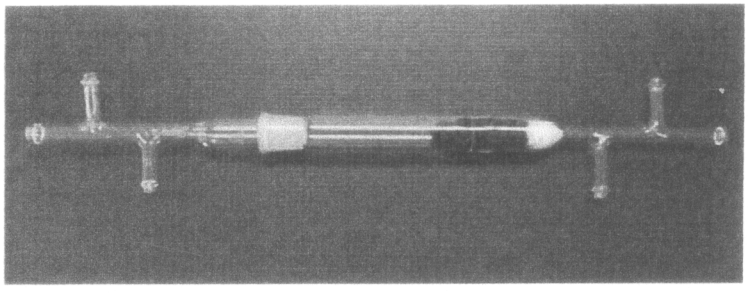

Figure 6.5 Glass adsorption column containing adsorbents and fiber glass.

NH_3 contaminated air stream was simulated for the test by passing air flow from air compressor through a NH_3 bottle. NH_3 solution of 25% w/w was filled in the bottle to pick up vaporized NH_3 gas and moisture to mix with the air stream at room temperature (28-29°C). The mixing stream was flowed through NH_3 mixing tank for continuously and steady flow to the adsorption column.

6.2.4 Operating parameters

Initial NH_3 concentration of 300-2000 ppmv and simulated waste air flow rate of 2-5 l/min was controlled by manual valves and flow meters (rotameters). NH_3 concentration in

air/NH_3 gaseous mixture was tested and measured by titration method. In the experiment, air samples were taken by sampling pump (224-PCXR8 Air Sampling Pump, SKC Inc.) for 2 min with air flow rate of 1 l/min. The NH_3 removal efficiency (%NH_3 Eff.) was calculated by equation (6.2) through concentration of NH_3 in inlet and outlet stream.

$$\%\,NH_3\ \text{Eff.} = \frac{C_i - C_o}{C_i} \times 100 \qquad (6.2)$$

where % NH_3 Eff. is percentage of NH_3 removal efficiency, C_i and C_o were NH_3 concentration (ppmv) in air streams at inlet and outlet point of adsorption column, respectively.

NH_3 inlet and outlet concentration in waste air was measured every 30 min until adsorption time of 4 h for NH_3 removal efficiency study and for breakthrough curve study, the concentration was measured every 10 min until C_i and C_o were the same.

6.3 Result and discussion

6.3.1 NH_3 adsorption by RWACs

1. Effect of H_2SO_4 concentration

Effect of H_2SO_4 concentrations (60-80%) for RWAC surface modification on NH_3 removal from waste air was investigated. Initial NH_3 concentration of 800 ppmv and waste air flow rate of 2 l/min in the adsorption experimental system was fixed. The results of NH_3 removal efficiency at each H_2SO_4 concentrations are ~~is~~ shown in Figure 6.6. On the NH_3 adsorption by using RWACs, the reaction between NH_3 and H_2SO_4 was shown in equation (6.3)

$$2NH_3(g) + H_2SO_4(aq) \rightarrow (NH_4)_2SO_4(s) \qquad (6.3)$$

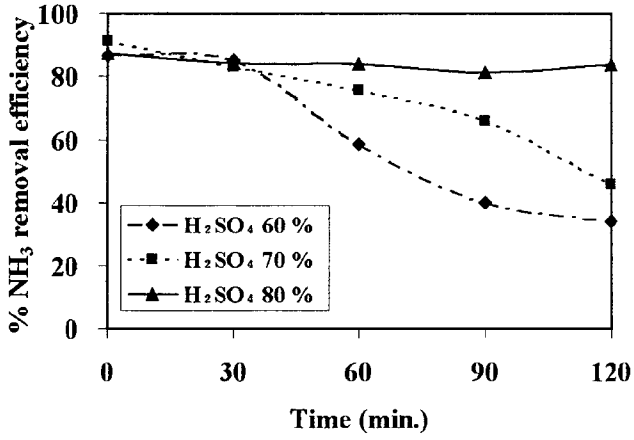

Figure 6.6 Effect of H_2SO_4 concentration for acidic adsorbent preparation on % NH_3 removal efficiency in adsorption system.

When RWACs was doped with higher H_2SO_4 concentration, the adsorption and reaction on the adsorbent surface was found better. Thus NH_3 was more removed from the waste air with more generation of $(NH_4)_2SO_4$ and more adsorption time. In the particular, the % NH_3 removal efficiency by H_2SO_4 80% RWACs was almost stable along 2 h experimental time.

2. Effect of adsorption parameter

The experiments of the adsorption for NH_3 contaminated waste air treatment were investigated. The adsorption parameters consisting of initial concentration and waste air flow rate on the NH_3 adsorption which was explained as follows.

2.1 Effect of initial NH_3 concentration

Effect of initial NH_3 concentration in waste air on % NH_3 removal efficiency by adsorption using H_2SO_4 70 % RWACs was demonstrated on Figure 6.7. Waste air flow rate of 2 l/min was constantly controlled. The result showed that %NH_3 removal efficiency (% Eff.) was decreased with initial NH_3 concentration (C_i) increased. It is because on the highly NH_3 concentration can generate more $(NH_4)_2SO_4$ on the activated carbon surface . Thus $(NH_4)_2SO_4$ crystals covered the pore mouth and then adsorption areas were reduced which effect to the decreasing in % NH_3 removal efficiency.

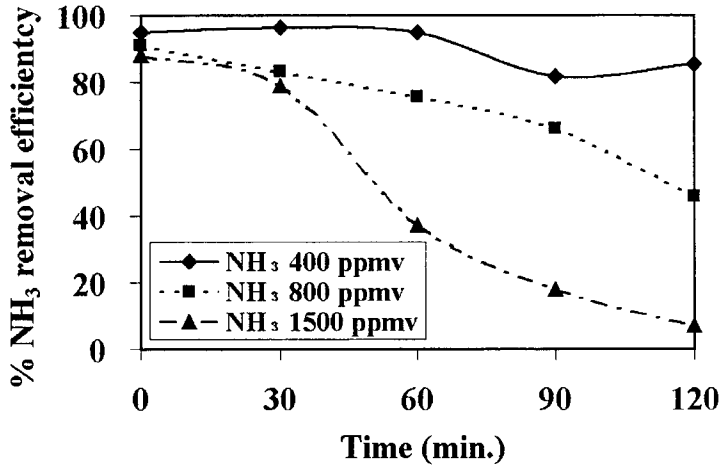

Figure 6.7 Effect of initial NH_3 concentration on % NH_3 removal efficiency by RWACs in adsorption system.

2.2 Effect of waste air flow rate

Effect of waste air flow rate (Q_T) on NH_3 removal efficiency by adsorption with 70 % w/w of RWACs and 800 ppmv of initial NH_3 concentration was shown in Figure 6.8

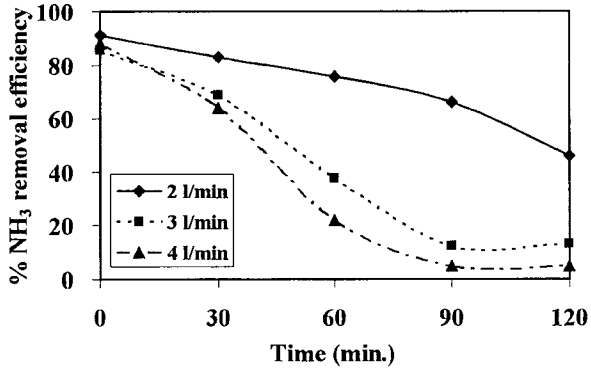

Figure 6.8 Effect of waste air flow rate on % NH_3 removal efficiency by RWACs.

The result demonstrated that when waste air flow rate was increased, % NH_3 removal efficiency was decreased. In consequence of higher waste air flow rate, the contact time between NH_3 in waste air and H_2SO_4 was shot so that the reaction was not complete and adsorption efficiency was low.

6.3.2 Comparisons of RWACs and RWBs of NH_3 adsorption

1. NH_3 removal efficiency from waste air

Effect of H_2SO_4 concentrations at 60-80% for RWACs and RWBs preparation on NH_3 removal from waste air are shown in Figure 6.9-6.10. Initial NH_3 concentration of 400 ppmv and waste air flow rate of 2 l/min were constantly controlled.

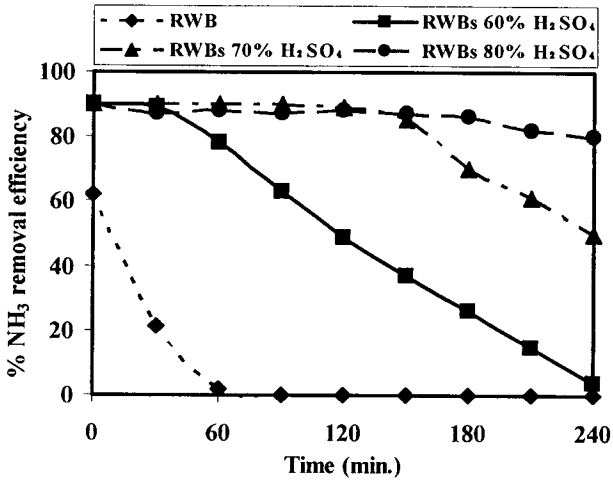

Figure 6.9 Effect of H_2SO_4 concentration for RWBs acidic adsorbent preparation on % NH_3 removal efficiency of the adsorption system.

The results showed that for original RWB and RWAC, the NH_3 removal efficiency were 60-80% and provided adsorption time only 1-2 h. However, after modified surface properties by H_2SO_4 impregnation, the % NH_3 removal efficiency was found higher than 90%. The increasing in acid concentration from 60 to 80% w/w for adsorbents surface modification, %NH_3 removal efficiency was increased. At H_2SO_4 80% w/w provides maximum NH_3 removal efficiency because the higher H_2SO_4 concentration on RWBs and RWACs surface increased the amount of H_2SO_4 reactant to react with NH_3. Thus NH_3 gas could be more removed from the waste air with more generating of $(NH_4)_2SO_4$.

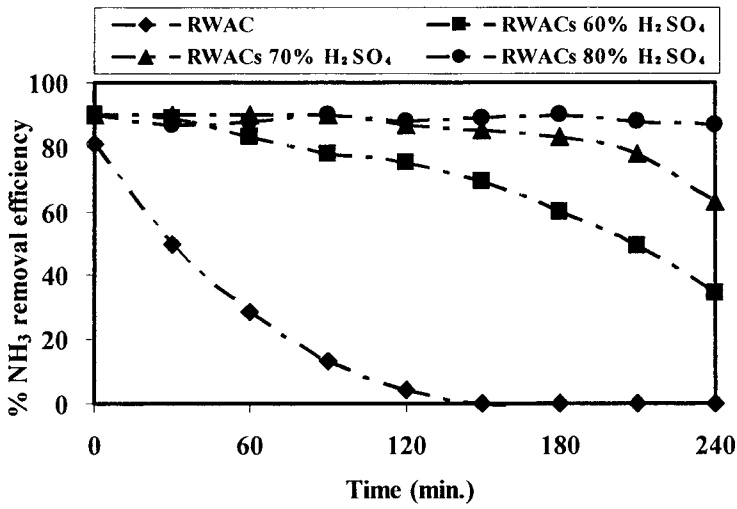

Figure 6.10 Effect of H_2SO_4 concentration for RWACs acidic absorbent preparation on % NH_3 removal efficiency of the system.

2. NH_3 breakthrough curve.

The breakthrough curves characterized the effects of H_2SO_4 concentration for RWBs preparation on performance of the NH_3 removal are shown in Figure 6.11-6.12. Initial NH_3 concentration of 800 ppmv and waste air flow rate of 2 l/min were constantly controlled. The results of adsorption time in NH_3 treatment for the breakthrough time of raw RWB and RWAC were lower than 2 h. On the other hand, the adsorbents soaking with H_2SO_4 had longer the adsorption time at more than 2 h and at 80 % H_2SO_4 of RWBs and RWACs provided adsorption time up to 3 h.

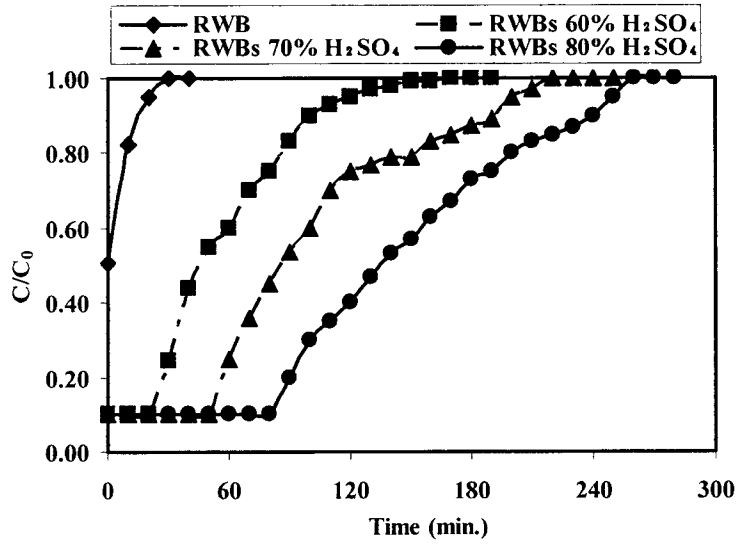

Figure 6.11 Effect of H_2SO_4 concentration for RWBs acidic adsorbent preparation on the breakthrough curve of NH_3 adsorption from waste air.

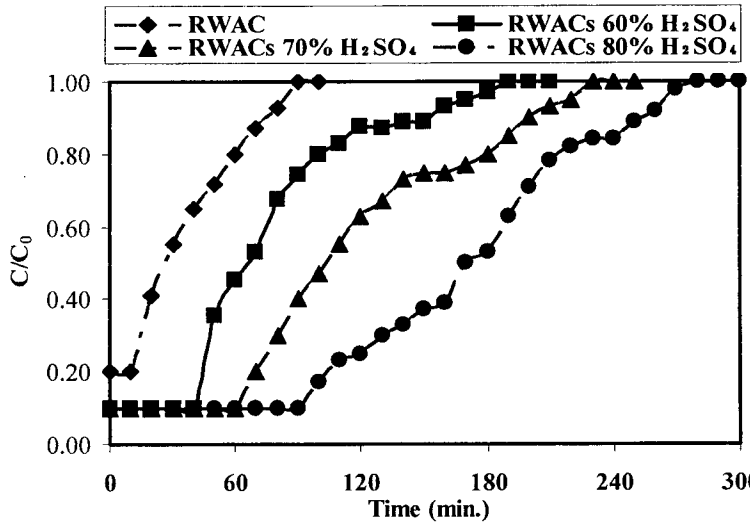

Figure 6.12 Effect of H_2SO_4 concentration for RWACs acidic adsorbent preparation on the breakthrough curve of NH_3 adsorption from waste air.

For comparison the result of breakthrough curve of NH_3 adsorption from waste air by RWBs and RWACs using 70% H_2SO_4, the data can be plotted as shown in Figure 6.13.

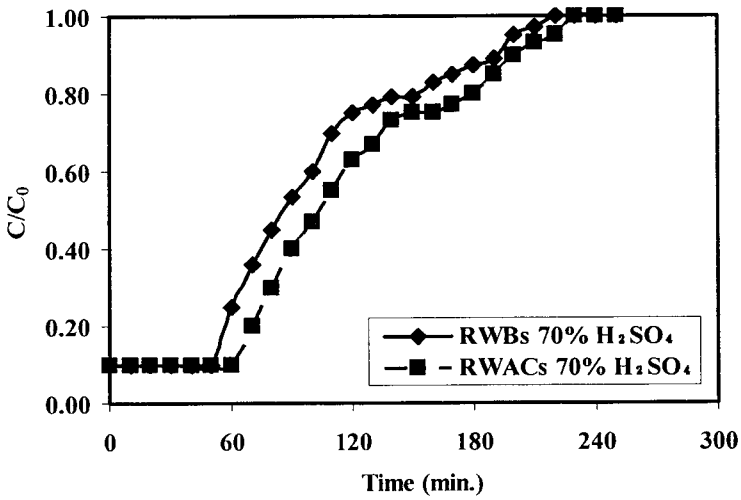

Figure 6.13 Breakthrough curve of NH_3 adsorption from waste air for comparison study between RWACs and RWBs at 70 % H_2SO_4 impregnation.

The result showed that slope of the breakthrough curve and breakthrough time of RWACs was slightly greater than RWBs as 2.20 h and 2.30 h, respectively. Since, the active sites on surface areas of the adsorbents after impregnation were a little difference as shown in table 6.2. The BET surface of RWACs and RWBs after impregnation with H_2SO_4 70 % were 6.73 and 2.22 m^2/g, respectively.

The table 6.2. showed BET surface area of RWACs and RWBs after impregnation with 70% H_2SO_4 and after using for NH_3 elimination till full with $(NH_4)_2SO_4$ crystals and inefficient in the same condition of NH_3 adsorption system. The BET surface areas of RWAC in Table 6.2 was much more than RWACs due to acid on RWACs was impregnated in pores site and stuck in micropores thus the surface areas were lower. On the other hand, BET surface area of RWB and RWBs were similar, because the mostly of pore structure of RWB were macropores and mesopores thus the molecule of H_2SO_4 was not stuck in there. Consequently, the result of breakthrough curve of RWACs and RWBs were similar.

Table 6.2 Characterization result of the fresh adsorbents (RWACs and RWBs) and after used to ammonia adsorption (RWACs^{u} and RWBs^{u}) at 70 % H_2SO_4 impregnation.

Sample	S_{BET} (m^2/g)	$S_{micropores}$ (m^2/g)
RWACs	6.73	0
RWACs^{u}	0.27	0
RWBs	2.22	0
RWBs^{u}	0.22	0

6.3.3 NH_3 adsorption by RWBs

After comparison study of NH_3 adsorption performance between RWACs and RWBs, the RWBs was selected to investigate the influence of initial NH_3 concentration in waste air, waste air flow rate, and concentration of H_2SO_4 impregnating on RWB were evaluated on NH_3 removal efficiency in adsorption column.

1. Effect of H_2SO_4 concentration

Effect of H_2SO_4 concentrations for RWB surface modification on NH_3 removal from waste air at inlet NH_3 concentration of 1300 ppmv and waste air flow rate 3 l/min is shown in Figure 6.14 The result showed that on the start up time, the % NH_3 removal efficiency was found higher than 80 %. The increasing in acid concentration from 40 to 80 % w/w for RWBs surface modification, %NH_3 removal efficiency was increased. At H_2SO_4 80% w/w provides maximum NH_3 removal efficiency because the higher H_2SO_4 concentration on RWBs surface increased the amount of H_2SO_4 reactant to react with NH_3. Thus NH_3 gas could be more removed from the waste air with more generating of $(NH_4)_2SO_4$.

Adsorption time at 50% NH_3 removal efficiency was considered at tie line of each experiment. The point was the ideal adsorption time for a breakthrough curve (Mccabe et al., 2005) and fitted as presented on Figure 6.15. The results confirm the effect of increasing in H_2SO_4 concentrations on RWBs surface to the increasing of NH_3 removal efficiency.

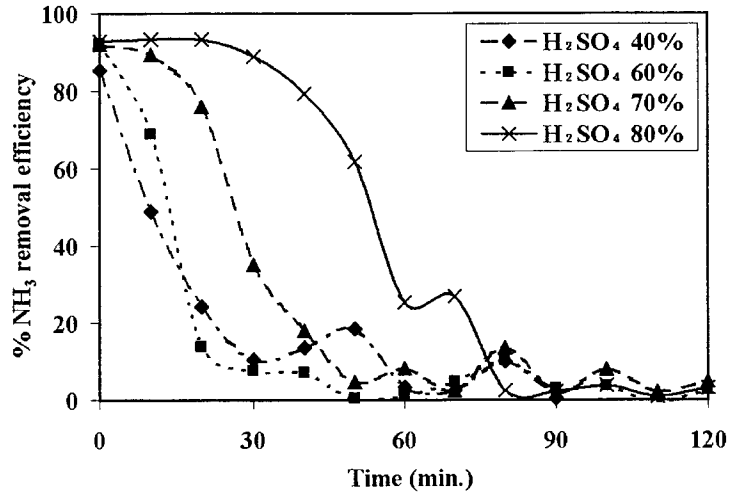

Figure 6.14 Effect of H_2SO_4 concentration for acidic adsorbent preparation on % NH_3 removal efficiency of the adsorption system.

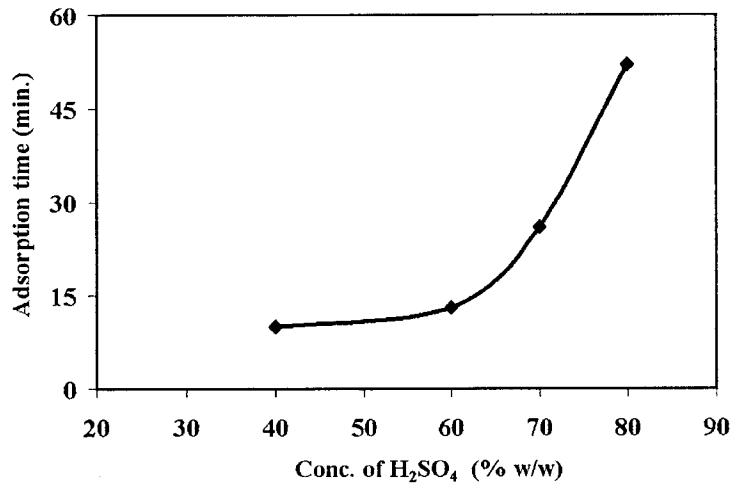

Figure 6.15 Effect of H_2SO_4 concentration for acidic adsorbent preparation on adsorption time at 50 % NH_3 removal efficiency of the system.

2. Effect of adsorption parameters

The experiments of the adsorption column were performed for NH_3 contaminated waste air treatment. The adsorption parameters consisting of initial concentration and waste air flow rate were investigated on the NH_3 adsorption which can be explained as following.

2.1 Effect of initial NH_3 concentration in waste air

Effect of initial NH_3 concentration in waste air on NH_3 removal efficiency by adsorption using H_2SO_4 40% w/w RWBs and waste air flow rate of 3 l/min was demonstrated in Figure 6.16. The result showed that at NH_3 concentration of 300 ppmv provides maximum NH_3 removal efficiency but when increasing NH_3 concentration NH_3 removal efficiency were decreased because at the highly NH_3 concentration can generate more $(NH_4)_2SO_4$ on the carbon surface. Thus $(NH_4)_2SO_4$ crystals covered the pore mouth and then adsorption areas were reduced which effect to the decreasing in NH_3 removal efficiency.

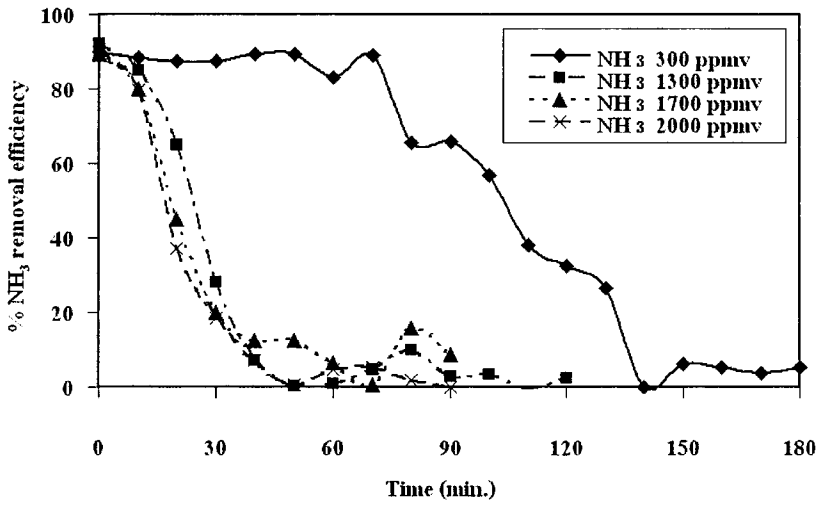

Figure 6.16 Effect of NH_3 Concentration in waste air on % NH_3 removal efficiency by RWBs.

Adsorption time at 50% NH_3 removal efficiency is shown for the effect of NH_3 inlet concentration in Figure 6.17. The trend of adsorption time was decreased when increasing inlet concentration of NH_3. At 300 ppmv of inlet NH_3 in waste air provided maximum adsorption time because the $(NH_4)_2SO_4$ crystal was slowly generated thus the crystal was not cover surface and pore mouth of RWBs and remaining more space for reaction. On the other hand, at the inlet of NH_3 concentration over 1300 ppmv , the adsorption time was too low due to the crystal of $(NH_4)_2SO_4$ was rapid generated and cover the surface of RWBs thus lacking of site to reaction and providing lower adsorption time.

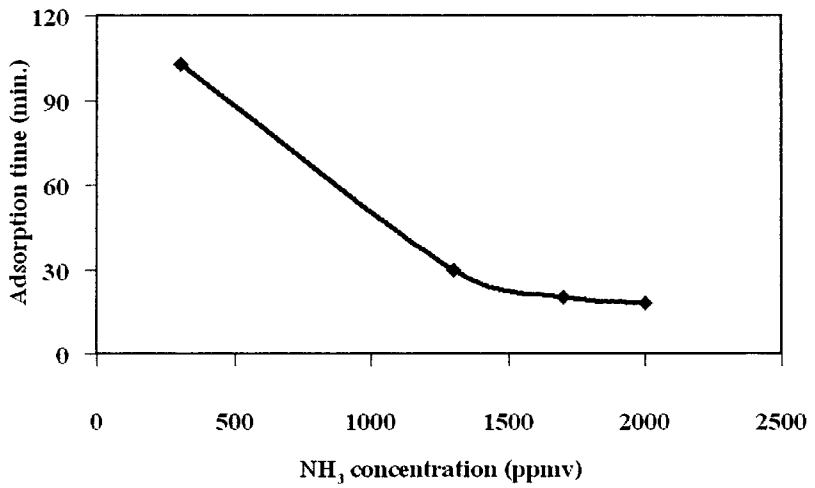

Figure 6.17 Effect of NH_3 inlet concentration on adsorption time at 50 % NH_3 removal efficiency of the system.

2.2 Effect of waste air flow rate

Effect of waste air flow rate on NH_3 removal efficiency by adsorption with 40 % w/w of RWBs and 1300 ppmv of initial NH_3 concentration was shown in Figure 6.18 and the effect of waste air flow rate on adsorption time at 50% NH_3 removal efficiency was manifested in Figure 6.19.

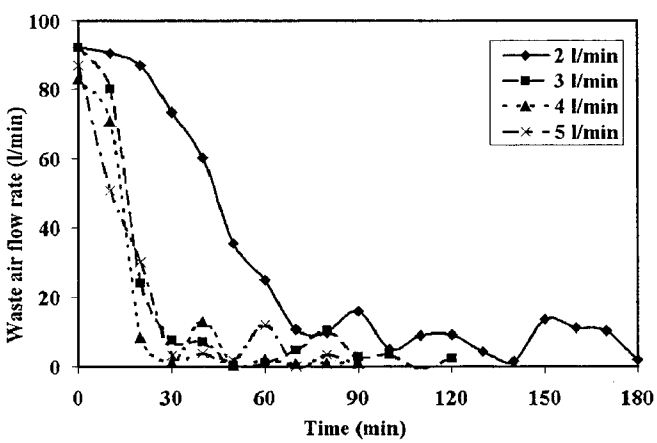

Figure 6.18 Effect of waste air flow rate on % NH_3 removal efficiency by RWBs

The result demonstrated that when waste air flow rate was increased from 2 to 5 l/min., % NH_3 removal efficiency was decreased. At waste air flow rate 2 l/min provides maximum %NH_3 removal efficiency. In consequence of higher waste air flow rate, the contact

time between NH_3 in waste air and H_2SO_4 on RWBs surface was rapid for the reaction was short so crystal from reaction between NH_3 in waste air and H_2SO_4 was fast to generate and cover surface and pore mouth thus the active site on surface are was deficiency and provided adsorption efficiency was lower.

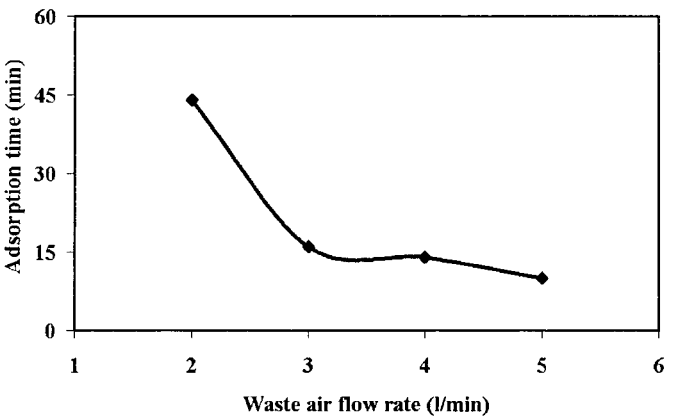

Figure 6.19 Effect of waste air flow rate on adsorption time at 50% NH_3 removal efficiency of the system.

6.5 Conclusion

The system of adsorption columns using rubber wood activated carbon impregnated with H_2SO_4 (RWACs) and rubber wood biochar impregnated with H_2SO_4 (RWBs) have effectively been used for NH_3 contaminated waste air treatment. Under the preparing RWACs and RWBs condition with high concentration of H_2SO_4, the NH_3 removal efficiency was increasing and reaches to 90% for eliminating NH_3. For the adsorption parameters; initial concentration and waste air flow rate, to NH_3 removal efficiency, the laboratory indicating that increasing of both parameters was decreasing NH_3 adsorption efficiency on the adsorbents. $(NH_4)_2SO_4$ was generated from reaction between NH_3 and H_2SO_4 on RWACs.

RWBs and RWACs have effectively been used for treatment of NH_3 contaminated waste air. Under the adsorbents preparing with high concentration of H_2SO_4, efficiency of NH_3 removal was increased up to 90%. From the removal efficiency and breakthrough curve of NH_3 adsorption, RWBs was slightly less removal efficiency and adsorption time than RWACs, so RWBs can be used for the adsorbent to eliminate NH_3 in waste air.

CHAPTER 7

MODELING AND OPTIMIZATION OF AMMONIA TREATMENT BY ACIDIC BIOCHAR USING RESPONSE SURFACE METHODOLOGY (RSM)

7.1 Introduction

Conventional and classical methods of studying a process by maintaining other factors involved at specified constant levels do not depict the combined effect of all the factors involved. Optimization of a multivariable system by conventional technique usually defines one factor at a time and needs to perform a lot of experiments. This method could not reveal the alternative effects between the components and also time consuming to determine optimum levels, which are unreliable. Recently, many statistical experimental design methods have been employed in chemical process optimization. The experimental design techniques are very useful tool for these purposes as it provides statistical models, which help to understand the interactions among the parameters. The CCD has been widely used for fitting a second-order model from experimental runs. These methods involve mathematical models for designing chemical processes and analyzing the process results. Among them, response surface methodology (RSM) is one of the suitable methods utilized in many fields. RSM is a collection of mathematical and statistical techniques useful for developing, improving, and optimizing processes and can be used to evaluate the relative significance of several affecting factors even in the presence of complex interactions. The main objective of RSM is to determine the optimum operational conditions for the system or to determine a region that satisfies the operating specifications (Mahalik et al., 2010). This method could effectively be used to form a process model and to predict results to achieve the optimal NH_3 removal efficiency of the adsorption column.

In this chapter, acidic rubber wood biochar was used for the removal of NH_3 from waste air through an chemical adsorption column. The acidic biochar had been prepared by impregnating the biochar with H_2SO_4 acid. The central composite design (CCD), a design of experiment, had been chosen to carry out the experiments at five levels in respect to an optimal

criterion. Three operating factors were chosen as independent variables, namely, the H_2SO_4 concentration for acidic biochar preparation, NH_3 concentration in waste air, and waste air flow rate. Using RSM, the interaction of possible influencing parameters on NH_3 removal efficiency can be evaluated. Graphical response surface and contour plots were used to localize the region of the optimum condition (Grutuito et al., 2008; Kayet et al., 2011).

7.2 Materials and methods

7.2.1 Materials

Rubber wood biochar (RWB) was carbonized in a stainless steel tube reactor (length 50 cm and i.d. 4 cm) under 4 l/min nitrogen at 500^{o}C for 2 h. The carbon products was crushed and sieved to the particle size of 2.36-3.36 mm. 95-97% H_2SO_4 and 25% NH_3 solution analytical grade obtaining from Merck were used as an impregnating reagent for acidic rubber wood biochar (RWBs) preparation and generating for NH_3 vapor to produce synthesized waste air, respectively.

7.2.2 Acidic biochar preparation and characterization

The RWBs acidic biochar was prepared by contacting 2 g of dried RWB into 10 ml of known H_2SO_4 concentration. Upon soaking time of 1 h at room temperature (28-29^{o}C), the samples was filtrated by a vacuum filter then dried in hot air oven at 110^{o}C for 1 h and cooled down in glass desiccators. Microscopic images of the RWBs were obtained by scanning electron microscope (JSM-5200). The SEM enables direct observation of the changes in the surface microstructures of the adsorbent due to the NH_3 adsorption.

7.2.3 NH_3 Adsorption experiments

Adsorption capacities of the RWBs adsorbent were tested in laboratory scale by continuous down-flow fixed-bed column. The schematic diagram of NH_3 contaminated waste air generation and adsorption unit is depicted in Figure 7.1 The adsorption column was a glass with an inside diameter of 2 cm and a column height of 15 cm. Fiber glass was installed in the bottom part of the column to support for the adsorbent.

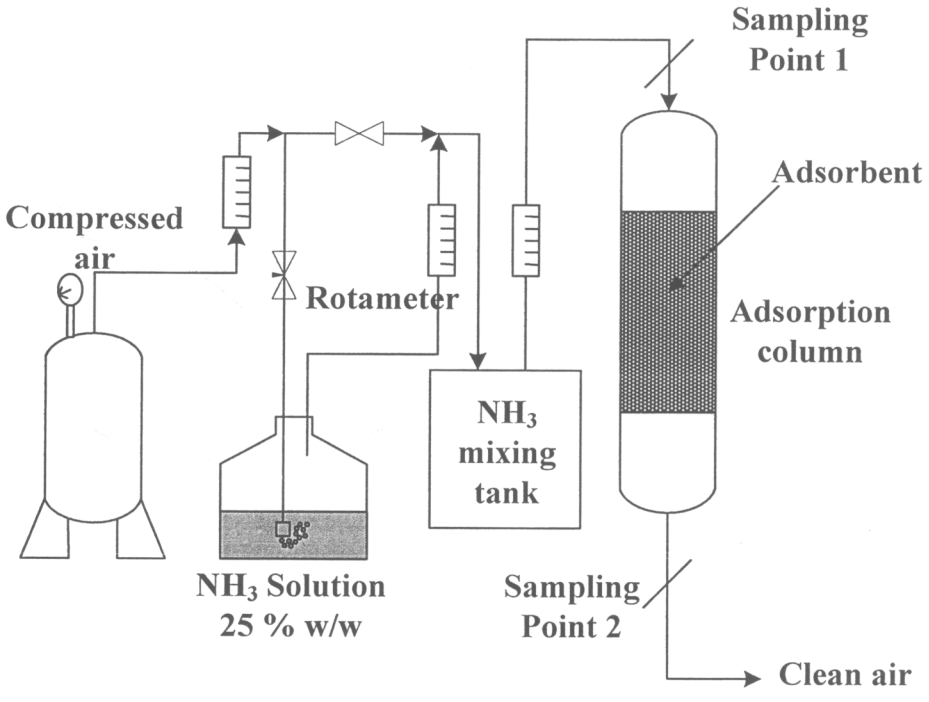

Figure 7.1 Schematic diagram of NH_3 contaminated waste air generation and adsorption system.

Waste air stream with NH_3 contamination was prepared for the adsorption test by flowing air stream from air compressor through NH_3 reservoir. NH_3 solution of 25% was filled in the reservoir to pick up the vaporized NH_3 gas and mix with the air stream at room temperature (28-29°C). The mixing stream was forced to flow through the mixing tank under continuous and steady flow to the adsorption column.

7.2.4 Air samples analysis

In the experiment, air samples from inlet and outlet waste air stream were taken by a sampling pump (224- PCXR8 Air Sampling Pump, SKC Inc.) every 10 min until concentrations of both streams were the same. The gaseous sample was bubbled through a 50 ml cold boric acid solution in an impinger (a glass gas wash bottle) at 2 l/min for 1 min. NH_3 absorbed was measured by titration method using 0.2% mixed indicators (methyl red and methylene blue) (American Public Health Association, 1995) and calculated for NH_3 concentration (ppmv) in synthesized waste air (Rodrigues et al., 2007). The percentage of NH_3 removal efficiency was calculated by Equation (7.1) through NH_3 concentration of inlet and outlet stream.

$$\text{Eff.}(\%) = \frac{C_i - C_o}{C_i} \times 100 \qquad (7.1)$$

where C_i and C_o are NH_3 concentration (ppmv) in the inlet and outlet waste air streams of adsorption test column. Eff. (%) is the percentage of NH_3 removal efficiency.

The symmetric adsorption time ($t_{1/2}$) of RWBs biochar adsorbent is defined as the ideal time at a proportion of 50% NH_3 adsorption efficiency for an operating curve or breakthrough curve at $C_i/C_o = 0.5$ (McCabe et al., 2005). The operating curves can be plotted between NH_3 adsorption efficiency versus operating time of waste air flowed through the bed. The $t_{1/2}$ can represent the adsorption capacity of the adsorbent and can be used for design of the adsorption column.

7.2.5 Experimental design and analysis

Basically, an optimization process involves three major steps, which are; performing the statistically designed experiments, estimating the coefficients in a mathematical model, and predicting the response and checking the adequacy of the model (Mahalik et al., 2010). Central composite design (CCD) has been applied in this work to study for the design of

NH_3 adsorption experiments. The design consists of a 2^n factorial or fraction (coded to the usual ± 1 notation) augmented by 2n axial points ($\pm\alpha$, 0, 0,..., 0), (0, $\pm\alpha$, 0,..., 0),..., (0, 0,..., $\pm\alpha$), and n_c center points (0, 0, 0,..., 0). In this case, the main effects and interactions may be estimated by fractional factorial designs running only a minimum number of experiments. The responses and the corresponding parameters were modeled and optimized using analysis of variance (ANOVA) to estimate the statistical parameters by means of RSM. If all variables are assumed to be measurable, the response surface can be expressed, in Equation (7.2), as follows.

$$Y = f(X_1, X_2, X_3, X_4....., X_n) \tag{7.2}$$

where Y is response of the system and X_i is the variables of action called factors. The goal of the RSM is to optimize the response variable (Y) and search for a suitable approximation of the functional relationship between the independent variables and the response surface. It is assumed that the independent variables are continuous and controllable by experiments with negligible errors.

The $t_{1/2}$ was applied for the response of the adsorption data in the RSM solution to develop an empirical model that is correlated to the three-process variables. NH_3 inlet concentration in waste air feeding, H_2SO_4 concentration for adsorbent preparation, and waste air flow rate were chosen as designed variables. Second degree quadratic equation as given by Equation (7.3) (Rajasimman and Murugaiyan, 2010) were used for model formation. Applying the relationships in Table 7.1, the values of the codes were calculated and shown in Table 7.2.

$$Y = \beta_0 + \sum_{i=1}^{k} \beta_i x_i + \sum_{i=1}^{k} \beta_{ii} x_i^2 + (\sum_{i=1}^{k-1} \sum_{j=i+1}^{k} \beta_{ij} x_i x_j)_{i<j} \tag{7.3}$$

where Y is the predicted response evaluated; x_i and x_j are the variables; β_0 is the constant coefficient; β_i, β_{ii} and β_{ij} are the coefficients of linear, quadratic, and the second-order terms, respectively; and k is the number of studied factors.

Table 7.1 Relationship between coded value and level of the variables (Mahalik et al., 2010).

Coded value	Level of variable
$-\alpha$	X_{min}
-1	$[(X_{max}+X_{min})/2]-[(X_{max}-X_{min})/2\beta]$
0	$(X_{max}+X_{min})/2$
+1	$[(X_{max}+X_{min})/2]+[(X_{max}-X_{min})/2\beta]$
$+\alpha$	X_{max}

Where X_{max} and X_{min} are maximum and minimum values of X, respectively; β is $2^{n/4}$, n = number of variables (in this study; $\beta = 2^{3/4} = 1.682$).

Table 7.2 Independent variables and their natural levels for CCD experimental design.

Independent Variables	Symbol	Natural variable levels				
		$-\alpha$	-1	0	+1	$+\alpha$
NH_3 inlet concentration (ppmv)	X_1	300	645	1150	1655	2000
H_2SO_4 concentration (%)	X_2	40	48	60	72	80
Waste air flow rate (l/min)	X_3	2	2.6	3.5	4.4	5

For statistical analysis, the experimental variables X_i have been coded as x_i according to the following Equation (7.4).

$$x_i = \frac{(X_i - X_0)}{\Delta X_i} \tag{7.4}$$

where x_i is the coded value (dimensionless) of the i^{th} independent variable, X_i is the uncoded value of the i^{th} independent variable, X_0 is the X_i at the center point, and ΔX_i is the step change value of the real variable i.

Total number of the tests (N_t) requiring for the three independent variables are shown in Equation (7.5).

$$N_t = 2^n + 2n + n_c = 2^3 + (2\times3) + 3 = 17 \quad (7.5)$$

The number of tests requiring for the CCD includes the standard 2^n factorial with its origin at the center, 2n points fixed axially at a distance, say α, from the center to generate the quadratic terms, and replicate tests at the center (n_c = 3); where n is the number of dependent variables. The axial points are chosen in such a manner that they allow rotatability, which ensures that the variance of the model prediction is constant at all points equidistant from the design center. Replicates of the test at the center are very important as they provide an independent estimate of the experimental error.

The quality of the fit of the polynomial model was expressed by the value of correlation coefficient (R^2) (Jain et al., 2011). The experimental design and optimization was generated using the Design-Expert program 8.0.6 trial version (Stat-Ease Inc., Minneapolis, USA).

7.3 Results and Discussions

7.3.1 Adsorption studies

NH_3 adsorption efficiency from waste air by acidic rubber wood biochar adsorbent in our work is at 90% (from 300 ppmv down to 30 ppmv). And since OSHA has set a permissible exposure limit concentration of 50 ppmv over an 8-h work day or a 40-h work week period for ammonia vapor in ambient air (Guo et al., 2005), our NH_3 outlet concentration resulted from a treatment of a quite high inlet waste air concentration is appreciably within OSHA standard.

From the experimental design table, we could present the adsorption capacity and determine the symmetric adsorption time ($t_{1/2}$) of each run by plotting the operating line and

breakthrough curve. The intersection between the operating line and the breakthrough curve generated the coordinate (50% Eff., $t_{1/2}$) and was a relatively straightforward approach to determine $t_{1/2.}$ Figure 7.2 shows the operating line and the breakthrough curve at experimental conditions of 1150 ppmv inlet NH_3 concentration, 80% H_2SO_4 concentration, and 3.5 l/min waste air flow rate.

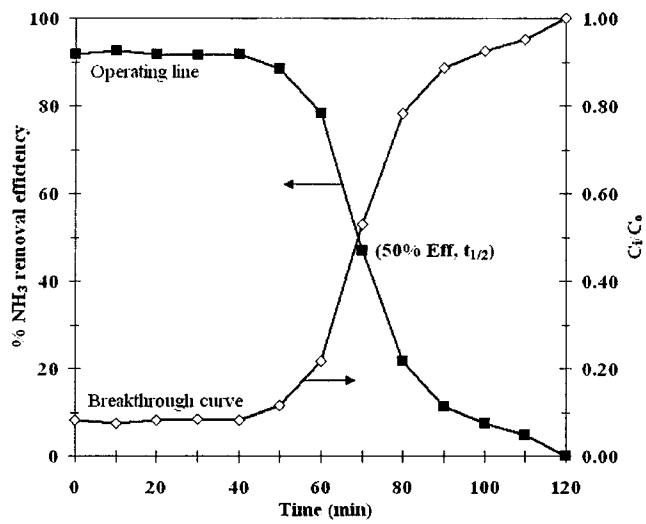

Figure 7.2 Correlation between operating line and breakthrough curve for symmetric adsorption time ($t_{1/2}$) determination in NH_3 adsorption system by biochar adsorbent.

Figure 7.3 presents the SEM surface images of RWBs at, before, and after NH_3 adsorption performed in the continuous waste air flow adsorption system. The inlet RWBs (see Figure 7.3a) shows a perfect honeycombed structure with clear opening of pores and thick walls. After NH_3 adsorption (see Figure 7.3b), the honeycombed structure was covered by crystals of $(NH_4)_2SO_4$.

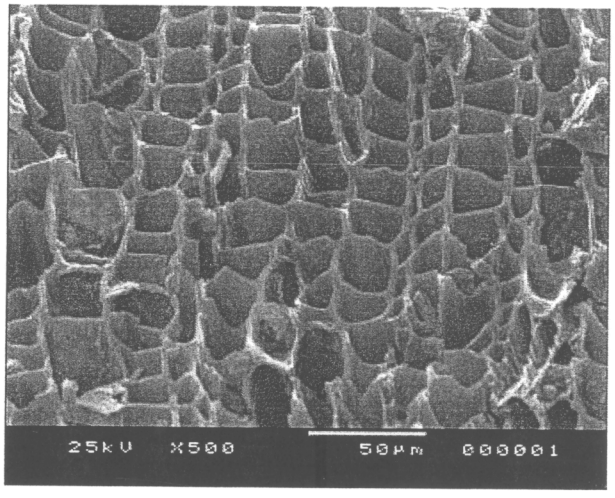

(a)

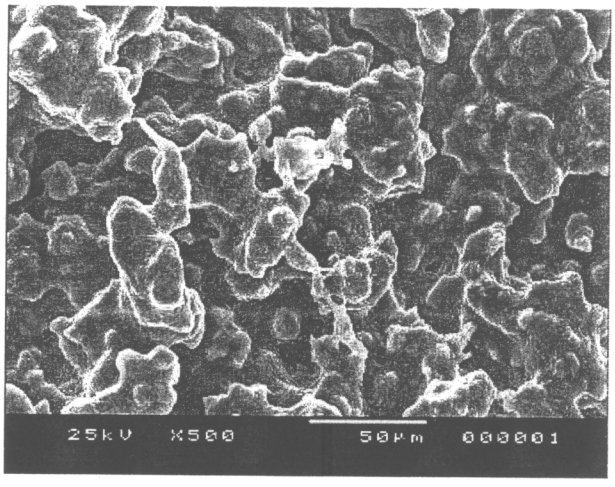

(b)

Figure 7.3 SEM photographs (500 x) of RWBs at before (a) and after (b) for NH_3 adsorption in continuous waste air flow adsorption system

7.3.2 ANOVA analysis and fitting of quadratic model

The statistical software package "Design Expert" has been used for regression analysis of the experimental data and to draw the response surface plot. ANOVA was used to estimate the statistical characteristics of the model fitting. The complete experimental design and results consisting of coded levels, actual variables, and responses are given in Table 7.3. In order to ensure a good model, a test for significance of the regression model and individual model coefficients was needed to be performed accompanying with the lack-of-fit test. Normally, the

significant factors can be ranked based on the F-value or p-value (also named "Prob. > F" value). The larger the magnitude of F-value and correspondingly the smaller the "Prob. > F" value, the more significant is the corresponding coefficient (Yi et al., 2010).

Table 7.3 Central composite design consisting of experiments for the study of experimental factors in coded and actual values with responses from experimental results.

Standard	Run	Coded values			Actual values			Response values
run no.		X_1	X_2	X_3	X_1 (ppmv)	X_2 (%)	X_3 (l/min)	$t_{1/2}$ (min)
1	15	-1	-1	-1	645	48	2.6	125
2	4	+1	-1	-1	1655	48	2.6	38
3	14	-1	+1	-1	645	72	2.6	148
4	11	+1	+1	-1	1655	72	2.6	56
5	2	-1	-1	+1	645	48	4.4	35
6	17	1	-1	+1	1655	48	4.4	22
7	16	-1	+1	+1	645	72	4.4	75
8	1	+1	+1	+1	1655	72	4.4	34
9	3	-α	0	0	300	60	3.5	117
10	13	+α	0	0	2000	60	3.5	41
11	12	0	-α	0	1150	40	3.5	28
12	10	0	+α	0	1150	80	3.5	70
13	7	0	0	-α	1150	60	2.0	65
14	6	0	0	+α	1150	60	5.0	25
15	5	0	0	0	1150	60	3.5	30
16	9	0	0	0	1150	60	3.5	32
17	8	0	0	0	1150	60	3.5	31

As there are many insignificant model terms from the full second quadratic model, they can be sorted out and then an improved model could be obtained. Thus, with the Design Expert program 8.0.6 trial version, the stepwise elimination procedure was selected to automatically eliminate the insignificant terms. The resulting ANOVA data for the reduced

quadratic model of total flux are given in Table 7.4. By applying multiple regression analysis on the experimental data, the reduced quadratic equation in terms of coded factors was obtained, as shown in Equation (7.6).

$$t_{1/2}=44.90 - 26.42X_1 + 11.98X_2 - 19.64X_3 + 15.63X_1X_3 + 15.28X_1^2 \quad (7.6)$$

where $t_{1/2}$ is the symmetric adsorption time. X_1, X_2, and X_3 are, respectively, the NH_3 inlet concentration, H_2SO_4 concentration, and waste air flow rate detailed in Table 7.2.

From Table 7.4 and Equation (7.6) significant terms for the response surface model can be determined. Firstly, the linear terms of the NH_3 inlet concentration (X_1), and the waste air flow rate (X_3) have largest negative effects on $t_{1/2}$, followed by H_2SO_4 concentration (X_2) which has a positive effect. The second order term of NH_3 inlet concentration X_1^2 and the interaction of X_1 and X_3 are also significant terms in the model. Ranking of these significant terms is as follows: $X_1>X_3>X_1^2>X_2>X_1X_3$. The predicted R^2 of 0.7749 is in reasonable agreement with the adjusted R^2 of 0.8745. The value of adequate precision is 15.0216, which is well above 4.

The application of the response surface methodology yields, on the basis of parameter estimates, an empirical relationship between the response variables (the symmetric adsorption time, $t_{1/2}$) and the test variables. These are related to the following quadratic expression in code unit, and after substituting Equation (7.6) to the refined model, the final model in terms of natural variables are obtained, as represented below:

$t_{1/2}$ = 340.2598 – (0.3111 × initial NH_3 concentration) + (1.0076 × H_2SO_4 concentration) – (61.8859 × waste air flow rate) + (0.0347 × initial NH_3 concentration × waste air flow rate) + (0.0001 × waste air flow rate^2) (7.7)

The quadratic equation obtained with multiple variables can be used to predict the $t_{1/2}$ within the limits of the experimental factors. Figure 7.4 reveals that the predicted response values of the reduced quadratic model are well in agreement with the actual ones in the range of the operating variables.

Table 7.4 ANOVA table (partial sum of squares) for reduce quadratic model.

Source	Sum of squares	DF	Mean Square	F-value	Prob > F	Remarks
Model	21757.20	5	4351.44	23.29	< 0.0001	significant
X_1	9532.82	1	9532.82	51.02	< 0.0001	significant
X_2	1960.66	1	1960.66	10.49	0.0079	significant
X_3	5269.86	1	5269.86	28.20	0.0002	significant
X_1X_3	1953.13	1	1953.13	10.45	0.0080	significant
X_1^2	3040.73	1	3040.73	16.27	0.0020	significant
Residual	2055.27	11	186.84			
Lack of Fit	2053.27	9	228.14	228.14	0.0044	significant
Pure Error	2.00	2	1.00			
Correlation Total	23812.47	16				
Standard deviation	13.67		R^2	0.9137		
Mean	57.18		Adjusted R^2	0.8745		
C.V. (%)	23.91		Predicted R^2	0.7749		
PRESS	5359.06		Adequate Precision	15.0216		

[a] DF= Degree of freedom

[b] C.V.= Coefficient of variation

[c] PRESS= Predicted residual sum of squares

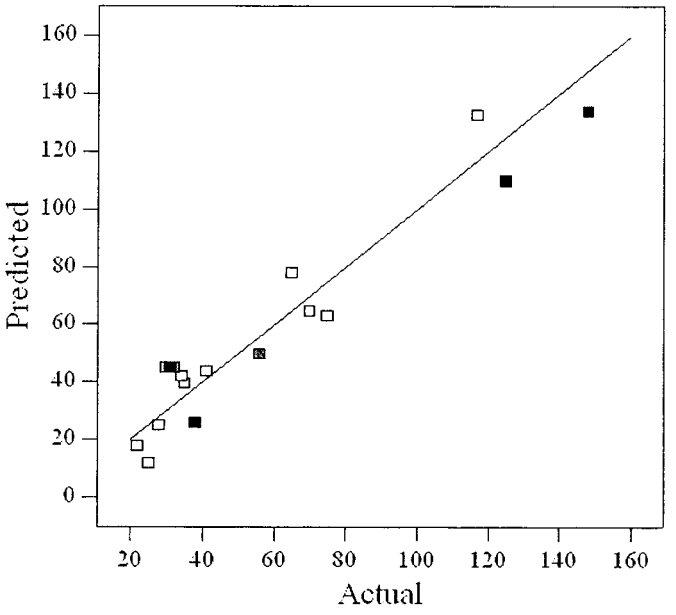

Figure 7.4 Plot of predicted response vs. actual value for $t_{1/2}$ response from reduced surface quadratic model.

7.3.3 Combined effect of operating parameters on the response

In order to visualize the relationship between the experimental variables and the response, and to study individual and interaction effects of the three factors consisting of the inlet NH_3 concentration, the H_2SO_4 concentration, and the waste air flow rate on the symmetric adsorption time ($t_{1/2}$) of NH_3 adsorption, response surfaces and contour plots were generated from the final model, as shown in Figure 7.5, and the contours were plotted in the x-y plane by projection of the response surface (Amari et al., 2008). These figures illustrate the response of different experimental variables and can be used to identify the major interactions between the variables. Each contour curve represents an infinite number of combinations of two test variables. Other factors are kept each time at their respective zero levels (Amari et al., 2008). A careful observation ANOVA results reveals that the inlet NH_3 concentration, the H_2SO_4 concentration, and the waste air flow rate have affected the response of symmetric adsorption time for NH_3 treatment. However, the inlet NH_3 concentration imposes the greatest effect while the H_2SO_4 concentration imposes the least. On the other hand, the quadratic effect of inlet NH_3 concentration

and the interaction effect of inlet NH_3 concentration and waste air flow rate impose also significant effects to the symmetric adsorption time of NH_3 treatment.

By keeping the waste air flow rate at 3.5 l/min, the combined effect of the inlet NH_3 concentration (X_1) and the H_2SO_4 concentration (X_2) was investigated as shown in 3D surface and its corresponding contour plotted in Figure 7.5a-b. As can be seen, the $t_{1/2}$ response decreases when the inlet NH_3 concentration changes from 300 ppmv to 2000 ppmv. The slope of the response surface is more negatively inclined with increasing inlet NH_3 concentration according to the additional term of X_1^2 in the quadratic model. The high NH_3 concentration generated more $(NH_4)_2SO_4$ crystals at the pore mouth which then reduced the adsorption area with an effect on the decrease in $t_{1/2}$. With the increase of H_2SO_4 concentration on the rubber wood biochar surface, $t_{1/2}$ also increased because the higher H_2SO_4 concentration on RWB surface increased the amount of H_2SO_4 reactant to react with NH_3 in the gas phase (Liang-hsing et al., 2006). Thus NH_3 gas could be more removed from the waste air with more generating of $(NH_4)_2SO_4$. The elliptical contour plot shows that the interaction term of X_1X_2, which indicates the higher H_2SO_4 concentration and lower inlet NH_3 concentration, has affected higher adsorption. The maximal $t_{1/2}$ of 182 min was obtained at 300 ppmv inlet NH_3 concentration and 80% H_2SO_4 concentration.

Figure 7.5c-d depicts the 3D plot and its corresponding contour plot to show the effects of H_2SO_4 concentration (X_2) and waste air flow rate (X_3) on $t_{1/2}$ response while keeping inlet NH_3 concentration (X_1) at 1150 ppmv. The graph shows that the maximum $t_{1/2}$ at 121 min occurs at 80% H_2SO_4 concentration and 2 l/min waste air flow rate which is in accordance with the model. Increasing the H_2SO_4 concentration, from 40 to 80 %, increased the $t_{1/2}$. It is very clear that H_2SO_4 concentration on the biochar surface has affected the NH_3 adsorption time. Increasing the waste air flow rate from 2 to 5 l/min, the $t_{1/2}$ was reduced. In consequence of higher waste air flow rate, the contact time between NH_3 in waste air and H_2SO_4 on the RWB surface was shortened, thus crystals from the reaction between NH_3 in the waste air and H_2SO_4 generated rapidly and covered the surface and the pore mouths of the RWB and hence the active sites on the surface were lessened, resulting in lower adsorption efficiency.

The combined effect of inlet NH_3 concentration (X_1) and waste air flow rate (X_3) has been analyzed. The $t_{1/2}$ from the response surface quadratic model, keeping H_2SO_4

concentration at 60%, is shown in the 3D surface plot and its corresponding contour plot in Figure 7.5e and Figure 7.5f, respectively. It can be observed that the slope of each contour curve of the waste air flow rate entirely depends on the inlet NH_3 concentration. The higher the waste air flow rate and the inlet NH_3 concentration, the lower the adsorption could be obtained. This indicates that the interaction effect between the waste air flow rate and the inlet NH_3 concentration is greatly pronounced, as confirmed by the significant test of the interaction term (X_1X_3) in the adsorption model. Because at higher waste air flow rate the retention time on the rubber wood biochar was short and higher NH_3 loading produced highly amount of NH_3 to react with H_2SO_4 on the surface, $(NH_4)_2SO_4$ crystals were immediately generated to cover the reactive surface and hence the adsorption areas were reduced with an effect in the drop of $t_{1/2}$. The maximum $t_{1/2}$ observed was 223 min when the inlet NH_3 concentration was 300 ppmv and the waste air flow rate was 2 l/min.

7.3.4 Process optimization using response surface methodology (RSM)

The optimum condition of NH_3 adsorption system was obtained using numerical optimization feature of the Design-Expert 8.0.6 software (Bhatia et al., 2009). The program searches for a combination of factor levels that simultaneously satisfy the requirements placed on each of the responses and factors. The reduced quadratic model was applied to determine the optimum condition for the response of $t_{1/2}$.The inlet NH_3 concentration of 300 ppmv was chosen and fixed for the NH_3 adsorption system because it is the level of NH_3 (200-300 ppmv) emitting in many industrial work places (Pollution Control Department, 2005).

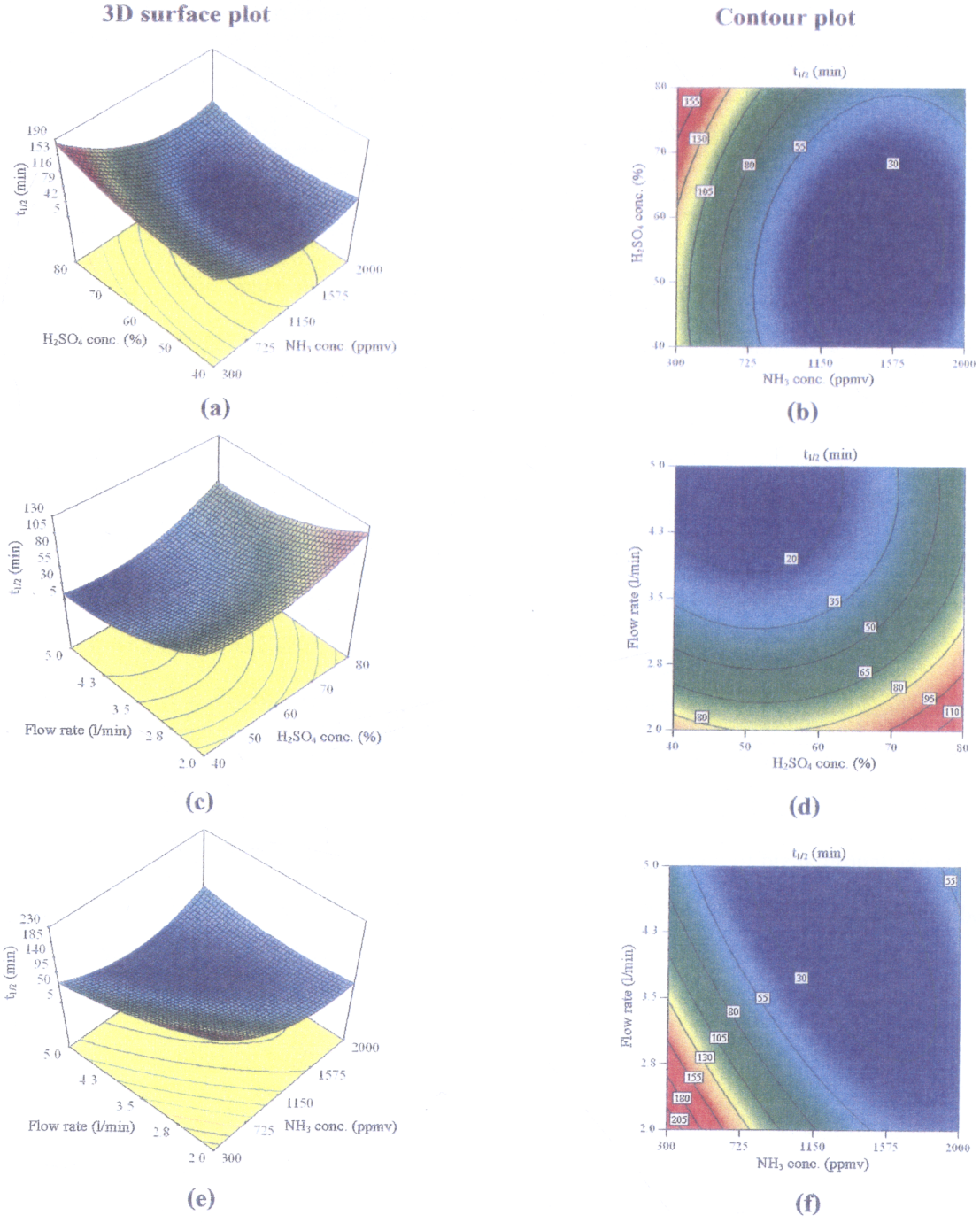

Figure 7.5 3D surface and contour plotted for combined effect of a,b) inlet NH_3 concentration and H_2SO_4 concentration of 3.5 l/min; c,d) H_2SO_4 concentration and waste air flow rate for 1150 ppmv NH_3; e,f) inlet NH_3 concentration and waste air flow rate under 60% H_2SO_4; on $t_{1/2}$ in the NH_3 adsorption system.

Table 7.5 Optimum condition and model validation of NH_3 adsorption system using acidic rubber wood biochar adsorbent.

NH_3 conc. (ppmv)	H_2SO_4 conc. (%)	Flow rate (l/min)	Symmetric adsorption time, $t_{1/2}$ (min)	
(X_1)	(X_2)	(X_3)	Predicted	Experimental
300	72	2.1	219	220

The most desirable experimental condition suggested by the software was selected for optimum condition to maximize the symmetric adsorption time ($t_{1/2}$). The predicted symmetric adsorption time for NH_3 adsorption from the waste air was at 219 min. The optimum result was verified by using 2 g of acidic biochar for adsorbing NH_3 from the waste air in a continuous adsorption unit according to experimental conditions given in Table 7.5. The verified experimental result of the symmetric adsorption time was at 220 min. It could be observed that the experimental value obtained from the adsorption system using biochar was in very good agreement with the value calculated from the model (Table 7.5).

For direct comparison, similar testing procedure was also applied on activated carbon commercial grade (AC; CGC – 11A in granular form with surface area of 1000-1100 m^2/g, purchased from Qualitech Supply Ltd.,Part., Songkhla, Thailand) Moreover, AC had been impregnated with H_2SO_4 to be acidic activated carbon (ACs). The result of breakthrough curve of NH_3 adsorption of 300 ppmv from waste air flow rate 2.1 l/min by AC and RWB, the data can be plotted as shown in Figure 7.6.

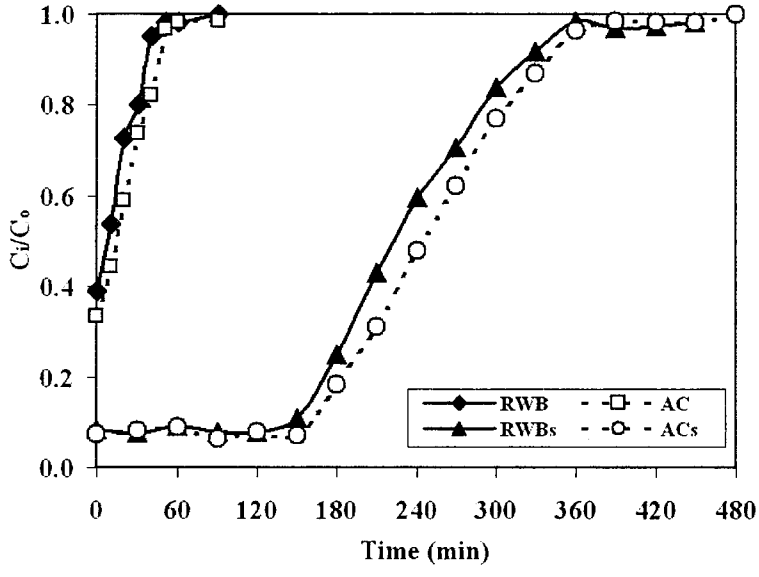

Figure 7.6 Breakthrough curve of NH_3 adsorption from waste air for comparison study between AC and RWB (without acid impregnation) and ACs and RWBs (with sulfuric acid impregnation)

From Figure 7.6, in comparing the NH_3 breakthrough curves of no-impregnation adsorbents (AC and RWB) and sulphuric acidic adsorbents (ACs and RWBs), it is obvious that NH_3 adsorption time of acidic adsorbents were much greater, and hence H_2SO_4 impregnation is a must. For either no-impregnated or impregnated adsorbent, the adsorption time of AC was slightly greater than RWB for the former, and the adsorption time of ACs was slightly greater than RWBs for the latter, meaning the use of AC is slightly better than the use of RWB. However, RWB is 3 times much cheaper than AC and the use of indigenous rubber wood biomass at an expense of slightly inferior adsorption property, instead of commercially available AC, can also render value-added aspect to the local product.

NH_3 adsorption capacity was calculated by integration of breakthrough curves (Rodrigues et al., 2007). Comparison with those of some other adsorbents reported in literature is given in Table 7.6. The value for NH_3 adsorption observed in this work is in good agreement with values found by other researches. Differences of NH_3 uptake are due to the properties of each adsorbent and experimental condition.

Table 7.6 Comparison of NH_3 adsorption capacity of various adsorbents reported in literatures.

Adsorbent	Adsorption capacity (mg g^{-1})	Reference
Natural clinoptilolite	12.70	Ciahotný et al. (2006)
Modified clinoptilolite Impregnated with acid	27.60-31.50	Ciahotný et al. (2006)
Activated carbon	0.60-1.80	Rodrigues et al. (2007)
Activated carbon impregnated with nitric acid	41.65	Huang et al. (2008)
Activated carbon impregnated with sulfuric acid	50.00	Liang-hsing et al. (2006)
Carbonaceous adsorbents from sewage sludge-based	18.7-20.6	Canals-Batlle et al. (2008)
Rubber wood biochar impregnated with sulfuric acid	46.35	This work

Table 7.6 details a literature review comparing some selective adsorbents that had been studied and reported. In general, adsorbents without acid impregnation yield markedly lower efficiency than those with acid impregnation. Activated carbon with nitric acid impregnation exhibited a slightly lower adsorption capacity than that impregnated with sulfuric acid. RWB impregnated with sulfuric acid showed a capacity value in between, with tendency towards the higher end, and thus can be considered one of the top choices for adsorbents.

7.4 Conclusion

In the present study, optimization of NH_3 removal from waste air with acidic rubber wood biochar (RWBs) was investigated to maximize the symmetric adsorption time ($t_{1/2}$) in a continuous NH_3 adsorption system. The NH_3 treatment process optimization focused on the influence of individual, as well as the interaction effect variables such as inlet NH_3 concentration, H_2SO_4 concentration, and waste air flow rate, employing response surface methodology (RSM) with central composite design (CCD). The multiple correlation coefficient of determination

R^2 obtained was 0.9137, inferring that the actual data fitted quite well with the predicted data applying the quadratic model. Regression analysis, ANOVA, and response surface plots were conducted using the Design Expert Software 8.0.6 trial version for predicting the responses in the experiment. The derived optimum condition for NH_3 adsorption by RWBs to yield the symmetric adsorption time at 219 min was an impregnation with 72% H_2SO_4 for removing NH_3 at 300 ppmv inlet concentration and 2.1 l/min waste air flow rate. By applying these parameter values, the maximal symmetric adsorption time has been predicted and confirmed experimentally. The by-product from the reaction between NH_3 and H_2SO_4 is $(NH_4)_2SO_4$ crystals which can be used as nitrogen fertilizer for plantation.

CHAPTER 8

REGENERATION OF RUBBER WOOD BIOCHAR

8.1 Introduction

The regeneration of adsorbents material is very important if processed are to be considered economically attractive. Steaming has been used for regenerating the spent activated carbon (Salvador and Sánchez Jiénez, 1999) with high pressure and temperature which is the causes damaging the porous structure of the adsorbent and has been high operating cost. Liang-hsing et al. (2006) employed low pressure steam at 103-105^{o}C for regeneration the spent adsorbent after adsorbs NH_3 by acidic activated carbon which was impregnated with H_2SO_4 which can be regenerated the adsorbent surface to 90%. The regeneration by-product is ammonium sulfate $(NH_4)_2SO_4$ solution, which is a perfect liquid fertilizer for local use. From the previous work, the hot water ($\approx$ 100 ^{o}C) is a possible alternative way to regenerate the spent adsorbents because $(NH_4)_2SO_4$ is highly soluble in water at low temperature and low pressure (http://en.wikipedia.org/wiki/Ammonium_sulfate).

This work aims to study for regeneration of the spent acidic rubber wood biochar (RWBs) after NH_3 adsorption in in the continuous down flow fixed-bed column system for NH_3 treatment. Leaching with hot water and refreshing the adsorbent with H_2SO_4 re-impregnation were applied and performed for reusing the RWBs. The influence of liquid water temperature and the regeneration times were investigated. The regenerated adsorbents were repacked in the continuous down flow fixed-bed column system for NH_3 in waste air treatment studies using breakthrough curve.

8.2 Research Methodology

8.2.1 Materials

Rubber wood biochar (RWB), as shown in Figure 8.1, was produced by carbonization in a stainless steel tube reactor (length 50 cm and i.d. 4 cm) under 4 l/min nitrogen at 500^{o}C for 2 h. The RWBs carbon products was crushed and sieved to particle size of 2.36-3.36 mm. H_2SO_4 acid 95-97% and NH_3 solution 25% obtained from Merck with analytical grade were used as an impregnating reagent and precursor for generating NH_3 gas contamination.

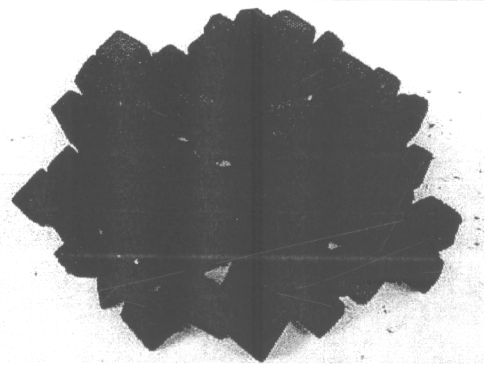

Figure 8.1 Picture of rubber wood charcoal (RWB)

8.2.2 Acidic adsorbent preparation

The RWBs acidic adsorbent was prepared by contacting 4 g of dried RWB into 10 ml of 70 % H_2SO_4. Upon soaking time of 1 h at room temperature (28-29^{o}C), the samples was filtrated by vacuum filter then dry in hot air oven at 110^{o}C for 1 h and cooled down in glass desiccators as shown in Figure 8.2.

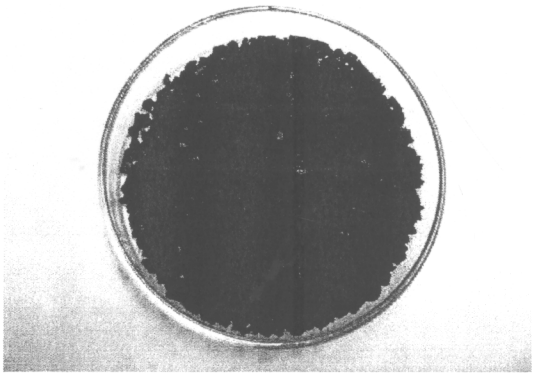

Figure 8.2 Impregnated rubber wood charcoal with H_2SO_4 (RWBs).

8.2.3 Adsorption experiments

The NH_3 adsorption RWBs were performed in laboratory scale of continuous down flow fixed-bed column. The schematic diagram of simulated waste air generation with NH_3 contaminated and adsorption unit are demonstrated in Figure 8.3. The adsorption column was designed using a glass with an inside diameter of 2 cm and column height of 15 cm. Fiberglass was installed in the bottom part to support RWBs in the column as shown in Figure 8.4.

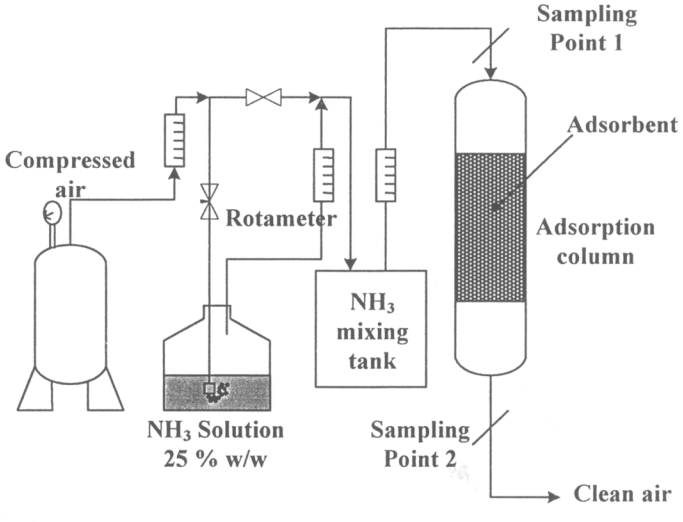

Figure 8.3 Schematic diagram of simulated waste air generation with NH_3 contaminated and treatment system of fix bed adsorption.

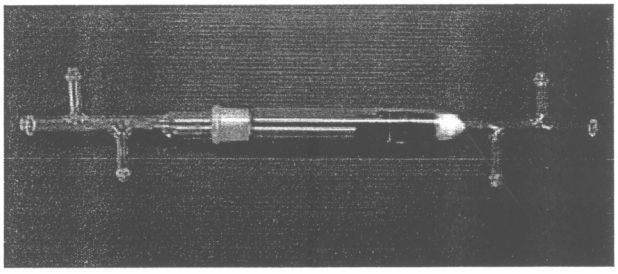

Figure 8.4 Glass adsorption column containing adsorbents and fiber glass.

NH_3 contaminated air stream was simulated for the test by passing air flow from air compressor through a NH_3 reservoir. NH_3 solution of 25% w/w was filled in the reservoir to pick up vaporized NH_3 gas and moisture to mix with the air stream at room temperature (28-29°C). The mixing stream was flowed through NH_3 mixing tank for continuously and steady flow to the adsorption column.

8.2.4 Adsorption operating parameters

The simulated NH_3 contaminated waste air was produced at initial NH_3 concentration of 300 ppmv and flow rate of 2 l/min by manual valves and flow meters (rotameters) controlling. NH_3 concentration in air/NH_3 gaseous mixture was tested and measured by titration method (Gue *et al.*, 2005). In the experiment, air samples were taken by sampling pump (224-PCXR8 Air Sampling Pump, SKC Inc.) for 2 min with air flow rate of 1 l/min. The breakthrough curve and breakthrough at 0.5 of each experiment was evaluated. NH_3 inlet concentration in waste air was measured every 30 min until inlet and outlet were the same, thus demonstrating the saturation of the adsorbent bed. Afterwards, regeneration was performed, and a new experiment was started.

8.2.5 Regeneration method

The apparatus for regeneration of the spent RWBs adsorbent is shown in Figure 8.5. The spent 4 g of RWBs was regenerated by leaching with 500 ml of tap water at various

temperatures (30-100°C) and stirring at 750 rpm for 3 h followed with dried at 110 °C for 3h and cooled in desiccators. Re-soaking with 10 ml of 70 % H_2SO_4 was performed for acid impregnation and new adsorption arrangement. The adsorption and regeneration cycles were repeated for 3 times to assess the reusability of RWBs.

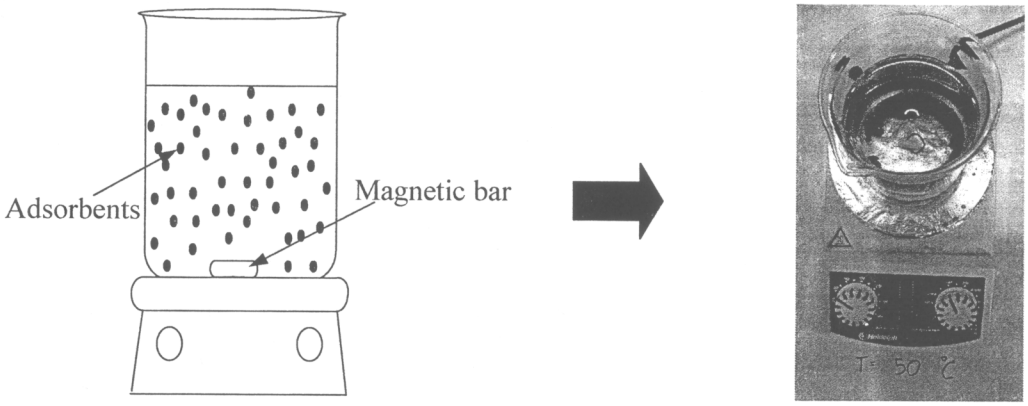

(a) Schematic diagram (b) Actual

Figure 8.5 Experimental set up for hot water regeneration of RWBs (a) Schematic diagram and (b) Actual

8.3 Results and Discussions

8.3.1 Breakthrough curve of NH_3 adsorption by RWBs

Breakthrough curves of RWBs on NH_3 removal from waste air for fresh adsorbent and the reusing without regeneration are shown in Figure 8.6.

Figure 8.6 showed the NH_3 adsorption breakthrough curve comparing between fresh RWBs ($RWBs^f$), reused RWBs with no re-impregnation ($RWBs^{no\text{-}nr}$), and used RWBs with re-impregnation with 70% H_2SO_4 ($RWBs^{no\text{-}r}$). $RWBs^{no\text{-}nr}$ and $RWBs^{no\text{-}r}$ were dried in hot air oven at 110°C before adsorption performing to evaporate water in the spent RWBs. The result showed that $RWBs^f$ provided breakthrough time of 6 h for NH_3 adsorption from original RWBs. On the other hand, NH_3 adsorption time of $RWBs^{no\text{-}nr}$ and $RWBs^{no\text{-}r}$ were 2 h and 3 h, respectively. After adsorption of NH_3 in waste air, ammonium sulfate ($(NH_4)_2SO_4$) crystal was generated and cover the pore mouth of RWBs and stuck in the pore as shown in Figure 8.7. Then the reusing without

any regeneration has effected to the lower adsorption time. The reusing of the adsorbent with H_2SO_4 acid re-impregnation also showed the very low NH_3 adsorption capacity.

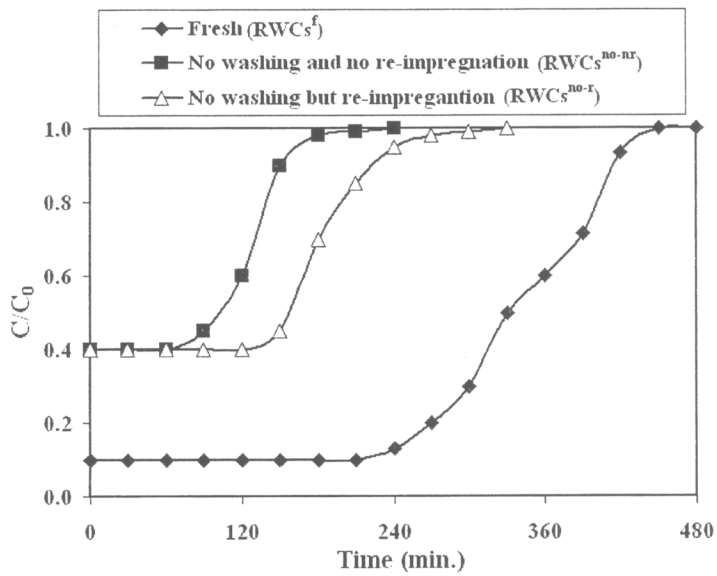

Figure 8.6 NH_3 adsorption Breakthrough curve of fresh RWBs ($RWBs^f$) (◆) and reused RWBs without regeneration at no washing and no re-impregnation ($RWBs^{no\text{-}nr}$) (■), and no washing and re-impregnation ($RWBs^{no\text{-}r}$) (△).

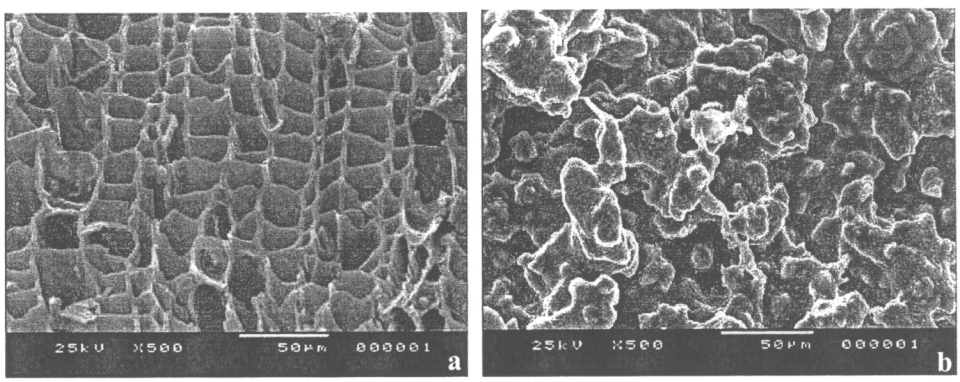

Figure 8.7 SEM photographs (500 x) of RWBs at before (a) and after (b) using for NH_3 adsorption

Drying of the spent adsorbent ($RWBs^{no\text{-}nr}$) in hot air oven has effected to changing the form of crystal in the pore structure. According to at temperature of 100°C, $(NH_4)_2SO_4$ was decomposed to other form of ammonium bisulfate (NH_4HSO_4) which is a salt of a strong acid and highly hygroscopic property (http://en.wikipedia.org/wiki/Ammonium_sulfte).

Therefore, the excess quantity of H_2SO_4 acid on the that $RWBs^{no\text{-}nr}$ can still adsorb react with NH_3 on the surface.

8.3.2 Breakthrough curves of NH_3 adsorption using 1st regenerated RWBs

Leaching method by hot water was chosen for regeneration the spent adsorbent in this work. Solubility of $(NH_4)_2SO_4$ in water can reach to 100% at 100 °C (http://en.wikipedia.org/wiki/Ammonium_sulfte). Figure 8.8 demonstrates the breakthrough curve of NH_3 adsorption from waste air by the effect of leaching temperature in the regeneration step of the spent RWBs. RWBs was re-impregnation by 70% H_2SO_4 for reusing adsorbed NH_3 at 300 ppmv

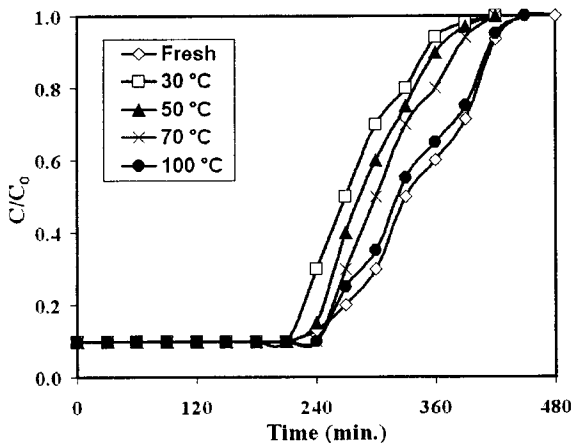

Figure 8.8 Effect of leaching temperature (30-100°C) on breakthrough curve of RWBs adsorption for 1st regeneration.

The result showed that when increasing the temperature of water in leaching step, the adsorption time was also increased. It was because of the solubility of $(NH_4)_2SO_4$ was raised with the higher leaching temperature (http://en.wikipedia.org/wiki/Ammonium_sulfte). The adsorption times of the 1st regenerated RWBs were found a little lower than fresh RWBs due to some of $(NH_4)_2SO_4$ crystal plugged in the adsorbent pore and the adsorbent surface was destroyed. The optimum temperature for the RWBs regeneration by leaching method was 100 °C that provided the NH_3 adsorption time of 6 h. pH of the leached water was 3-4.

8.3.3 Breakthrough curves of NH_3 adsorption using 2nd regenerated RWBs

For economical use of the biochar adsorbent in actual operating, many time of regeneration for the reusing should be performed the adsorption time was decreased. The 2nd regeneration of RWBs was studied by leaching the spent adsorbent with hot water. Breakthrough curves of NH_3 removal from waste air by adsorption performing are shown in Figure 8.9 at different leaching temperature. The result showed that the adsorption time was increased as the increasing in leaching temperature. After 2nd regeneration, higher adsorption time of the spent RWBs for NH_3 removal was found comparing to the fresh RWBs.

Table 8.1 shows BET surface area of the fresh adsorbents (RWBs), 1st regenerated RWBs, and 2nd regenerated RWBs impregnating with 70% H_2SO_4. The regeneration was performed by leaching with water at 30°C. For more times of regeneration and acid re-impregnation on RWBs, the surface of RWBs was corroded and destroyed. Higher BET surface area was generated to increase active site of the RWBs for NH_3 adsorption. After regeneration, the weigh of RWB of each time was lost estimated to 0.06 g. The optimum temperature of 2nd regeneration spent RWBs to NH_3 adsorption was 100°C and provided adsorption time to 9 h.

Table 8.1 Characterization results of the fresh adsorbents (RWBs), 1st regenerated RWBs, and 2nd regenerated RWBs by impregnating with 70% H_2SO_4 and regenerating with water at leaching temperature of 30 °C.

Sample	S_{BET} (m^2/g)	Smicropores (m^2/g)
Fresh RWBs	2.22	0
1st regenerated RWBs	1.80	0
2nd regenerated RWBs	3.25	0

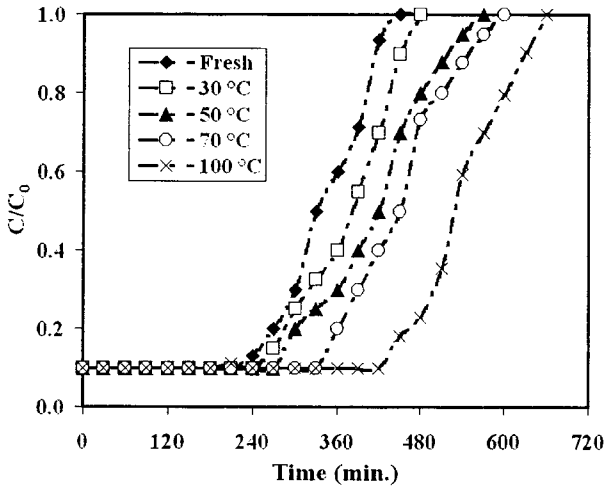

Figure 8.9 Effect of leaching temperature (30-100°C) on breakthrough curve of RWBs adsorption for 2nd regeneration.

8.4 Cost evaluation

8.4.1 Adsorbent preparation cost

For applying the rubber wood biochar (RWBs) on the treatment of NH_3 in waste air releasing from industry, adsorbent preparation cost of the adsorbent was evaluated. The prices of the main materials were offered such as rubber wood biochar and H_2SO_4 solution as shown in table 8.2. Moreover, cost of activated carbon commercial grad (AC) was offered to cost comparisons with rubber wood biochar (RWB).

From Table 8.2, the price of RWB is much cheaper than AC about 20 times. From the result in Figure 7.6, indicated that the adsorption time of AC was slightly greater than RWB for the former, and the adsorption time of ACs was slightly greater than RWBs for the latter, meaning the use of AC is slightly better than the use of RWB. However, the use of indigenous rubber wood biomass at an expense of slightly inferior adsorption property, instead of commercially available AC, can also render value-added aspect to the local product.

Table 8.2 Cost of chemical reagent for NH_3 adsorption/ kg biochar.

Materials cost	
Rubber wood biochar (RWB) from local market[a]	5-6 Baht/kg.
Activated carbon (AC)[b]	110-120 Baht/kg
H_2SO_4 70% w/w (solution)[c]	19 Baht/kg.
$(NH_4)_2SO_4$ (powder)[c]	21 Baht/kg.
Acidic adsorbent preparation (1 kg)	
H_2SO_4 70% w/w (kg / kg of adsorbents)	2.54 kg/kg of adsorbents
Acidic rubber wood biochar (RWBs)	14-15 Baht/kg
Acidic activated carbon (ACs)	45-47 Baht/kg

[a] Hatyai, Songkhla, Thailand

[b] Qualitech Supply Ltd.,Part., Songkhla, Thailand

[c] Boss Optical Limited Partnership, Songkhla, Thailand

8.4.2 Operating cost estimation of RWBs for NH_3 adsorption

Fresh RWBs for NH_3 adsorption:

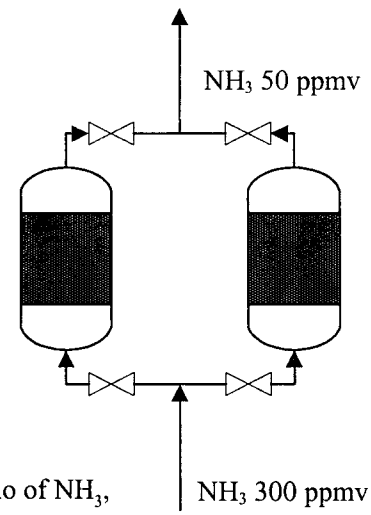

Molecular weight of

NH_3 17.031 g/mol

H_2SO_4 98.079 g/mol

$(NH_4)_2SO_4$ 132.14 g/mol

From stoichiometric ratio:

$2NH_{3(g)} + H_2SO_{4(aq)} \rightarrow (NH_4)_2SO_{4(s)}$

Reaction stoichiometry describes the 2:1:1 ratio of NH_3, H_2SO_4, and $(NH_4)_2SO_4$ moles in the above equation.

From the experiment, 1 kg of biochar absorbed 70 % H_2SO_4 of 1.65 L.

Density of 70 % H_2SO_4 is 1.54 g/cm^3, so, amount of 70 % H_2SO_4 is equal to:

$$1.54\frac{g}{cm^3} \times 1000\frac{cm^3}{L} \times 1.65\,L \times 0.001\frac{kg}{g} = 2.54\,kg$$

Base on 2.54 kg of 70 % H_2SO_4 on 1 kg biochar

Transform in unit of mole:

$$70\,\%\ H_2SO_4\ 2.54\,kg \times \frac{1\,mole}{98.079\,g} \times 1000\frac{g}{kg} = 25.90\,mole$$

From the reaction, 1 mole of H_2SO_4 reacted with 2 mole of NH_3, so, the amount of NH_3 for reaction with 70 % H_2SO_4 25.90 mole is:

$$NH_3 = 25.90\ mol \times 2 = 51.80\,mole \times 17.031\frac{g}{mole} = 882.21\ g$$

In NH_3 adsorption system, the inlet, outlet and waste air flow rate was defined as:

NH_3 inlet concentration 300 ppmv or 0.206 mg/l

NH_3 outlet concentration 50 ppmv or 0.034 mg/l

Waste air flow rate 100 m^3/h

From material balance

input – output = accumulate

So; 300 ppmv – 50 ppmv = 250 ppmv

Or: $0.206\ mg/l - 0.034\ mg/l = 0.172\frac{mg}{L} \times 1000\frac{L}{m^3} \times 0.001\frac{g}{mg} = 0.172\,g/m^3$

From waste air flow rate at100 m^3/h, calculated amount of NH_3 that accumulated in the adsorption column per hour as:

$$100\ m^3/h \times 0.172\ g/m^3 = 17.2\ g/h$$

From amount of NH_3 that reacted H_2SO_4 followed by stoichiometry and the amount of accumulated NH_3 per hour, can calculate the adsorption time of NH_3 by fresh RWBs as:

$$882.21\ g \times \frac{1}{17.2}\ h/g = 51.30\ h \text{ or } 2.14\ days$$

The by-product of reaction between NH_3 and H_2SO_4 is $(NH_4)_2SO_4$ which is the good nitrogen fertilizer so we can trade the $(NH_4)_2SO_4$ to the farmer.

From stoichiometric, the ratio of H_2SO_4: $(NH_4)_2SO_4$ is 1:1. Thus, H_2SO_4 25.90 mole produced $(NH_4)_2SO_4$ as:

$$(NH_4)_2SO_4 = 25.90\,mole \times 132.14\frac{g}{mole} = 3422.43\,g \text{ or } 3.42\,kg$$

From the data in Table 8.2, we can calculate the cost and profit of the NH_3 adsorption by fresh RWBs 1 kg.

Weight of RWBs was the sum of acid weight and biochar weight.

So; Weight of biochar + Weight of acid = Weight of RWBs

1 kg + 2.54 kg = 3.54 kg

Price of 70 % H_2SO_4 is 19 Baht/kg and Biochar is 6 Baht/kg, the price of RWBs 1 kg is;

$$6\ \frac{\text{baht}}{\text{kg}}\ (1\ \text{kg}) + 19\ \frac{\text{baht}}{\text{kg}}\ (2.54\ \text{kg}) \longrightarrow \frac{54.26\ \text{Baht}}{3.54\ \text{kg}} = 15.33\ \text{Baht/kg RWBs.}$$

The price of $(NH_4)_2SO_4$ is 21 Baht/kg and the weight of $(NH_4)_2SO_4$ from stoichiometry is 3.42 kg on the RWBs 3.54 kg. Thus, we calculated the price of $(NH_4)_2SO_4$ / kg RWBs;

$$21\ \frac{\text{baht}}{\text{kg}}\ (3.42\ \text{kg}) \longrightarrow \frac{71.82\ \text{baht}}{3.54\ \text{kg}} = 20.29\ \text{Baht/kg RWBs.}$$

Finally, we calculated the profit from NH_3 adsorption by RWBs as;

Income of $(NH_4)_2SO_4$–Budget of RWBs = Profit of NH_3 adsorption;

20.29 baht/kg RWBs – 15.33 baht/kg RWBs = 4.96 baht/kg RWBs

Regeneration:

After regeneration, biochar was re-impregnated with 70 % H_2SO_4 so the cost of original biochar was not include for calculated operating cost. Thus, we calculated cost and profit of the NH_3 adsorption by RWBs.

Price of 70 % H_2SO_4 is 19 Baht/kg, the price of RWBs 1 kg is;

$$0\ \frac{\text{baht}}{\text{kg}}\ (1\ \text{kg}) + 19\ \frac{\text{baht}}{\text{kg}}\ (2.54\ \text{kg}) \longrightarrow \frac{48.26\ \text{Baht}}{3.54\ \text{kg}} = 13.63\ \text{Baht/kg RWBs.}$$

The income of $(NH_4)_2SO_4$ / kg RWBs is 20.29 Baht/kg RWBs.

Finally, we calculated the profit from NH_3 adsorption by RWBs as;

Income of $(NH_4)_2SO_4$–Budget of RWBs = Profit of NH_3 adsorption;

20.29 baht/kg RWBs – 13.63 baht/kg RWBs = 6.66 baht/kg RWBs

Summary

Base on 2.54 kg of 70 % H_2SO_4 on 1 kg biochar can eliminate NH_3 300 ppmv about 2 days and the by-produce is $(NH_4)_2SO_4$ can sell and provided profit of 4.96 Baht/ kg RWBs of fresh RWBs. For regenerated RWBs, the original biochar was not include so the cost was decreased. Thus the profit from NH_3 adsorption by regenerated RWBs was 6.66 Baht/ kg RWBs.

Standard heat of reaction between NH_3 and H_2SO_4

From Hess's law;

$$\Delta\hat{H}_r^o = \sum_i v_i \Delta\hat{H}_{fi}^o = \sum_{products} |v_i| \Delta\hat{H}_{fi}^o - \sum_{reactants} |v_i| \Delta\hat{H}_{fi}^o$$

When v_i is the stoichiometric coefficient of the i^{th} species participating in a reaction (+ for products, - for reactants) and $\Delta\hat{H}_{fi}^o$ is the standard heat of formation of this species.

From stoichiometric ratio:

$$2NH_{3(g)} + H_2SO_{4(aq)} \rightarrow (NH_4)_2SO_{4(s)}$$

Standard heat of formation of:

NH_3	$-46.19_{(g)}$	kJ/mol
H_2SO_4	$-907.51_{(aq)}$	kJ/mol
$(NH_4)_2SO_4$	$-1179.3_{(s)}$	kJ/mol

From Hess's law;

$$\Delta\hat{H}_r^o = \left(\Delta\hat{H}_f^o\right)_{(NH_4)_2SO_{4(s)}} - \left(\Delta\hat{H}_f^o\right)_{H_2SO_{4(aq)}} - 2\left(\Delta\hat{H}_f^o\right)_{NH_{3(g)}}$$

$$\Delta\hat{H}_r^o = [-1179.3 - (-907.51) - 2(-46.19)]\,kJ/mol$$

$$= -179.41\ kJ/mol$$

So, the reaction between NH_3 and H_2SO_4 is exothermic reaction.

Notices: The heat from reaction between NH_3 and H_2SO_4 was decreased by waste air flow through the bed and convect the heat to the discharge.

8.5 Conclusions

RWBs can effectively be used for NH_3 adsorption from waste air and regenerated by leaching method using hot water. The leaching temperature of 100^oC gave optimum condition for RWBs regeneration and reusing in the adsorption column. From the breakthrough curve of NH_3 adsorption, 2^{nd} regeneration provided the higher adsorption time comparing to fresh and 1^{st} regeneration which can be adsorbed NH_3 to 9 h.

CHAPTER 9

SUMMARY AND FUTURE WORKS

9.1 Summary

Activated carbon producing from rubber wood chip by H_3PO_4 activation provided higher yield (%).On the other hand, the H_2SO_4 acid performed a higher BET and micropore surface area of the activated carbon. So, mixing acid between H_3PO_4 and H_2SO_4 was selected to activate rubber wood off-cut for high yield and well develops porosity of activated carbon. The optimum condition for activated carbon preparation from rubber wood off-cut is the acid mixing of H_3PO_4 50% w/w and H_2SO_4 40% w/w. The temperature and time for activation performing were 400^{o}C and 2 hour that provided 40% yield of the product, 1200 m^2/g BET surface area, and 700 m^2/g Micropores surface area. The optimum condition for biochar preparation was obtained from 500^{o}C and 2 hour activation which provided 25% yield, 3 m^2/g BET surface area.

The system of adsorption columns using rubber wood adorbents impregnated with H_2SO_4 (RWACs and RWBs) has effectively be used for NH_3 contaminated waste air treatment. Under the preparing the acidic adsorbents condition with high concentration of H_2SO_4, the NH_3 removal efficiency was increasing and reaches to 90% for eliminating NH_3. For the adsorption parameters; initial concentration and waste air flow rate, to NH_3 removal efficiency, the laboratory indicating that increasing of both parameters was decreasing NH_3 adsorption efficiency on the acidic adsorbents. From the removal efficiency and breakthrough curve of the NH_3 adsorption, RWBs was slightly less removal efficiency and adsorption time than RWACs. By-product of the treatment is ammonium sulfate ($(NH_4)_2SO_4$) which is a good nitrogen fertilizer.

A central composite design (CCD) coupled with response surface methodology (RSM) was successfully employed to obtain the optimum process conditions while the interactions between process variables were demonstrated and elucidated. The adsorption time at 50% NH_3 removal efficiency on acidic rubber wood biochar was significantly decreased by

increasing inlet NH_3 concentration and waste air flow rate. On the other hand, increasing of H_2SO_4 concentration, the adsorption time to removal NH_3 from waste air was also increased. The optimum condition for the NH_3 adsorption by acidic rubber wood biochar is impregnation with 72% H_2SO_4 for removing NH_3 at 300 mg/m_3 of inlet concentration on 2.1 l/min waste air flow rate to give the adsorption at 50% NH3 removal efficiency at 219 min. The simulated data fitted the experimental data satisfactorily.

RWBs has effectively been used and regenerated for NH_3 adsorption from waste air by hot water leaching. The leaching temperature of 100^{o}C gave optimum condition for RWBs regeneration and reusing in the adsorption column.

9.2 Future works

1) Study the adsorption isotherm and kinetic of adsorption of acidic rubber wood biochar for NH_3 adsorption.
2) Operating cost evaluation between acidic rubber wood activated carbon and acidic rubber wood biochar for NH_3 adsorption.
3) Further study of regeneration rubber wood biochar by hot water and analysis the by-product and estimated the cost.
4) Study the alternative acid for modified surface of adsorbent for NH_3 adsorption.
5) Apply this method to eliminate NH_3 in the industries.

REFERENCES

Amari, A., Gannouni, A., Chlendi, M., and Bellagi, A. 2008. Optimization by response surface methodology (RSM) for toluene adsorption onto prepared acid activated clay. The Canadian journal of chemical engineering 86, 1093-1102.

American Public Health Association. 1995. Standard methods for the examination of water and wastewater . U.S.A., pp. 4-77.

Anupam, K., Dutta, S., Bhattacharjee, C., and Datta, S. 2011. Adsorptive removal of chromium (VI) from aqueous solution over powdered activated carbon: Optimisation through response methodology. Chemical Engineering Journal. 173, 135-143.

Arulkumar, M., Sathishkumar, P., and Palvannan, T. 2011. Optimization of Orange G dye adsorption by activated carbon of thespesia populnea pods using respons surface methodology. Journal of Hazardous Materials. 186, 827-834.

Asada, T., Ohkudo, T., Kawata, K., and Oikawa, K. 2006. Ammonia adsorption on bamboo Charcoal with Acid Treatment. Journal of Health Science, 52(5): 585-589.

Aslan, N. 2008. Application of response surface methodogy and central composite rotatable design for modeling and optimization of a muti-gravity separator for chromite concentration. Powder Technology. 185, 80-86.

Barrett, E.P., Joyner, L.G., and Halenda, P.H. 1951. Journal America Chemical Society. 73, 373.

Bashir, M., Aziz, H., and Yusoff, M. 2011. New sequential treatment for mature landfill leachate by cationic/anioic and anionic/cationic processes: Optimization and comparative study. Journal of Hazardous Materials.186, 92-102.

Benaddi, H., Legras, D., Rouzaud, J.N., and Beguin, F. 1998. Influence of the atmoshere in the chemical activation of wood by phosphoric acid. Carbon. 36, 306-309.

Bell, M.J., and Worrall, F. 2011. Charcoal addition to soils in NE England: A carbon sink with environmental. Science of the Total Environment. 409, 1704-1714.

Berčič, G, and Pinter, A. 1996. Desorption of phenol from activated carbon by hot water regeneration. Desorption isotherms. Industrial & Engineering Chemistry Research. 35, 4619-4625.

Bhatia, S., Wong, C., and Abdullah, A. 2009. Optimization of air-borne butyl acetate adsorption on dual-function Ag-Y adsorbent-catalyst using response surface methodology. Journal of Hazardous Materials. 164, 1110-1117.

Biomass Cleating House, 2006. Biomass, 1st ed. Energy for environment Foundation, Thailand.

Brunauer, S., Emmett, P.H., and Teller, E. 1938. Journal America. Chemical. Society. 60, 309.

Budinova, T., Ekinci, E., Yardim, F., Grimm, A., Björnbom, E., Minkova, V., and Goranova, M. 2006. Characterization and application of activated carbon produced by H3PO4 and water vapor activation. Fuel Processing Technology. 87, 899-905.

Canals-Batlle, C., Ros, A., Lillo-Ródenas, M.A., Fuente, E., Montes-Morán, M.A., Martin, M.J., and Linares-Solano, A. 2008. Carbonaceous adsorbents for NH3 removal at room temperature. Carbon. 46, 176-178.

Ciahotný, K., Melenová, L., Jirglová, H., Pachtová, O., Kočiřík, M., and Eić, M. 2006. Removal of ammonia from waste air streams with clinoptilolite tuff in its natural and treated forms. Adsorption. 19, 219-226.

De, S., and White, J. 2001. Rubber Technologist's Handbook, Rapra Technology Limited, United Kingdom, pp. 11-19.

Duku, M., Gu, S., and Hagan, E. 2011. Biochar production potential in Ghana-A review. Renewable and Sustainable Energy reviews. 15, 3539-3551.

Dumroese, R., Heiskanen, J., Englund, K., and Tervahauta, A. 2011. Pelleted biochar: Chemical and physical properties show potential use as a substrate in container nurseries. Biomass & Bioenergy. 35, 2018-2027.

Fortier, H., Westreich, P., Selig, S., Zelenitetz, C., and Dahn, J. R. 2008. Ammonia, cyclohexane, nitrogen and water adsorption capacities of an activated carbon impregnated with increasing amount of $ZnCl_2$, and designed to chemisorb gaseous NH_3 from an air stream. Journal of Colloid and Interface Science, 320: 423-435.

Gerçel, Ö., Özcan, A., Özcan, A., and Gerçel, H. 2007. Preparation of activated carbon from a renewable bio-plant of Euphorbia rigida by H_2SO_4 activation and its adsorption behavior in aqueous solutions. Applied Surface Science. 253, 4843-4852.

Girgis, B., Attia, A., and Fathy, N. 2007. Modification in adsorption characteristics of activated carbon produced by H_3PO_4 under flowing gases. Colloids and Surfaces A: Physicochem. Eng. Aspects. 299, 79-87.

Gómez-Serrano, V., Cuerda-Correa, E.M., Fernández-González, M.C., Alexandre-Franco, M.F., and Macías-García, A. 2005. Preparation of activated carbons from chestnut wood by phosphoric acid-chemical activation. Study of microporosity and fractal dimension. Materials Letters. 59, 846-853.

Gratuito, M.K.B., Panyathanmaporn, T., Chumnanklang, R.-A., Sirinuntawittaya, N., and Dutta, A. 2008. Production of activated carbon from coconut shell: Optimization using response surface methodology. Bioresource Technology. 99, 4887-4895.

Guo, J., and Lua, A. 1999. Textural and chemical charactersations of activated carbon prepared from oil-plam stone with H_2SO_4 and KOH impregnation. Microporous and Mesoporous Materials. 32, 111-117.

Guo, J., Xu,W. S., Chen,Y. L., and Lua, A. C. 2005. Adsorption NH_3 onto activated carbon prepared from palm shells impregnated with H_2SO_4. Journal of Colloid and Interface Science. 281, 285-290.

Guo, X., Tak, J., and Johnson, R. 2009. Ammonia removal from air stream and biogas by a H_2SO_4 impregnated adsorbent originating from waste-shavings and biosolids. Journal of Hazardous Materials. 166, 372-376.

Guo, Y., and Rockstraw, D. 2007. Activated carbons prepared from rice hull by one-step phosphoric acid activation. Microporous and Mesoporous Materials. 100, 12-19.

Haimour, N.M., and Emeish, S. 2006. Utilization of date stones for production of activated carbon using phosphoric acid. Water Management. 26, 651-660.

Huang, C., Li, H., and Chen, C. 2008. Effect of surface acidic oxides of activated carbon on adsorption of ammonia. Journal of Hazardous Materials. 159, 523-527.

Jain, M., Garg, V.K., and Kadirvelu, K. 2011. Investigation of Cr(VI) adsorption onto chemically treated Helianthus annuus: Optimization using Response Surface Methodology. Bioresource Technology. 102, 600-605.

Kalavathy, M. H., Karthikeyan, T., Rajgopal, S., and Miranda, L. R. 2005. Kinetic and isotherm studies of Cu(II) adsorption onto H_3PO_4-activated rubber wood sawdust. Journal of Colloid and Interface Science. 292, 354-362.

Karagöz. S., Tay, T., Ucar, S., and Erdem, M. 2008. Activated carbons from waste biomass by sulfuric acid activation and their use on methylene blue adsorption. Bioresource Technology. 99, 6214-6222.

Khayet, M., Zahrim, A.Y., and Hilal, N. 2011. Modelling and optimization of coagulation of highly concentration industrial grad leather dye by response surface methodology. Chemical Engineering Journal. 167, 77-83.

Krukanont, P., and Prasertsan, S. 2004. Geographical distribution of biomass and potential sites of rubber wood fired power plants in southern Thailand. Biomass & Bioenergy. 26, 47-59.

Kumar, A., Prasad, B., and Mishra, I.M. 2008. Optimization of process parameters for acrylonitrile removal by a low-cost adsorbent using Box-Behnken design. Journal of Hazardous Materials. 150, 174-182.

Kumar, A., Prasad, B., and Mishra, I.M. 2009. Optimization of acrylonitrile removal by activated carbon-granular using response surface methodology. The Canadian journal of chemical engineering. 87, 637-643.

Kumar, B.G., Miranda, L., and Velen, M. 2005. Adsorption of Bismark Brown dye on activated carbons prepared from rubberwood sawdust (Hevea brasiliensis) using different activation methods. Journal of Hazardous Materials. B126, 63-70.

Kumar, B.G., Shivakamy, K., Miranda, L., and Velan, M. 2006. Preparation of stream activated carbon from rubber wood sawdust (Hevea brasiliensis) and its adsorption kinetics. Journal of HazardouS Materials. B136, 922-929.

Lammirato, C., Miltner, A., and Kaestner, M. 2011. Effects of wood char and activated carbon on the hydrolysis of cellobiose by β-glucosidase from Aspergillus niger. Soil Biology & Biochemistry. 43, 1936-1942.

Lee, K., and Kim, J. 1996. High-temperature properties of ferroelastic $(NH_4)_2SO_4$. Journal of the Korean Physical Society (Proc. Suppl.). 29, S424-S428.

Lei, X., Li, M., Zhang, Z., Feng, C., Bai, W., and Sugiura N. 2009. Electrochemical regeneration of zeolites and the removal of ammonia. Journal of Hazardous Materials. 169, 746–750.

Liang-hsing, C., Ru-in, T., Jen-ray, C., and Maw-tien, L. 2006. Regenerable adsorbent for removing ammonia elvoed from anaerobic reaction of animal urine. Journal of Environmental Sciences. 18, 1176-1181.

Mahalik, K., Sahu, J.N., Patwardhan, A., and Meikap, B.C. 2010. Statistical modeling and optimization of hydrolysis of urea to generate ammonia for flue gas conditioning. Journal of Hazardous Materials. 182, 603-610.

Mccabe, W. L., Smith, J. C., and Harriott, P. 2005. Unit operations of chemical engineering. The McGraw-Hill companies, Singapore, pp. 846-847.

Montgomery, D. 2005. Design and Analysis of Experiments. John Wiley & Sons, Inc., U.S.A., pp. 418-419.

Patnaik, P. 2002. Handbook of inorganic chemicals. McGraw-Hill, New York, U.S.A., pp. 43-45.

Özçimen, D., and Ersoy-Meriçboyu, A. 2010. Characterization of biochar and bio-oil sample obtained from carbonization of various biomass materials. Renewable Energy. 35, 1319-1324.

Prahas, D., Kartika, Y., Indraswati, N., and Ismadji, S. 2008.Activated carbon from jackfruit peel waste by H_3PO_4 chemical activation: pore structure and surface chemistry characterization. Chemical Engineering Journal. 140, 32-42.

Rajasimman, M., and Murugaiyan, K. 2010. Sorption of Nickel by Hypnea Valentiae: Application of Response Surface Methodology. World Academic of Science, Engineering and Technology C: Civil and Environmental Engineering. 3:1, 7-12.

Rodrigues, C. C., Moraes, D., Nóbrega, S. W., and Bardoza, M. G. 2007. Ammonia adsorption in a fixed bed of activated carbon. Bioresource Technology. 98, 886-891.

Salvador, F., and Sánchez Jiénez. C. 1999. Effect of regeneration treatment with water at high pressure and temperature on the characteristics of three commercial activated carbons. Carbon. 37, 577-583.

Sánchez-Romeu, J., País-Chanfrau, J.M., Pestana-Vila,Y., López-Larraburo, I., Masso-Rodríguez,Y., Linares-Domínguez, M. et al. 2008. Statistical optimization of immunoaffinity purification of hepatitis B surface antigen using responsesurface methodology. Biochem Engineering Journal. 38, 1–8.

Scott, A., and Damblon, F. 2010. Charcoal: Taphonomy and significance in geology, botany and archaeology. Palaeogeography, Palaeoclimatology, Palaeoecology. 291, 1-10.

Singh, C.K., Sahu, J.N., Mahalik, K.K., Mohanty, C.R., Mohan, B., and Meikap, B.C. 2008. Studies on the removal of Pb(II) from wastewater by activated carbon developed from Tamarind wood activated with sulphuric acid. Journal of Hazardous Materials. 153, 221-228.

Srinivasakannan, C. and Bakar, M. Z. A. 2004. Production of activated from rubber wood sawdust. Biomass and Bioenergy. 27, 89-96.

Steppan, D. D., Werner, J. and Yeater, R. P. 1998. Essential regression and experimental design for chemists and engineers.

Taghizadeh-Toosi, A., Clough, T., Sherlock, R., and Condrom, L. 2011. A wood based low-temperature biochar captures NH_3-N generated from ruminant urine-N, retaing its bioavailability. Plant and Soil. Publish online: 8 October 2011.

Xiarchos, I., Jaworska, A., and Zakrzewska-Trznadel, G. 2008. Response surface methodology for the modeling of copper removal from aqueous solutions using using micellar-enhanced ultrafiltration. Journal of MemnranE Science. 321, 22-231.

Yi, S., Su, Y., Qi, B., Su, Z., and Wan, Y. 2010. Application of response surface methodology and central composite rotatable design in optimization the preparation condition of vinyltriethoxysilane modified silicalite/polydimethylsiloxane hybrid pervaporation membranes. Separation and Purification Technology. 71, 252-262.

Yu, X., Mu, C., Gu, C., Liu, C. and Liu, X. 2011. Impact of woodchip biochar amendment on the sorption and dissipation of pesticide acetamiprid in agricultural soils. Chemosphere. 85, 1284-1289.

Zheng, Y., Liu, Y., and Wang, A. 2011. Fast removal of ammonium ion using a hydrogel optimized with response surface methodology. Chemical Engineering Journal. 171, 1201-1208.

http://en.wikipedia.org/wiki/Activated_carbon [April 25, 2012]

http://en.wikipedia.org/wiki/Ammonium_sulfte [April 25, 2012]

http://en.wikipedia.org/wiki/Phosphoric_acid [April 25, 2012]

http://en.wikipedia.org/wiki/Sulfuric_acid [April 25, 2012]

http://www.csiro.au/files/files/poei.pdf [April 25, 2012]

http://www.statease.com/dx8descr.html [April 25, 2012]

APPENDIX

APPENDIX A

Experimental Results

A-1 Activated carbon production from rubber wood by H_2SO_4 and H_3PO_4 acid activation.

Table A-1.1 Characterizations of rubber wood activated carbon by H_2SO_4 activation.

Conc.(%)	Yield (%)	S_{BET} (m^2/g)	S_{micro} (m^2/g)
20	30	334	249
30	30	456	366
40	30	497	400
50	28	557	466
60	28	499	462
70	27	474	389
80	22	398	335

Conc.= concentration

S_{BET}= BET surface area

S_{micro}= Micropores surface area

Table A-1.2 Characterizations of rubber wood activated carbon by H_3PO_4 activation.

Conc.(%)	Yield (%)	S_{BET} (m^2/g)	S_{micro} (m^2/g)
20	29	3	0
30	34	27	10
40	38	66	22
50	43	85	14
60	44	122	44
70	45	314	18
80	52	620	150

A-2 Preparation of activated carbon from rubber wood off-cut by mixed acid activation.

Table A-2.1 Characterizations of rubber wood activated carbon by mixed acid activation at constant H_3PO_4 at 40 %.

Conc. (%)	Yield (%)	S_{BET} (m^2/g)	S_{micro} (m^2/g)
20	40	105	27
30	38	290	139
40	37	515	251
50	36	506	101

Table A-2.2 Characterizations of rubber wood activated carbon by mixed acid activation at constant H_3PO_4 at 50 %.

Conc. (%)	Yield (%)	S_{BET} (m^2/g)	S_{micro} (m^2/g)
20	42	341	82
30	40	382	220
40	38	731	403
50	37	672	182

Table A-2.3 Effect of carbonization temperature on characterizations of activated carbon by the acid mixing of H_3PO_4 50% and H_2SO_4 40% at 2 h activation time.

Temperature (°C)	Yield (%)	S_{BET} (m^2/g)	S_{micro} (m^2/g)
400	39.7	1244	702
500	38.3	906	375
600	38.0	876	355
700	37.7	731	403

Table A-2.4 Effect of carbonization time on characterizations of activated carbon by the acid mixing of H_3PO_4 50% and H_2SO_4 40% at 2 h activation time.

Time (h)	Yield (%)	S_{BET} (m^2/g)	S_{micro} (m^2/g)
1	42	1138	681
2	40	1244	702
3	39	1189	657

A-3 NH_3 treatment in waste air using rubber wood activated carbon impregnated with sulfuric acid

A-3.1 Effect of H_2SO_4 concentration for acidic rubber wood activated carbon preparation on % NH_3 removal efficiency in adsorption system. Inlet NH_3 concentration of 800 ppmv and waste air flow rate of 2 l/min in 120 min.

Table A-3.1.1 NH_3 removal efficiency using rubber wood activated carbon impregnated with 60% H_2SO_4.

Time (min)	NH_3 concentration (ppmv)		NH_3 removal efficiency (%)
	Inlet	Outlet	
0	791	100	87
30	831	125	85
60	836	340	59
90	780	467	40
120	799	524	34

Table A-3.1.2 NH_3 removal efficiency using rubber wood activated carbon impregnated with 70% H_2SO_4.

Time (min)	NH_3 concentration (ppmv)		NH_3 removal efficiency (%)
	Inlet	Outlet	
0	810	69	91
30	800	136	83
60	874	213	76
90	836	283	66
120	814	442	46

Table A-3.1.3 NH_3 removal efficiency using rubber wood activated carbon impregnated with 80% H_2SO_4.

Time (min)	NH_3 concentration (ppmv)		NH_3 removal efficiency (%)
	Inlet	Outlet	
0	805	108	87
30	819	130	84
60	807	132	84
90	809	151	81
120	812	126	84

Table A-3.1.4 Experimental result and Calculated value of NH_3 weight on various H_2SO_4 concentrations.

H_2SO_4 concentration (%)	Weight of NH_3 (g)	
	Experimental	Calculation
60	0.014	0.016
70	0.015	0.016
80	0.023	0.016

A-3.2 Effect of inlet NH_3 Concentration on % NH_3 removal efficiency by acidic rubber wood activated carbon in adsorption system. H_2SO_4 70 % and Waste air flow rate of 2 l/min in 120 min.

Table A-3.2.1 Effect of inlet NH_3 Concentration at 400 ppmv on % NH_3 removal efficiency.

Time (min)	NH_3 concentration (ppmv)		NH_3 removal efficiency (%)
	Inlet	Outlet	
0	384	20	95
30	407	15	96
60	465	25	95
90	430	78	82
120	362	53	85

Table A-3.2.2 Effect of inlet NH_3 Concentration at 1500 ppmv on % NH_3 removal efficiency.

Time (min)	NH_3 concentration (ppmv)		NH_3 removal efficiency (%)
	Inlet	Outlet	
0	1547	185	88
30	1479	312	79
60	1311	821	37
90	1555	1277	18
120	1455	1352	7

Table A-3.2.3 Experimental result and Calculated value of NH_3 weight on various inlet NH_3 Concentration

NH_3 concentration (ppmv)	Weight of NH_3 (g)	
	Experimental	Calculation
400	0.015	0.010
800	0.015	0.016
1500	0.012	0.019

A-3.3 Effect of waste air flow rate on NH_3 removal efficiency by adsorption with 70 % w/w of RWACs and 800 ppmv of inlet NH_3 concentration in 120 min.

Table A-3.3.1 Effect of waste air flowrate at 3 l/min on % NH_3 removal efficiency.

Time (min)	NH_3 concentration (ppmv)		NH_3 removal efficiency (%)
	Inlet	Outlet	
0	771	112	85
30	821	253	69
60	791	493	38
90	833	729	12
120	840	729	13

Table A-3.3.2 Effect of waste air flowrate at 4 l/min on % NH_3 removal efficiency.

Time (min)	NH_3 concentration (ppmv)		NH_3 removal efficiency (%)
	Inlet	Outlet	
0	899	107	88
30	811	293	64
60	807	132	22
90	729	568	5
120	820	781	5

Table A-3.3.3 Experimental result and Calculated value of NH_3 weight on various waste air flow rate

Waste air flow rate (l/min)	Weight of NH_3 (g)	
	Experimental	Calculation
2	0.015	0.016
3	0.012	0.014
4	0.008	0.015

A-4 NH_3 adsorption from waste air using acid modification rubber wood activated carbon and biochar.

A-4.1 Effect of H_2SO_4 concentration for acidic rubber wood activated carbon preparation on % NH_3 removal efficiency in adsorption system. Inlet NH_3 concentration of 400 ppmv and waste air flow rate of 2 l/min in 240 min.

Table A-4.1.1 NH_3 removal efficiency using rubber wood activated carbon without H_2SO_4 impregnation.

Time (min)	NH_3 concentration (ppmv)		NH_3 removal efficiency (%)
	Inlet	Outlet	
0	411	79	81
30	402	200	50
60	451	325	28
90	446	387	13
120	362	347	4
150	398	398	0
180	405	405	0
210	416	416	0
240	387	387	0

Table A-4.1.2 NH_3 removal efficiency using rubber wood activated carbon impregnated with 60% H_2SO_4.

Time (min)	NH_3 concentration (ppmv)		NH_3 removal efficiency (%)
	Inlet	Outlet	
0	402	42	90
30	435	48	89
60	360	62	83
90	467	94	78

Time (min)	NH_3 concentration (ppmv)		NH_3 removal efficiency (%)
	Inlet	Outlet	
120	422	105	75
150	409	125	69
180	452	180	60
210	405	205	49
240	456	300	34

Table A-4.1.3 NH_3 removal efficiency using rubber wood activated carbon impregnated with 70% H_2SO_4.

Time (min)	NH_3 concentration (ppmv)		NH_3 removal efficiency (%)
	Inlet	Outlet	
0	384	37	90
30	467	48	90
60	415	42	90
90	380	37	90
120	402	53	87
150	423	63	85
180	395	67	83
210	440	99	78
240	339	126	63

Table A-4.1.4 NH_3 removal efficiency using rubber wood activated carbon impregnated with 80% H_2SO_4.

Time (min)	NH_3 concentration (ppmv)		NH_3 removal efficiency (%)
	Inlet	Outlet	
0	413	40	90
30	450	59	87

Time (min)	NH_3 concentration (ppmv)		NH_3 removal efficiency (%)
	Inlet	Outlet	
60	392	46	88
90	391	38	90
120	387	45	88
150	429	47	89
180	448	43	90
210	388	45	88
240	433	55	87

A-4.2 Effect of H_2SO_4 concentration for acidic rubber wood biochar carbon preparation on % NH_3 removal efficiency in adsorption system. Inlet NH_3 concentration of 400 ppmv and waste air flow rate of 2 l/min in 240 min.

Table A-4.1.1 NH_3 removal efficiency using rubber wood activated biochar without H_2SO_4 impregnation.

Time (min)	NH_3 concentration (ppmv)		NH_3 removal efficiency (%)
	Inlet	Outlet	
0	473	180	62
30	392	310	21
60	360	62	2
90	467	467	0
120	422	422	0
150	409	409	0
180	452	452	0
210	405	405	0
240	456	456	0

Table A-4.1.2 NH_3 removal efficiency using rubber wood activated biochar impregnated with 60% H_2SO_4.

Time (min)	NH_3 concentration (ppmv)		NH_3 removal efficiency (%)
	Inlet	Outlet	
0	396	38	90
30	384	42	89
60	421	94	78
90	433	160	63
120	414	211	49
150	389	246	37
180	477	352	26
210	398	339	15
240	352	338	4

Table A-4.1.3 NH_3 removal efficiency using rubber wood activated biochar impregnated with 70% H_2SO_4.

Time (min)	NH_3 concentration (ppmv)		NH_3 removal efficiency (%)
	Inlet	Outlet	
0	393	38	90
30	407	42	90
60	367	38	90
90	376	38	90
120	410	45	89
150	386	56	85
180	356	105	70
210	410	161	61
240	411	206	50

Table A-4.1.4 NH_3 removal efficiency using rubber wood activated biochar impregnated with 80% H_2SO_4.

Time (min)	NH_3 concentration (ppmv)		NH_3 removal efficiency (%)
	Inlet	Outlet	
0	373	37	90
30	432	56	87
60	387	46	88
90	394	52	87
120	384	45	88
150	445	59	87
180	458	63	86
210	434	79	82
240	469	95	80

A-4.3 Effect of H_2SO_4 concentration for acidic rubber wood activated carbon preparation on the breakthrough curve of NH_3 adsorption from waste air. Inlet NH_3 concentration of 800 ppmv and waste air flow rate of 2 l/min in 240 min.

Table A-4.3.1 Breakthrough of NH_3 adsorption using rubber wood activated carbon without H_2SO_4 impregnation.

Time (min)	NH_3 concentration (ppmv)		C/C_0
	Inlet	Outlet	
0	839	166	0.20
10	832	165	0.20
20	829	341	0.41
30	812	446	0.55
40	872	565	0.65
50	821	589	0.72

Time (min)	NH_3 concentration (ppmv)		C/C_0
	Inlet	Outlet	
60	756	605	0.80
70	786	684	0.87
80	812	755	0.93
90	845	845	1.00
100	802	802	1.00

Table A-4.3.2 Breakthrough of NH_3 adsorption using rubber wood activated carbon impregnated with 60% H_2SO_4.

Time (min)	NH_3 concentration (ppmv)		C/C_0
	Inlet	Outlet	
0	768	77	0.10
10	794	79	0.10
20	848	85	0.10
30	816	82	0.10
40	813	81	0.10
50	827	294	0.36
60	809	366	0.45
70	823	436	0.53
80	781	529	0.68
90	770	572	0.74
100	846	677	0.80
110	765	635	0.83
120	848	742	0.87
130	802	699	0.87
140	836	744	0.89

Time (min)	NH_3 concentration (ppmv)		C/C_0
	Inlet	Outlet	
150	821	731	0.89
160	859	800	0.93
170	820	779	0.95
180	837	813	0.97
190	813	813	1.00
200	803	803	1.00
210	795	795	1.00

Table A-4.3.3 Breakthrough of NH_3 adsorption using rubber wood activated carbon impregnated with 70% H_2SO_4.

Time (min)	NH_3 concentration (ppmv)		C/C_0
	Inlet	Outlet	
0	833	83	0.10
10	811	81	0.10
20	788	79	0.10
30	773	77	0.10
40	829	83	0.10
50	839	84	0.10
60	805	81	0.10
70	781	157	0.20
80	780	234	0.30
90	856	342	0.40
100	793	373	0.47
110	793	436	0.55
120	772	486	0.63

Time (min)	NH_3 concentration (ppmv)		C/C_0
	Inlet	Outlet	
130	838	561	0.67
140	826	603	0.73
150	852	639	0.75
160	854	641	0.75
170	832	641	0.77
180	824	659	0.80
190	795	676	0.85
200	798	718	0.90
210	761	708	0.93
220	852	809	0.95
230	773	773	1.00
240	747	747	1.00
250	791	791	1.00

Table A-4.3.4 Breakthrough of NH_3 adsorption using rubber wood activated carbon impregnated with 80% H_2SO_4.

Time (min)	NH_3 concentration (ppmv)		C/C_0
	Inlet	Outlet	
0	798	80	0.10
10	842	84	0.10
20	750	75	0.10
30	834	83	0.10
40	765	77	0.10
50	848	85	0.10
60	742	74	0.10

Time (min)	NH_3 concentration (ppmv)		C/C_0
	Inlet	Outlet	
70	794	79	0.10
80	792	79	0.10
90	811	81	0.10
100	754	128	0.17
110	823	189	0.23
120	843	211	0.25
130	874	262	0.30
140	845	279	0.33
150	811	300	0.37
160	782	305	0.39
170	819	410	0.50
180	805	427	0.53
190	742	467	0.63
200	830	589	0.71
210	836	652	0.78
220	814	667	0.82
230	763	641	0.84
240	801	673	0.84
250	808	719	0.89
260	791	728	0.92
270	782	766	0.98
280	844	844	1.00
290	819	819	1.00
300	793	793	1.00

A-4.4 Effect of H_2SO_4 concentration for acidic rubber wood biochar preparation on the breakthrough curve of NH_3 adsorption from waste air. Inlet NH_3 concentration of 800 ppmv and waste air flow rate of 2 l/min in 240 min.

Table A-4.4.1 Breakthrough of NH_3 adsorption using rubber wood biochar carbon without H_2SO_4 impregnation.

Time (min)	NH_3 concentration (ppmv)		C/C_0
	Inlet	Outlet	
0	701	355	0.51
10	847	698	0.82
20	829	745	0.95
30	812	802	1.00
40	872	867	1.00

Table A-4.4.2 Breakthrough of NH_3 adsorption using rubber wood biochar carbon impregnated with 60% H_2SO_4.

Time (min)	NH_3 concentration (ppmv)		C/C_0
	Inlet	Outlet	
0	806	81	0.10
10	789	79	0.10
20	815	82	0.10
30	872	215	0.25
40	786	345	0.44
50	801	441	0.55
60	813	488	0.60
70	803	562	0.70
80	774	581	0.75
90	821	682	0.83

Time (min)	NH_3 concentration (ppmv)		C/C_0
	Inlet	Outlet	
100	805	725	0.90
110	816	759	0.93
120	842	800	0.95
130	810	786	0.97
140	764	749	0.98
150	812	804	0.99
160	806	798	0.99
170	770	770	1.00
180	782	782	1.00
190	801	801	1.00

Table A-4.4.3 Breakthrough of NH_3 adsorption using rubber wood biochar carbon impregnated with 70% H_2SO_4.

Time (min)	NH_3 concentration (ppmv)		C/C_0
	Inlet	Outlet	
0	787	79	0.10
10	839	84	0.10
20	761	76	0.10
30	856	86	0.10
40	806	81	0.10
50	849	85	0.10
60	763	191	0.25
70	776	279	0.36
80	812	365	0.45
90	797	427	0.54

Time (min)	NH_3 concentration (ppmv)		C/C_0
	Inlet	Outlet	
100	821	493	0.60
110	776	543	0.70
120	792	594	0.75
130	817	629	0.77
140	832	657	0.79
150	783	619	0.79
160	809	671	0.83
170	795	676	0.85
180	792	692	0.87
190	814	724	0.89
200	787	748	0.95
210	846	821	0.97
220	778	778	1.00
230	809	809	1.00
240	817	817	1.00
250	842	842	1.00

Table A-4.4.4 Breakthrough of NH_3 adsorption using rubber wood biochar carbon impregnated with 80% H_2SO_4.

Time (min)	NH_3 concentration (ppmv)		C/C_0
	Inlet	Outlet	
0	818	82	0.10
10	815	82	0.10
20	803	80	0.10
30	824	82	0.10

Time (min)	NH_3 concentration (ppmv)		C/C_0
	Inlet	Outlet	
40	780	78	0.10
50	792	79	0.10
60	783	78	0.10
70	773	77	0.10
80	763	76	0.10
90	807	161	0.20
100	798	239	0.30
110	761	266	0.35
120	802	321	0.40
130	796	374	0.47
140	817	433	0.53
150	762	434	0.57
160	761	479	0.63
170	765	513	0.67
180	827	604	0.73
190	803	602	0.75
200	823	658	0.80
210	784	651	0.83
220	762	648	0.85
230	858	746	0.87
240	757	681	0.90
250	807	767	0.95
260	818	818	1.00
270	772	772	1.00
280	833	833	1.00

A-5 Removal of NH_3 from waste air by rubber wood biochar impregnated with H_2SO_4 and regenteration

A-5.1 Effect of H_2SO_4 concentration for acidic rubber wood biochar preparation on % NH_3 removal efficiency of the adsorption system

Table A-5.1.1 Effect of H_2SO_4 concentration for acidic rubber wood biochar preparation on % NH_3 removal efficiency of the adsorption system. at inlet NH_3 concentration of 1300 ppmv and waste air flow rate 3 l/min.

Time (min)	NH_3 removal efficiency (%)			
	40%	60%	70%	80%
0	85	92	92	93
10	49	69	89	93
20	24	14	76	93
30	11	8	35	89
40	14	7	18	79
50	18	0	5	62
60	3	1	8	25
70	2	5	2	27
80	10	10	14	3
90	0	3	2	2
100	0	3	8	4
110	0	0	2	1
120	0	2	5	3

Table A-5.1.2 Effect of H_2SO_4 concentration for acidic rubber wood biochar preparation on adsorption time at 50 % NH_3 removal efficiency of the system.

H_2SO_4 concentration (%)	Time (min.)
40	10
60	13
70	26
80	52

A-5.2 Effect of NH_3 Concentration in waste air on % NH_3 removal efficiency by acidic rubber wood biochar.

Table A-5.2.1 Effect of NH_3 Concentration in waste air on % NH_3 removal efficiency by acidic rubber wood biochar using H_2SO_4 40% w/w RWBs and waste air flow rate of 3 l/min.

Time (min)	NH_3 removal efficiency (%)			
	300 ppmv	1300ppmv	1700 ppmv	2000 ppmv
0	90	92	89	91
10	88	85	80	80
20	88	65	45	37
30	88	28	20	18
40	89	7	12	7
50	89	0	12	1
60	83	1	6	5
70	89	5	1	5
80	66	10	16	2
90	66	3	9	0
100	57	3	-	-
110	38	0	-	-
120	33	2	-	-
130	27	-	-	-

Time (min)	NH_3 removal efficiency (%)			
	300 ppmv	1300ppmv	1700 ppmv	2000 ppmv
150	6	-	-	-
160	5	-	-	-
170	4	-	-	-
180	5	-	-	-

Table A-5.2.2 Effect of NH_3 inlet concentration on adsorption time at 50 % NH_3 removal efficiency of the system.

NH_3 concentration (ppmv)	Time (min)
300	103
1300	30
1700	20
2000	18

A-5.3 Effect of waste air flow rate on % NH_3 removal efficiency by acidic rubber wood biochar.

Table A-5.3.1 Effect of waste air flow rate on % NH_3 removal efficiency by adsorption with 40 % w/w of acidic rubber wood biochar and 1300 ppmv of initial NH_3 concentration

Time (min)	NH_3 removal efficiency (%)			
	2 l/min	3 l/mim	4 l/min	5 l/min
0	92	92	83	87
10	91	80	71	51
20	87	24	8	30
30	73	8	1	3
40	60	7	13	4
50	36	0	0	2
60	25	1	2	12

Time (min)	NH_3 removal efficiency (%)			
	2 l/min	3 l/mim	4 l/min	5 l/min
70	11	5	1	0
80	10	10	1	4
90	16	3	1	1
100	5	3	-	-
110	9	0	-	-
120	9	2	-	-
130	4	-	-	-
140	1	-	-	-
150	13	-	-	-
160	11	-	-	-
170	10	-	-	-
180	2	-	-	-

Table A-5.3.2 Effect of waste air flow rate on adsorption time at 50% NH_3 removal efficiency of the system.

Waste air flow rate (l/min)	Time (min)
2	44
3	16
4	14
5	10

A-5.4 Acidic rubber wood biochar regeneration by hot water.

Table A-5.4.1 NH_3 adsorption Breakthrough curve of fresh acidic rubber wood biochar ($RWBs^{f}$), no washing and no re-impregnation acidic rubber wood biochar ($RWBs^{no\text{-}nr}$), and no washing and re-impregnation acidic rubber wood biochar ($RWBs^{no\text{-}r}$).

Time (min)	C/C_0		
	$RWBs^{no\text{-}nr}$	$RWBs^{no\text{-}r}$	$RWBs^{f}$
0	0.4	0.4	0.1
30	0.4	0.4	0.1
60	0.4	0.4	0.1
90	0.5	0.4	0.1
120	0.6	0.4	0.1
150	0.9	0.5	0.1
180	1.0	0.7	0.1
210	1.0	0.9	0.1
240	1.0	1.0	0.1
270	-	1.0	0.2
300	-	1.0	0.3
330	-	1.0	0.5
360	-	-	0.6
390	-	-	0.7
420	-	-	0.9
450	-	-	1.0
480	-	-	1.0

Table A-5.4.2 Effect of water temperature for 1st regeneration on breakthrough curve of acidic rubber wood biochar.

Time (min)	C/C_0			
	30°C	50 °C	70 °C	100 °C
0	0.1	0.1	0.1	0.1
30	0.1	0.1	0.1	0.1

Time (min)	C/C_0			
	30°C	50 °C	70 °C	100 °C
60	0.1	0.1	0.1	0.1
90	0.1	0.1	0.1	0.1
120	0.1	0.1	0.1	0.1
150	0.1	0.1	0.1	0.1
180	0.1	0.1	0.1	0.1
210	0.1	0.1	0.1	0.1
240	0.3	0.2	0.1	0.1
270	0.5	0.4	0.3	0.3
300	0.7	0.6	0.5	0.4
330	0.8	0.8	0.7	0.6
360	0.9	0.9	0.8	0.7
390	1.0	1.0	0.9	0.8
420	1.0	1.0	1.0	1.0
450	-	-	-	1.0

Table A-5.4.3 Effect of water temperature for 2nd regeneration on breakthrough curve of acidic rubber wood biochar.

Time (min)	C/C_o			
	30°C	50 °C	70 °C	100 °C
0	0.1	0.1	0.1	0.1
30	0.1	0.1	0.1	0.1
60	0.1	0.1	0.1	0.1
90	0.1	0.1	0.1	0.1
120	0.1	0.1	0.1	0.1
150	0.1	0.1	0.1	0.1
180	0.1	0.1	0.1	0.1

Time (min)	C/C_o			
	30°C	50 °C	70 °C	100 °C
210	0.1	0.1	0.1	0.1
240	0.1	0.1	0.1	0.1
270	0.2	0.1	0.1	0.1
300	0.3	0.2	0.1	0.1
330	0.3	0.3	0.1	0.1
360	0.4	0.3	0.2	0.1
390	0.6	0.4	0.3	0.1
420	0.7	0.5	0.4	0.1
450	0.9	0.7	0.5	0.2
480	1.0	0.8	0.7	0.2
510	-	0.9	0.8	0.4
540	-	1.0	0.9	0.6
570	-	1.0	1.0	0.7
600	-	-	1.0	0.8
630	-	-	-	0.9
660	-	-	-	1.0

A-6 Modeling and optimization of ammonia treatment by acidic biochar using response surface methodology (RSM)

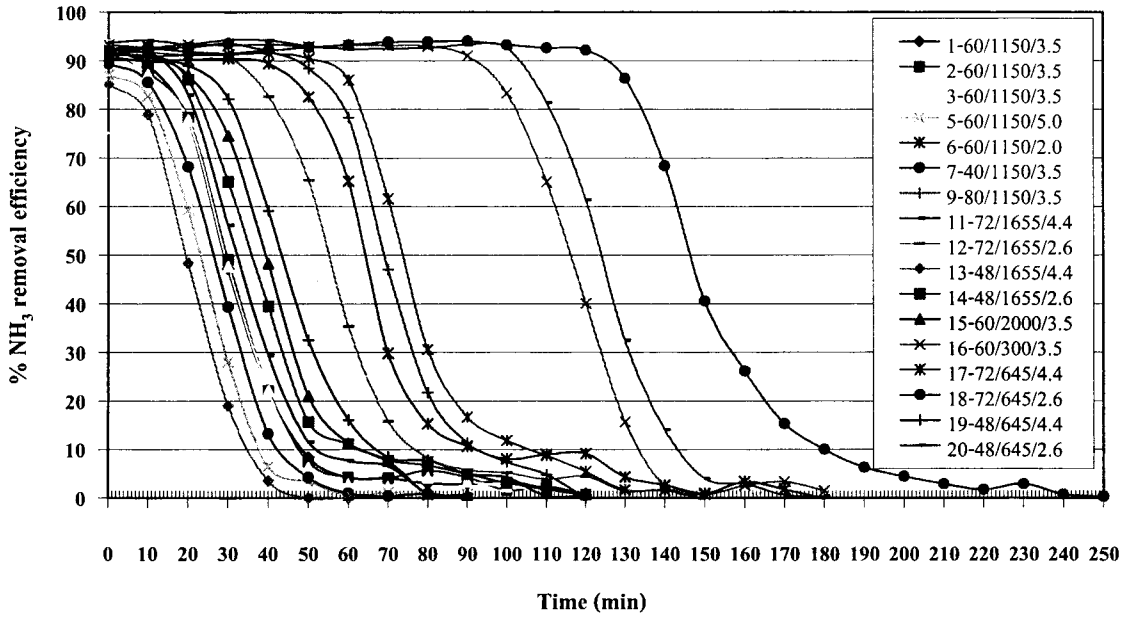

Figure A-6.1 the NH_3 removal efficiency on RSM methods for determined $t_{1/2}$

Table A-6.1 Breakthrough curve of NH_3 adsorption (300 ppmv) from waste air (2.1 l/min) for comparison study between commercial activated carbon (AC) and rubber wood biochar (RWB).

Time (min)	C/C_o	
	AC	RWB
0	0.3	0.4
10	0.4	0.5
20	0.6	0.7
30	0.7	0.8
40	0.8	1.0
50	1.0	1.0
60	1.0	1.0
90	1.0	1.0

Table A-6.2 Breakthrough curve of NH_3 adsorption (300 ppmv) from waste air (2.1 l/min) for comparison study between acidic commercial activated carbon (ACs) and acidic rubber wood biochar (RWBs) (with 72 % sulfuric acid impregnation).

Time (min)	C/C_o	
	ACs	RWBs
0	0.1	0.1
30	0.1	0.1
60	0.1	0.1
90	0.1	0.1
120	0.1	0.1
150	0.1	0.1
180	0.2	0.3
210	0.3	0.4
240	0.5	0.6
270	0.6	0.7
300	0.8	0.8
330	0.9	0.9
360	1.0	1.0
390	1.0	1.0
420	1.0	1.0
450	1.0	1.0

APPENDIX B

Analytical Methods

B-1 Determination of ammonia content in waste air

(refer by American Public Health Association, 1995 and Rodrigues et al., 2007)

B-1.1 Analysis

Titration was used to determine ammonia concentration. The air/ammonia gaseous mixture was bubbled through a 50 ml cold boric acid solution for 1 min. The following reaction ensues:

$$H_3BO_3(l) + NH_3(g) \longrightarrow NH_4H_2BO_3(l) \qquad (1)$$

The resulting $NH_4H_2BO_3$ solution is colourless, turning green following the addition of 0.2% mixed indicators alcohol solution (methyl red and methylene blue) (American Public Health Association, 1995). It is then titrated by hydrochloric acid 0.02 M until it is violet. The following reaction ensues:

$$NH_4H_2BO_3(l) + HCl(l) \longrightarrow H_3BO_3(l) + NH_4Cl(l) \qquad (2)$$

Thus, $NH_4H_2BO_3$ concentration can be calculated by means of the following equation:

$$V_{NH_4H_2BO_3} \cdot M_{NH_4H_2BO_3} = V_{HCl} \cdot M_{HCl} \qquad (3)$$

in which:

$V_{NH_4H_2BO_3}$ = volume of ammonium borate [ml];

$M_{NH_4H_2BO_3}$ = molarity of ammonium borate [mol];

V_{HCl} = volume of hydrochloric acid [ml];

M_{HCl} = molarity of hydrochloric acid [mol];

After calculating $NH_4H_2BO_3$ concentration, it is then possible to determine the mass of ammonia in the solution, following the bubbling of the gaseous mixture, using the equation below:

$$m_{NH_3} = M_{NH_4H_2BO_3} \cdot V_{NH_4H_2BO_3} \cdot PM_{NH_3} \qquad (4)$$

in which:

m_{NH_3} = ammonia mass [mg];

PM_{NH_3} = molecular weight of ammonia [g/mol].

After calculating the mass of ammonia, ammonia concentration in the gaseous mixture is determined dividing the mass by the volume of bubbling gas in the boric acid solution, making use of the equation:

$$C_{NH_3} = \frac{m_{NH_3}}{Q_T \cdot t_b} \qquad (5)$$

in which:

C_{NH_3} = ammonia concentration [mg/l];

Q_T = total flow of gaseous mixture [l/min];

t_b = bubbling time [min].

B-2 Parts per Million by Volume (or mole) in Air

(refer by http://www.lenntech.com/calculators/ppm/converter-parts-per-million.htm)

In air pollution literature ppm applied to a gas, always means parts per million by volume or by mole. These are identical for an ideal gas, and practically identical for most gases of air pollution interest at 1 atm. Another way of expressing this value is ppmv. One part per million (by volume) is equal to a volume of a given gas mixed in a million volumes of air:

$$1\ ppm = \frac{1\ gas\ volume}{10^6\ air\ volumes}$$

A micro liter volume of gas in one liter of air would therefore be equal to 1 ppm:

$$1\ ppm = \frac{1\ \mu L\ gas}{1\ L\ air}$$

Today's more and more there is an interest to express gas concentrations in metric units, i.e. $\mu g/m^3$. Although expressing gaseous concentrations in $\mu g/m^3$ units, has the advantage of metric expression, it has the disadvantage of being greatly influenced by changes in temperature

and pressure. Additionally, because of difference in molecular weight, comparisons of concentrations of different gases are difficult.

To convert ppmv to a metric expression like $\mu g/m^3$, the density of the concerning gas is needed. The density of gas can be calculated by the Law of Avogadro's, which says: equal volumes of gases, at the same temperature and pressure, contain the same number of molecules. This law implies that 1 mole of gas at STP a volume of 22.71108 liters (dm^3) enfolds, also mentioned as the molar volume of ideal gas. Standard Temperature and Pressure (STP) is defined as a condition of 100.00 kPa (1 bar) and 273.15 K (0 °C), which is a standard of IUPAC. The amount of moles of the concerning gas can be calculated with the molecular weight.

$$1\ \text{ppm} = \frac{V_m}{M}\ \frac{1\ \mu\text{g gas}}{1\ \text{L air}}$$

Where:

V_m = standard molar volume of ideal gas (at 1 bar and 273.15 K) [22.71108 L/mol]

M = molecular weight of gas[g/mol]

For converting ppm by mole, the same equation can be used. This can be made clear by the following notation:

$$1\ \text{ppm} = \frac{1\ \mu\text{mole gas}}{1\text{mole air}} = \frac{V_m}{M}\ \frac{1\ \mu\text{g gas}}{1\ \text{L air}}$$

By checking the dimensions of the most right part of the equation, there will be found a dimensionless value, like the concentration in ppm is.

To calculate the concentration in metric dimensions, with other temperature and pressure conditions the Ideal Gas Law comes in handy. The volume (V) divided by the number of molecules (n) represents the molar volume (V_n) of the gas with a temperature (T) and pressure (P).

$$V_n = V/n = R\ \frac{T}{p}$$

where:

V_n = specific molar volume of ideal gas (at pressure P and temperature T) [L/mol]

V = volume of the gas[m^3]

n = amount of molecules[mol]

R = universal gas law constant [8.314510 J K^{-1} mol^{-1}] or [m^3 Pa K^{-1} mol^{-1}]

T = temperature[K]

P = pressure [Pa]

With this equation it comes clear that the percentage notation by ppm is much more useful, because the independency of the temperature and pressure.